Interference mitigation techniques for 4G networks

Daniel Jaramillo Ramirez

N° d'ordre : 2014-02-TH

SUPELEC

ECOLE DOCTORALE STITS

"Sciences et Technologies de l'Information des Télécommunications et des Systèmes"

THESE DE DOCTORAT

DOMAINE : STIC

Spécialité : Télécommunications

Présentée par

Daniel JARAMILLO-RAMIREZ

Techniques de lutte contre l'interférence inter-cellulaire dans les réseaux de 4ème génération

Interference mitigation techniques for 4G networks

Rapporteur :	Roberto BUSTAMANTE	Prof. Université de los Andes
Examinateur :	Bruno CLERCKX	Prof. Imperial College London
Président du jury :	Pierre DUHAMEL	Prof. CNRS/Supélec
Membre invité :	Eric HARDOUIN	Ingénieur Orange Labs
Encadrant de thèse :	Marios KOUNTOURIS	Prof. Dpt. Télécom. Supélec
Rapporteur :	Didier LE RUYET	Prof. CNAM
Directeur de thèse :	Hikmet SARI	Dir. Dpt. Télécom. Supélec

Acknowledgments

This thesis summarizes three years of research under a CIFRE convention between Orange Labs and Supélec, partially funded by the French national association for research and technology (ANRT). The excellent relation between both sides carried all along these three years, based on respect, willingness to work and cooperation, provided me the most suitable environment for professional development.

In this regard, I am deeply thankful to Marios Kountouris and Eric Hardouin: it was a great pleasure working with you two. I will always remember our meetings as a hearty duel between practical and theoretical communications. Marios had the patience for taking me inside many of the basic concepts of modern communications that I was missing when I arrived, always available for my long list of dumb questions. He also had to teach me all the rules of being a researcher and publishing papers; and firmly proved to me the importance of doing practical research from a solid theoretical grounding. Eric was always an excellent reference on the industry's point of view. He was truly helpful on technical details. He provided a great balance on this tree-year industrial-academic marriage, always available and fully committed on the guidance process.

Next to Marios and Eric I had the great chance of finding two excellent work environments in Supélec and Orange Labs. The telecommunications department and the ALU Chair were I met Samir, Subhash, Farhan, Meryem, Germán, Apostolos, Axel, Stefano, Luca, Marco, Jakob, Salam, Laura, Karim, Ejder, Bhanu, Giovanni, Loig, Emil, Nikos and so many great people. Special thanks to Catherine, Jose and Huu for all their help. In Orange Labs I am very thankful to Alexandre Gouraud for his valuable discussions and all the team for the very good moments: Pierre, Hajer, Sarah, Atoosa, Baozhu, Yohan, Arturo, Sofía, Ahmed, Boubou, Najet, Ali, Alexandre N. Thanks also to Suzette that was always kindly available.

My sincere thanks to all the jury members for participating in my defense, contributing with interesting questions, their kind comments and motivating messages. Starting from Roberto, who was the first person pushing me to pursuit a doctoral degree. Roberto and professor Didier le Ruyet thoroughly reviewed my thesis manuscript in a short time, providing useful comments

and corrections. Special thanks to Hikmet Sari who was my thesis director and helped me normalize my situation in France.

Quiero hacer un agradecimiento especial a mis amigos más cercanos en París. Simón, M. José, Luis y Alinda, quienes estuvieron siempre presentes acompañando mis continuos “no tengo tiempo” y mis cortos pero muy amenos ratos de descanso. Así como a mis amigos en Colombia y en otros lugares que fueron siempre de gran apoyo. A mis hermanos y en especial a mis padres que son los primeros responsables de cualquier logro en mi vida personal y profesional. Sabrán perdonarme también por no haber estado muy disponible durante estos años, aun cuando vinieron a verme.

Finalmente dejo unas palabras para el más profundo, sincero y efusivo agradecimiento que guardo con la persona que ha sido mi mayor soporte y mi mejor compañía en los grandes momentos, en los pequeños detalles, en los días grises y en los de sol radiante.

Abstract

Wireless communications have become a fundamental feature of any modern society. In particular, cellular technology is used by most of the world's population and has been established as the principal means of access to the Internet. Cellular networks are essential for societal welfare and development but the increasing demand for data traffic and higher data rates set enormous scientific and engineering challenges. Increasing the network capacity is one of the most important challenges, which is also closely related to the problem of *interference mitigation*. As one of the most promising concepts for overcoming interference in cellular networks, network cooperation has been extensively studied in recent years and several different techniques have been proposed. Focusing on the downlink, which in general is technically more challenging, this dissertation investigates network cooperation at the transmitter side under imperfect channel state information, as well as explores the potential gains from a new technique of network cooperation that takes advantage of signal processing capabilities at the receiver side. In the first part, different transmission techniques commonly referred to as Coordinated Multi-Point Transmission (CoMP), are studied under the effect of feedback quantization and delay, unequal pathloss and other-cell interference (OCI). An analytical framework is provided, which yields closed-form expressions to calculate the ergodic throughput and outage probabilities of Coordinated Beamforming (CBF) and Joint Transmission (JT). The results indicate the optimal configuration for a system using CoMP and provide guidelines and answers to key questions, such as how many transmitters to coordinate, how many antennas to use, how many users to serve, which SNR regime is more convenient, whether to apply CBF or prefer a more complex JT, etc. The cell regions where CoMP increases the achievable sum rate compared to

non-cooperative transmission are identified and the gains are quantified. Furthermore, CoMP is shown to be highly sensitive to the feedback quality. Although single-user or multi-user JT may be useful in some regimes, CBF appears to find a good compromise between implementation complexity, backhaul requirements and the gains provided, especially for cell-edge users.

Second, a new coordination technique at the receiver side is proposed to obtain sum-rate gains by means of Successive Interference Cancellation (SIC). The conditions that guarantee network capacity gains by means of SIC at the receiver are provided. To take advantage of these conditions, network coordination is needed to adapt the rates to be properly decoded at the different users involved. This technique is named *Cooperative SIC* and is shown to provide significant throughput gains for cell-edge users in different cells, or even if multiple users are located inside one cell SIC allows the neighbor transmitters to serve some users and help increasing the sum rate. The cooperative SIC strategy is initially established for one receiver suppressing multiple interference signals, but can also be extended for simultaneous receivers doing SIC. The effect of small-scale fading is proved to be beneficial to increase the gains of SIC with respect to receivers that treat interference as noise (IaN). Finally, an algorithm is proposed for a centralized scheduler to implement the cooperative SIC strategy in large networks, proving that important gains can be achieved specially for cell-edge users.

Résumé

Les communications sans fils sont devenues un outil fondamental pour les sociétés modernes. Plus spécifiquement, les réseaux cellulaires sont utilisés pour la plupart des populations et sont actuellement le moyen préféré pour l'accès à Internet. En conséquence, les réseaux cellulaires ont un rôle essentiel pour le bien être et le développement social, mais l'augmentation de la demande du trafique des données fait apparaître de nouveaux défis scientifiques et d'ingénierie. L'augmentation de la capacité du réseau est étroitement liée au problème de la mitigation des interférences. Dans cette problématique, les réseaux coopératifs ont été largement étudiés dans les années récentes. Cette thèse porte sur deux techniques de coopération dans la voie descendante : l'une déjà connue réalisée à l'émission et une deuxième proposée du coté des récepteurs.

La première partie étudie les effets de quantification et délais sur les informations de retour (en anglais feedback) nécessaires pour la mise en opération des différentes techniques d'émission coordonnée, connues sous le nom de CoMP pour *Coordinated Multipoint Transmission*. CoMP est connue comme une solution qui promet des augmentations importantes sur la capacité du réseau en conditions idéales, or ses vrais résultats sous le feedback limité n'avaient pas encore été décrits de manière analytique. En particulier, pour les modes d'émission connus comme JT (*Joint Transmission*) et CBF (*Coordinated Beamforming*), des expressions analytiques ont été déduites pour calculer la capacité du réseau et la probabilité de succès de transmission. Ces expressions permettent de trouver la configuration optimale du système (en termes de capacité) indiquant le nombre des stations qui doivent être coordonnées, le nombre d'antennes à utiliser, la puissance d'émission et le mode préféré entre JT en CBF. Il est aussi possible de trouver les régions dans l'espace où CoMP dépasse la performance d'autres tech-

niques non coopératives. Ces régions entourent les bordures de cellules en proportion avec la qualité du feedback. Si JT montre bien les meilleurs résultats en termes de capacité, CBF apparaît comme la technique la plus adaptée avec une performance légèrement inférieure à JT et une complexité acceptable avec des besoins de *backhaul* toujours réalistes.

La deuxième partie propose une nouvelle technique de coopération de réseau pour les récepteurs avancés du type SIC (en Anglais *Successive Interference Cancellation*). La condition qui garantit des gains de capacité grâce à l'utilisation des récepteurs SIC est obtenue. Pour profiter de cette condition, une méthode de coopération est nécessaire pour assurer une adaptation de lien adéquate pour que l'interférence soit décodable et le débit somme soit supérieur à celui atteint avec des récepteurs traditionnels. Cette technique montre des gains importants de capacité pour des utilisateurs en bordure de cellule. Initialement établie pour la suppression d'une seule source d'interférence, cette technique est étendue pour supprimer un nombre indéfini des signaux d'interférence impliquant la coopération du même nombre de stations de base (émetteurs). L'effet des évanouissements rapides (*small-scale fading*) a été aussi étudié. Malgré son impact sur la capacité finale du système, il est montré que ceci est plus important dans les systèmes de récepteurs traditionnels. Finalement, l'utilisation de la technique SIC coopérative dans les réseaux avec un grand nombre de cellules requiert l'implémentation d'un *scheduler* centralisé et des algorithmes avancés pour garantir sa faisabilité. Un algorithme à été proposé et montre des gains de capacité très importants pour les utilisateurs en bordure de cellule.

Contents

List of Figures

List of Tables

Part I

Introduction

History and motivations

0.1 Brief history of wireless communications and cellular networks

The 21-st century has become the stage of the *Information Age* expansion as a large majority of the world's population is connected and most of the economic activity is carried out or somehow related to the Internet. Simultaneously and pushed by the Internet's momentum, wireless communications became the preferred Internet access technology [1]. Sensors, machines and devices connect to the Internet and a huge variety of new activities become wireless with the development of applications and standards such as RFID (Radio Frequency Identification), NFC (Near Field Communications), LiFi (Wi-Fi over light), Bluetooth or DLNA (Digital Living Network Alliance). By far, the more widespread and useful technology of wireless communications is the cellular network. After several decades of enormous scientific and engineering achievements a leading industrial consortium (Third Generation Partnership Project 3GPP) has standardized a worldwide used cellular technology named LTE.

From analog radio communications to the cellular concept

Although radio communications are said to be born at Marconi's demonstration in 1897, transmitting a Morse code message in the Isle of Wight [2], the genesis of mobile communications dates back to the 1940's where only in the United States thousands of analog radios were used mainly for public services. In the early 60's the number of mobile users in that country grew to more than a million with the development of cordless telephones, however, they were not con-

nected to the public switched telephone network and the coverage areas were restricted [3, 4]. Important advances in related areas such signal processing and electronics enhanced the capacity of the radio devices to the point that in the early 80's the cellular concept, previously developed in Bells Labs, gave birth to the first generation of cellular networks with a variety of technologies such as AMPS (Advanced Mobile Phone System) in the USA, TACS (Total Access Communication System) in Japan and the UK, NMT (Nordic Mobile Telephone) in the Scandinavian countries, Radiocom2000 in France and C-NETZ in Germany. These systems were based on analog modulation and coding, frequency division multiple access (FDMA), and were very limited in terms of coverage. Additionally, the user terminals had important dimensions which limited their portability.

The second generation and GSM

During the 90's, cellular systems became digital. Japan migrated to PDC (Personal Digital Communication), the USA developed the first Coded Division Multiple Access (CDMA) standard IS-95 and Europe standardized GSM, the most successful technology from the 2^{nd} *generation* deployed all over the world and still carrying important amounts of voice traffic nowadays. GSM is responsible for spreading the massive use of cellular phones mainly for voice and text messages (sms) but the data services were slow and limited; first under GPRS (General Packet Radio Service), then using EDGE (Enhanced Data rates for GSM Evolution) with rates in the order of 200 Kbit$/$s per cell.

Smart-phones in the third generation

The increasing demand for larger data rates brought the development of two new standards of the so called 3^{rd} *generation* of cellular networks. CDMA2000 was installed in North America and some Asian countries, while UMTS (Universal Mobile Telecommunications System) defined by the 3GPP was deployed all over the world. UMTS was based on Wideband Code Division Multiple Access (W-CDMA) and paved the way for the arrival of the smart-phones. These powerful terminals provide an immense variety of applications and most importantly be-

came the main user terminal for Internet access. By 2013 the International Telecommunications Union reported nearly 6.8 billion users of cellular phones (96% of world's population) [1].

Towards forth generation cellular networks

The data rate capacity kept increasing up to 42 Mbit$/$s with the introduction of HSPA and HSPA+ (High Speed Packet Access) but the market's response being overwhelmingly positive led the 3GPP consortium into defining new technical requirements for the 4^{th} *generation* of cellular networks, called the UMTS *Long Term Evolution* (LTE). Drastic changes on the core network and the introduction of *Orthogonal Frequency Division Multiple Access* (OFDMA) and Multiple-antenna (MIMO) radio technologies allow data rates up to 150 Mbit/s in the downlink and 50 Mbit/s in the uplink [5]. At the beginning of 2013, LTE deployments had captured more than 50 million clients in some 20 countries and strong investments make promise for worldwide use of this technology in the short-term future.

0.2 Motivations and contributions of this thesis

As will be explained in detail in Chapter 1, one of the main bottlenecks in cellular networks is the interference on the radio interface. The design of transmission strategies that achieve a better spectral efficiency has become one of the hot topics on research in the recent years. The radio electric spectrum is almost completely allocated for different communication services and will probably host many more services and devices with the arrival of future cellular networks. From a different perspective, is important to consider that in the large majority of cellular networks the use of data has been always asymmetric: the downlink is usually required to have ten times more capacity than the uplink. The increasing penetration of smart-phones in the market allows users to generate more content, shrinking the figure to seven times more traffic in the downlink. This asymmetry is also seen in the scarcity of resources and the efforts made by the research community looking after more efficient transmission schemes. Similarly, all research presented in this thesis targets increasing the downlink capacity of wireless networks.

Some of the most promising families of techniques for interference mitigation widely known in the literature are Relays, Massive MIMO, Small cells and Network Cooperation. A brief description of each can be found in section 1.2.3. The work of this thesis is mainly dedicated to Network Cooperation.

Interference mitigation at the transmitter side

Some of the most studied techniques are Coordinated Scheduling (CS), Coordinated Beamforming (CBF) and Joint Transmission (JT). The 3GPP consortium and the associated research community has grouped under the name CoMP for *Coordinated Multi-Point Transmission*. Despite the large amount of papers published on CoMP, few of them address the problem of limited feedback on FDD systems. Being quantization and delay the major drawbacks of feedback systems, an analytic framework was derived to approximate the performance in terms of throughput and outage probability. In this subject, the following publications are described on chapter 2:

- D. Jaramillo-Ramírez, M. Kountouris, and E. Hardouin, "Coordinated multi-point transmission with imperfect channel knowledge and other-cell Interference", *Proc., IEEE Personal Indoor and Mobile Radio Communications (PIMRC)*. Sydney, Australia, September 2012.

- D. Jaramillo-Ramírez, M. Kountouris, and E. Hardouin, "Coordinated multi-point transmission with quantized and delayed feedback", *Proc., IEEE Global Telecommunications Conference (GLOBECOM)*, Anaheim, CA, USA, December 2012.

- D. Jaramillo-Ramírez, M. Kountouris, and E. Hardouin, "Coordinated multi-point transmission with imperfect CSI and other-cell interference", in revision for *IEEE Transactions on Wireless Communications*.

Summary: The impact of quantized and delayed channel state information (CSI) on the average achievable rate of JT and CBF systems is investigated. Closed-form expressions and accurate approximations are derived on the expected sum rate and success probability of CoMP systems with imperfect CSI assuming small-scale Rayleigh fading, pathloss attenuation, and other-cell

interference (OCI). For analytical tractability, a moment matching technique approximates the distributions of the received desired and interference signals. The proposed approximate framework enables us to identify key system parameters, such as feedback resolution, delay, pathloss, and transmit SNR for which CoMP becomes a judicious choice of transmission strategy as compared to non-cooperative transmission. Moreover, adaptive feedback bit allocations are proposed on chapter 3. Results on adaptive feedback bit allocation were published at

- D. Jaramillo-Ramírez, M. Kountouris, and E. Hardouin, "Adaptive feedback bit allocation for coordinated multi-point transmission systems", *Proc., IEEE Personal Indoor and Mobile Radio Communications (PIMRC)*. London, UK, September 2013.

Interference mitigation at the receiver side

Additionally the final chapter of this thesis proposes a new technique for network cooperation called *Cooperative Successive Interference Cancellation* (coop. SIC). For many years, SIC has been known to be a capacity achieving technique for the multiple access channel (MAC) in information theory, but it has not been applied yet in the downlink of wireless systems. The main idea is that neighbor BS cooperate so that one of the users is able to decode and suppress an interference signal to get its desired signal at a larger rate, increasing the system throughput. The results of cooperative SIC can be found in

- D. Jaramillo-Ramírez, M. Kountouris, and E. Hardouin, "Successive interference cancellation in downlink cooperative cellular networks", accepted in *IEEE ICC 2014*.

- D. Jaramillo-Ramírez, M. Kountouris, and E. Hardouin, "Cooperative Successive interference cancellation in wireless networks", to be submitted to *IEEE Transactions on Wireless Communications*.

Summary: The improvement in sum rate of downlink cellular networks using successive interference cancellation (SIC) is studied. First, considering a two-cell cellular network and proposing a cooperative SIC scheme, in which one user receives its data at the single-user capacity using SIC while the rate in the other cell is accordingly adapted to maximize the sum rate. The

cooperative SIC scheme is then extended for N-cells. Characterizing the corner points of the capacity region of a N-user interference channel, we derive conditions for which using SIC increases the sum rate as compared to treating interference as noise (IaN). Finally, a centralized cell scheduling for performing cooperative SIC in multiuser multi-cell networks is proposed. Numerical results show that significant sum-rate improvement is achieved using SIC receivers, even with few users per cell and especially at the cell edge.

The results regarding network cooperation for SIC were presented at a recent 3GPP meeting for discussion on advanced receivers:

- D. Jaramillo-Ramirez and E. Hardouin, "NAICS: How to coordinate link adaptation for CWIC receivers". 3GPP meeting Barcelona, Spain, $19\text{th} - 23\text{rd}$ August 2013.

Related to this work, a patent was also filed in France.

- Patent: D. Jaramillo-Ramirez, E. Hardouin and M. Kountouris, filed August 2013.

Small Cells

The first contribution of this thesis was focused on evaluating the impact of user selection (scheduling) on outage probabilities and spectral efficiency for two-tier networks (e.g. a macro-cells tier and a small-cells tier). For instance, two-tier networks can be seen as a simplified version of a heterogeneous network composed by a macro BS underlaying multiple small cells following a two-dimensional Poisson point process (PPP) distribution. These results are not included in this manuscript but can be tracked on

- D. Jaramillo-Ramírez, M. Kountouris, and E. Hardouin, "Downlink Beamforming in Multi-Antenna Two-Tier Networks with User Selection", *Proc., IEEE GLOBECOM Workshop*, Houston, TX, USA, December 2011.

Chapter 1

Preliminary concepts

1.1 Basic Concepts of Wireless Channels

For the average user controlling the television remotely or participating on a video-call while enjoying a picnic in a park, wireless communications systems may seem like black magic. In reality, conveying information throughout electromagnetic radiation requires a fascinating engineering process involving technologies developed during the last hundred years. Moreover, the actual wireless standards for cellular networks not only transmit information but they do it so effectively that they approach the mathematical limits of communication efficiency described on the foundations of information theory. The corner stone of such remarkable achievement relies on a profound understanding of the wireless channel, i.e. all the phenomena that affect by the wave carrying the information message.

1.1.1 Propagation phenomena

The electromagnetic waves describe the physical event of the fastest possible way that energy can travel in space. Moreover, they are the only mean of energy propagation that can travel through the vacuum space. Their speed, undulating nature and ability to traverse any mean make them ideal to carry information. In particular, the portion of the spectrum where the wireless communications take place is known as radio waves. As the energy propagates in the

space as a radio wave, three main effects are distinguished and form the basis for modeling the wireless channel:

- Path-loss: As the wave travels, the space covered by the wave is enlarged and the amount of energy per unit area is naturally reduced as the inverse of the square of the distance. In a wireless channel the path-loss is usually described as d^{α}, where d is the distance between the transmitter and the receiver, while the exponent varies as $2 < \alpha < 4$ according to the propagation environment.

- Shadowing: This effect accounts for big obstacles that strongly attenuate the signal power. In outdoor urban environments it could represent buildings. Shadowing is usually modeled as a random variable following a heavy-tail distribution.

- Small-scale fading: When radio waves face obstacles, part of their energy may go through the obstacle, but part of it may also be reflected. This effect is known as scattering. The receiver will then see multiple copies of the signal arriving at different times with different intensities. The resulting wave may increase its amplitude if the multiple copies arrive aligned on phase or may suffer a strong fading if the copies arrive with opposite phases. Consequently, the received power varies in a very large range: a signal sample can be a million times (60 dB) stronger or weaker than a sample taken an instant later, some meters further or in the adjacent frequency. This fact constitutes the main challenge for wireless communications, since a very low signal power cannot be distinguished from noise or from other signals, not even by means of the most sophisticated receiver. The adjective *fast* often used to describe the fading can be controversial, but a conventionally accepted definition proposes that if the signal power variations change faster than the duration of the transmitted symbols then the channel presents fast fading [3].

To counter these effects, multiple mechanisms have been used in the evolution of cellular networks. In the state of the art, the LTE standard is based on three main techniques described as follows.

- MIMO: Multiple antenna techniques have been used since the 70's at the receiving end [6] to take advantage of the multi-path nature of any wireless channel, by constructively combining the different copies of the received signal [7]. However, in the late 90's, seminal theoretic articles [8–11] demonstrated the huge benefits of using coding techniques combined with MIMO systems: not only a *diversity gain* could help healing the faded signal, but a *power gain* is obtained combining multiple copies of the same signal and the *multiplexing gain* allows the transmission of multiple streams on the same time-frequency resources generating a multiplication of the spectral efficiency. Furthermore, the way the multiple antennas are used compromises the multiplexing gain and the diversity gain as described by the fundamental diversity-multiplexing trade-off [12]. In cellular networks, diversity and multiplexing MIMO techniques are specified in LTE and LTE-A (LTE Advanced) [5].

- OFDM: Since fast fading creates frequency selective channels, the transmission bandwidth can be divided into narrow band sub-channels in which longer symbols are transmitted allowing the insertion of guard intervals that avoid inter-symbol interference. *Orthogonal Frequency Division Multiplexing* involves signal processing techniques guaranteeing the non-interference of the sub-carriers. This feature allows a more efficient use of the spectrum and facilitates the deployment of *Single Frequency Networks* (SFN). The downlink of LTE uses an OFDM waveform and OFDMA as the access technique, enhancing interference avoidance combining OFDMA with the scheduler.

- Link Adaptation and H-ARQ: The link adaptation consist on a loop mechanism where the receiver informs the transmitter of the estimated channel conditions. Based on this information, the transmitter will increase the symbol rate to take advantage of a good channel or reduce the rate to avoid information loss under severe propagation conditions. Additionally, *Hybrid-Automatic Repeat reQuest* (H-ARQ) combines coding with retransmission of data blocks that contain errors after the initial decoding attempt. In summary both techniques exploit the temporal selectivity of the wireless channel. A basic mechanism of link adaptation was used in EDGE. Later, more sophisticated schemes were introduced

for HSDPA and LTE using H-ARQ, where the modulation and coding schemes include high order modulations as 64-QAM together with a wide range of coding rates.

1.2 Interference in cellular networks

The combination of the above described techniques effectively counters the main propagation effects. Nevertheless, even if fast fading is no longer the main limiting factor for the radio access network, the cellular technology is prone to changes and improvements. Academia and industry continue to be actively involved on its evolution and the future cellular networks are expected to be different from the current ones. The main reason being, to mitigate *interference*.

1.2.1 Spectrum scarcity

From all frequencies on the radio-electric spectrum, some are preferred for broadcast communications services such television or radio broadcasting, air navigation systems or radio communications for police and other public services. All these services have been historically allocated a spectrum slice. Yet, with the arrival of cellular telephony a few chunks were still available. The appropriate spectrum for cellular services is scarce and henceforth expensive. The operators of cellular telephony pay large amounts of money to local authorities to rent a piece of spectrum. Additionally, the 2G, 3G and 4G signals have to use different channels and even if the new technologies could replace the 2G services, many users still own 2G terminals and cannot be disconnected. In general, all wireless technologies avoid interference using *orthogonal* time-frequency resource allocation, i.e. separating contiguous transmissions in time or frequency as a means to avoid interference. This technique although effective is inefficient given the spectrum scarcity. To increase the total network capacity or equivalently the area spectral efficiency (in bit/s/Hz/m^2) it is sometimes better to *treat* the interference than to *avoid* it.

1.2.2 Types of interference

An intrinsic feature of the cellular service is that its coverage spans large areas, typically countries of thousands or millions of square kilometers. It is therefore unfeasible to achieve this coverage with one single transmitter. In average, cellular networks have transmitters every kilometer or less depending on the density of users. Regarding path-loss, the closer the transmitter, the stronger the received signal and the better the cellular service. Every transmitter has a coverage area called the *cell*, but wireless signals do not stop when they reach the cell edge, they travel in space creating interference on the neighboring cells. Thus, if all transmitters in a cellular network emit signals at the same time on the same frequency band, interference becomes the principal bottleneck to increase the capacity of cellular networks. Many types of interference can be found on the literature but is worth attempting a rough classification of them, focused on cellular networks as follows:

- Inter-Symbol Interference (ISI): Denotes the interference of subsequent symbols that reach a receiver at the same time due to a multi-path channel where the delay of the different signal copies is larger than the symbol period. A short inter-site distance in SFN can also generate ISI. Most of the efforts to reduce ISI are handled by OFDM and other techniques. ISI is outside the focus of this research.

- Inter-User Interference (IUI): Multiple-antennas at the transmitter generate the so called spatial *degrees-of-freedom*: the possibility to spatially separate several signals being transmitted from the same point. However, a precise information of the spatial channel response is required at the transmitter, together with multiple and sufficiently separated antennas at the receiver. In absence of these ideal characteristics multi-user transmission systems (MU-MIMO) always imply IUI [13]. This type of interference occurs inside a given cell and the transmitter and receivers inside may to some extent control its impact. In single-user MIMO transmissions, multiple streams may also be considered as IUI.

- Inter-Cell Interference (ICI): Even in the ideal case where IUI is completely eliminated, in cellular networks the neighbor transmitter is probably applying the same techniques so

that its users do not interfere with each-other. The transmitted signals from neighbor cells cannot be controlled unless there exists a *cooperation* mechanism. However, network cooperation is limited to some neighbor cells and therefore, covering a large area with multiple transmitters operating in the same time-frequency resources always implies ICI.

1.2.3 Interference mitigation for area spectral efficiency

One of the main purposes of design of the future cellular networks is to increase the spectral efficiency. More precisely, to increase the area spectral efficiency; i.e. the amount of bits per second per Hertz per square meter that can be transmitted. This section briefly describes solutions that have been subject of academic research and industrial implementation at different levels.

Relays

The use of relays is generally instrumental for extending coverage with multi-hop communications. In places with difficult coverage, it is usually assumed that the transmitter cannot reach the receiver and hence, the relay sets a bridge in between. Several relay types have been investigated such as amplify-and-forward, decode-and-forward or compress-and-forward in both half-duplex and full-duplex relays [14]. The use of relays can also be considered a network cooperation technique or part of the so called heterogeneous networks.

Massive MIMO

Not feasible for mobiles terminals, the use of very large antenna arrays at the transmitter end to serve multiple users has proved to be effective countering fading and enhancing the spatial multiplexing capability of the transmitter [15]. The need for accurate channel state information implies that massive MIMO techniques should be based on time division duplexing (TDD). Although this technique makes promise of simpler and cost-effective implementations to increase the network capacity [16], pilot contamination sets a saturation on the gains and remains an active subject of research.

Small cells

In contrast to the traditional cellular approach, where relatively big areas were covered by one transmitter or base station, the next generation of cellular networks seeks to be based on a more heterogeneous topology, including many low power transmitters with limited coverage known popularly as small cells, e.g. micro, pico or femto cells. Although this approach generates more interference, there is a substantial increase in the spatial spectrum reuse. As the majority of wireless traffic is generated indoor [17], small cells allow users to be closer to a network node, considerably reducing the path-loss. Heterogeneous networks are called to be designed with self-organizing capabilities and help off-loading the macro-cellular traffic and reducing the infrastructure costs to the operators [18].

Network Cooperation

Network cooperation may be seen as an attempt to transform several independent base stations into one single base station with multiple antennas distributed along the coverage area. There are many levels at which cooperation can be realized: from exchanging some information for soft-handover implementation to exchanging channel state information and the transmitted data to obtain multiplexing and diversity gains. A higher degree of cooperation implies larger gains at the expense of complexity and high capacity backhaul links. Network cooperation can be classified as *Interference coordination* schemes for those exchanging only channel state information and *full cooperation* schemes for those implying additionally the exchange of the transmitted data [14]. However, even under ideal system conditions, network cooperation gains are limited to some extent [19] and its optimization is an active field of research.

Among the many different network cooperation schemes cited in the literature, we differentiate four techniques that have been intensively studied in the recent years.

- Interference Alignment: Making use of the spatial degrees of freedom available at MIMO channels, Interference Alignment [20] has proved to be optimal in terms of the degrees of freedom, allowing a multi-user-multi-cell network operating at high signal-to-noise-ratio (SNR), to provide half of the capacity that could be achieved in complete absence

of interference. Stringent feedback requirements apply for interference alignment that remains to the date, more a theoretical benchmark than a practical scheme.

- Coordinated scheduling (CS): At a more practical level, coordinated scheduling has been subject to research and implementation for scheduling optimization in LTE networks, taking advantage of frequency selectivity and OFDMA in the downlink resource allocation. Using a centralized scheduler, several base stations may avoid interfering with each other. This techniques is known as resource orthogonalization but is a spectral-inefficient transmission strategy [2]. More sophisticated CS schemes can be seen for instance in [21].

- Coordinated Beamforming (CBF): If the channel state information of different users is exchanged, their serving BSs can align their beam-forming precoders to null the interference towards neighbor users [22]. Different from interference alignment, CBF can work on MISO transmissions and comes at the price of losing some diversity gain to obtain a larger multiplexing gain serving multiple users on the same time-frequency resources.

- Joint Transmission (JT): The real concept of network MIMO also known as joint transmission is implemented if CSI and data are exchanged between the cooperative BSs [23]. Each of them should find the right precoder to simultaneously transmit the same signal from multiple points to serve the intended user(s). With this technique both diversity and multiplexing gains can be achieved. Additionally, the interference is notably reduced as the closest BSs will be emitting desired signals.

1.3 Introduction to Coordinated Multi-Point Transmission

BS cooperative communication is used to harness multi-cell interference, allowing for aggressive frequency reuse that results in significant sum rate gains. The main goal is to provide mobile users with homogeneous quality of service (QoS) over the whole coverage area, despite the physical constraints of low received power and high interference at cell edges. Roughly speaking, the more BSs cooperate, the less interference is generated, resulting in enhanced

throughput gains at the expense of sharing data and control information among the involved cells.

1.3.1 Transmission techniques

CoMP can be in general classified into many different categories [14, 24]. Different techniques named for example Distributed Antenna Systems (DAS) fall into the scope of CoMP and are prone to be applied on heterogeneous networks [25]. For the purpose of this thesis and fixing the scope on the downlink we distinguish two families of CoMP techniques.

Coordination

It is generally named BS coordination when several BS exchange CSI or scheduling information to decide the transmission strategy in a distributed or centralized approach.

- In OFDMA systems such LTE, Coordinated Scheduling (CS) takes place when a central processor receives CSI from different BSs and performs the resource allocation to avoid interference between the active users in a cluster. Although this strategy is not efficient in terms of spectrum, it is specially desirable to exploit the time-frequency selectivity of fading channels. CS does not require the use of multiple antennas and its backhaul and latency requirements are relatively low. CS is not investigated in this thesis.

- Coordinated Beam-forming (CBF) aims at using multiple antennas from several BSs to provide multiplexing gain, i.e. serving multiple users on the same resource. Using beam-forming techniques to null the IUI, some or full spatial diversity gain is given up. The concept of CBF appeared in the 90's as a power control maximization problem (see for instance [26]). The problem was later solved for individual SINR constraints [27], and several algorithms were proposed to find the optimal precoders efficiently [28]. Zero-Forcing Beam-forming (ZFBF) is known to be a good equilibrium between performance and complexity [29]. Hence, its use in multi-cell cooperation has been widely accepted. See for instance [30].

Full cooperation

In this case, the data being transmitted and the CSI from all users is shared among the cooperative BSs, requiring the use of significant resources in the uplink and the backhaul. Furthermore, stringent delay and quantization resolution conditions must be fulfilled.

- Transmit Point Selection (TPS) may be seeing as a special form of macro diversity transmission, where the best beam-forming from the multiple BSs is selected to serve one user at each time interval. Since there are no multiple signals being transmitted at the same time, there are less synchronization requirements and consequently, there is no multiplexing or diversity gains. TPS is not in the scope of this research.

- The most profit of full cooperation is taken by means of Joint Transmission (JT). Several users can be served from multiple BSs on the same time-frequency resources without interfering with each other. This technique implements the real network MIMO concept, adding a per BS power constraint to the broadcast channel formed in the downlink of a single-cell multi-user MIMO system [23]. Different levels of cooperation and backhaul capacity demand an adaptive policy that switches among different transmission techniques as shown in [31]. On ideal conditions with full synchronization, absence of delay and perfect CSI, JT may provide both diversity and multiplexing gains. In particular, if only one user is served the scheme is called single-user JT (SU-JT) with no multiplexing gain. Otherwise is called multi-user JT (MU-JT).

1.3.2 Performance Metrics

Multi-antenna transmission schemes are usually measured in terms of two performance metrics. The ***diversity order*** is used to evaluate the reliability of a communication link, which is related to the outage probability and ultimately to the quality of service provided. Graphically, in a log-log scale plot, the diversity order is the slope of the outage probability vs. the SNR curve for a fixed rate. Yet, in actual systems link adaptation continuously changes the rate, hence, a

more general definition is [12]

$$d = -\lim_{\mathrm{SNR}\to\infty} \frac{\log(\mathbb{P}_{out}(\mathrm{SNR}, \hat{R}))}{\log(\mathrm{SNR})} \tag{1.1}$$

where $\hat{R} = f(\mathrm{SNR})$ depends on the MCS and the link adaptation policy. The diversity order is directly related to a ***power gain***. For example, assume a single BS with N_t antennas transmits with $\mathrm{SNR} = p$ to a single-antenna user. If the transmitter has perfect CSI, the average signal value is $N_t p$, the power gain is N_t and a diversity order $d \leq N_t$ where the equality is obtained if Shannon codes are used with instantaneous link adaptation.

Additionally, the ***multiplexing gain*** is a measure of the system capacity. Using the same rate function as in (1.1), the multiplexing gain is defined as

$$r = \lim_{\mathrm{SNR}\to\infty} \frac{\hat{R}}{\log(\mathrm{SNR})} \tag{1.2}$$

Graphically, the multiplexing gain is the slope of the rate vs SNR curve setting the horizontal axis in a logarithmic scale.

Finally, in cellular networks and specially in multi-cellular cooperative transmissions, the ***coverage*** is determined by the outage probability. A comparison of different transmission schemes is presented in table 1.1.

Remark: The use of the spatial *degrees of freedom* generated with multiple antennas allows a system to trade-off multiplexing gain and diversity order [12]. Beamforming techniques such ZF used here for JT and CBF, exploit the degrees of freedom to null the interference creating parallel channels that generate multiplexing gain. In modern cellular systems, diversity is generally obtained with time-frequency selectivity using OFDMA and H-ARQ [6].

Figure 1.1 shows the capacity of different transmission schemes for both single-cell and cooperative multi-cell layout with equal diversity order. Single cell schemes have dot markers and multi-cell schemes have circle markers. In both cases the total system $\mathrm{SNR} = P$. In the case of perfect-CSI, a MISO channel with N_t users and transmit antennas is used. In the case of no-CSI, the diversity order is ensured with a MIMO channel with $N_t = N_r$ antennas. The gaps observed between perfect-CSI and the corresponding no-CSI curve can be closed by means of

Scheme	N_t	N_r	CSIT	Power G.	Multiplexing G.	Coverage
Single-Cell TDMA	1	1	no	1	1	1 Cell
Single-Cell ZF	N	1	perfect	$1/N$	N	1 Cell
Single-Cell DPC	N	1	perfect	1	N	1 Cell
Multi-Cell TDMA	1	1	no	1	1	M Cells
Multi-Cell CBF	N	N	no	$1/(MN_t)$	0	M Cells
Multi-Cell MU-JT	N	N	no	$1/N_t$	0	M Cells
Multi-Cell CBF	N	1	perfect	$1/(MN_t)$	N_t	M Cells
Multi-Cell MU-JT	N	1	perfect	$1/N_t$	N_t	M Cells
Multi-Cell DPC	N	1	perfect	1	N_t	M Cells

Table 1.1: Transmission schemes comparison. M BSs, $N = N_t = N_r$ antennas.

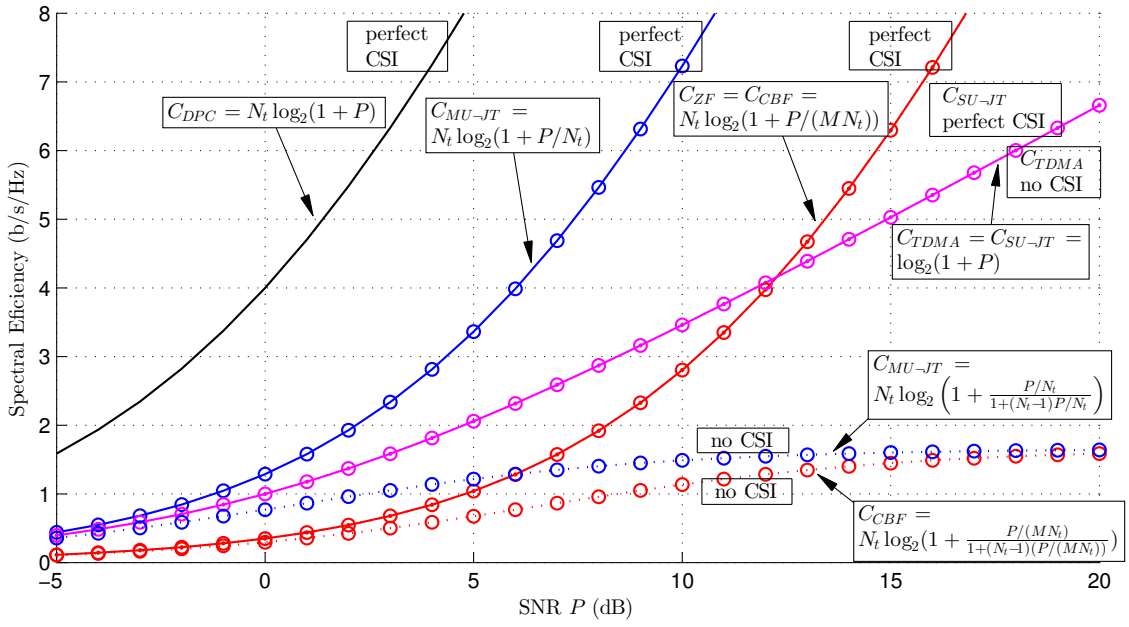

Figure 1.1: Achievable rates for single-cell and multi-cell MISO and MIMO channels. $N_t = N_r = M = 4$. Both single-cells and multi-cell schemes use a total system $\mathrm{SNR} = P$ constraint.

effective feedback mechanisms which should be designed to improve the TDMA performance ($d = 1, r = 1$), where no cooperation no multiple antennas and no spatial CSI is needed.

1.3.3 Limited Feedback

The significant performance gains promised by CoMP techniques come at the expense of CSI and heavily depend on the feedback quality. Although in time division duplexing (TDD), CSI can be obtained by channel reciprocity, in frequency division duplexing (FDD) cellular systems, channel reciprocity cannot be exploited and explicit feedback has to be acquired through a finite rate reverse channel, which is subject to delay, channel estimation errors, and quantization error. In real systems, multiple steps have to be performed with non-ideal systems to obtain the CSI, as follows.

1. Using pilot symbols, the receiver has to estimate both channel's magnitude and direction (phase) on the downlink. This estimation can be done with relative high precision and this error's impact is often ignored in the literature.

2. The channel direction has to be quantized with a finite number of bits, creating inevitably the quantization error. Both parts agree on a codebook, and the receiver sends back the index of the codebook element closest to the CSI. The codebook index is reported back to the BS through an uplink channel, which is not necessarily error and delay free.

3. In this thesis, only the impact of quantized and delayed CSI (QD-CSI) is considered; the important issues of synchronization, channel estimation, and link adaptation are beyond the scope.

Although systems relying on limited feedback or partial channel knowledge have been extensively studied in single-cell multi-antenna systems [13, 32–36], there is relatively less work on the effect of imperfect CSI in CoMP systems. Information theory basis for downlink CoMP with imperfect CSI are presented in [31]. The effect of reducing the backhaul capacity is showing in [37]. In [38], uplink CoMP systems under constrained backhaul and feedback are studied. In [39], the authors study the effect of the training frame length and derive the optimal number of cooperative BS in uplink CoMP systems. The effect of delayed CSI, ignoring the effect of channel quantization, is studied in [40], while the impact of quantized CSI is studied in [41].

The effect of QD-CSI in adaptive bit partitioning schemes is studied in [42]. An adaptive interference cancellation scheme is proposed in [43] and multi-mode transmission under incomplete CSI is proposed in [44].

1.4 Introduction to Successive Interference Cancellation

The multiple access channel (MAC) has been known in information theory for years [45]. It refers to the situation, where several sources communicate with the same destination in the same channel use. Since there are multiple individual links, the capacity of the MAC is not a single rate. It is a set of rates for each of the point-to-point channels that can be found on the MAC. This set of rates is called the *Capacity Region*. The capacity region of the MAC was fully characterized in [46] even for the particular case of the Gaussian MAC, which is of special interest in this work. From all the points that form the capacity region, some of them are known to have the maximum sum rate. The technique that achieves these maximum sum rate points is known as Successive Interference Cancellation.

1.4.1 Multiple Access Channel

The information-theoretic bound on the maximum possible achievable rate for each user on a MAC. The union of all possible sets of maximum rates forms the capacity region. In its most simple instance, a MAC is formed by two transmitters and one receiver. Its capacity region is determined by three constrains: *i)* Tx_1 cannot exceed its point-to-point Shannon capacity. *ii)* The same individual condition for Tx_2. *iii)* The sum of both rates cannot exceed the Shannon capacity of a link where both transmit powers (SNRs) are added. (A formal justification can be found in [2], Appendix B.9). These three constraints are written as follows

$$\begin{aligned} R_1 &\leq \log_2(1+\mathrm{SNR}_1) \\ R_2 &\leq \log_2(1+\mathrm{SNR}_2) \\ R_1+R_2 &\leq \log_2(1+\mathrm{SNR}_1+\mathrm{SNR}_2) \end{aligned}$$

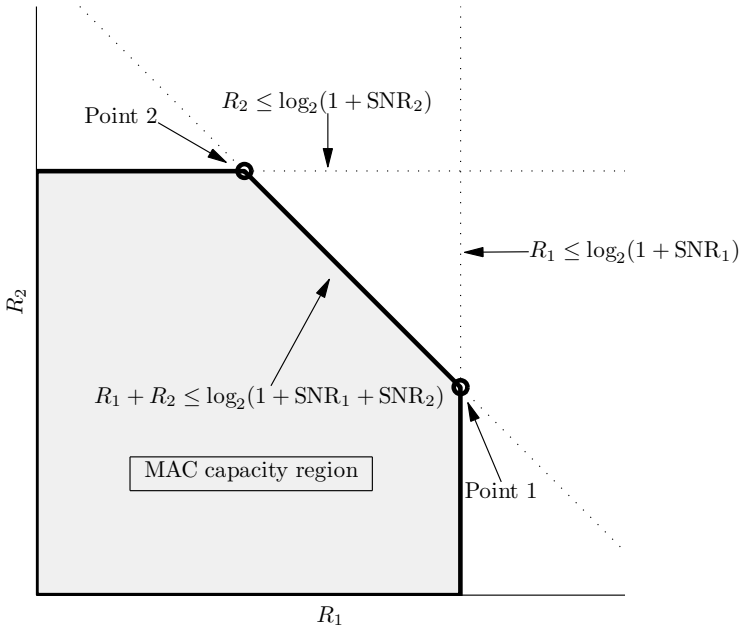

Figure 1.2: Capacity region of the 2-Tx MAC.

Figure 1.2 shows the capacity region of a 2-Tx MAC. Note that all points in the diagonal line achieve the (same) maximum sum rate possible. In particular, the corner points in the capacity region, imply that one of the links achieves the point-to-point capacity while simultaneously the other link can still convey some information at a non-zero rate, limited by the interference generated. But how can one of the signals be decoded free of interference? The technique that achieves this corner points is known as Successive Interference Cancellation (SIC) [47]. The receiver should decode both signals. If the signal from Tx_1 is decoded first, it should be suppressed from the remaining signal so that the signal from Tx_2 can be decoded free of interference (see point 2 in Figure 1.2). Decoding the signal from Tx_2 first, leads the system to operate in the other corner point (see point 1 in Figure 1.2).

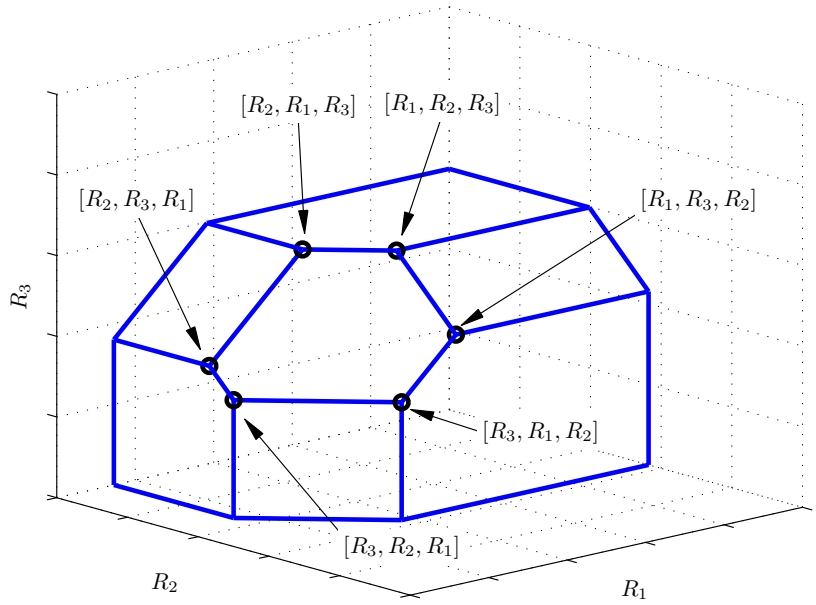

Figure 1.3: Capacity region of the 3-Tx MAC with all possible SIC decoding orders.

1.4.2 Successive Interference Cancellation

The MAC capacity region can be generalized to the case where N sources communicate with the same destination. The capacity region of a MAC has $2^N - 1$ constrains that intersect in $N!$ corner points of maximum sum rate, each one representing a different decoding order. The general form a capacity region is

$$\sum_{i \in \mathcal{S}} R_i < \log_2 \left(1 + \sum_{i \in \mathcal{S}} \mathrm{SNR}_i \right), \tag{1.3}$$

where $\mathcal{S}$ is any non-empty subset of the set of all users $[1 \ldots N]$. Figure 1.3 shows the capacity region of a MAC formed by 3 users, pointing out the $3! = 6$ possible decoding orders obtained with SIC.

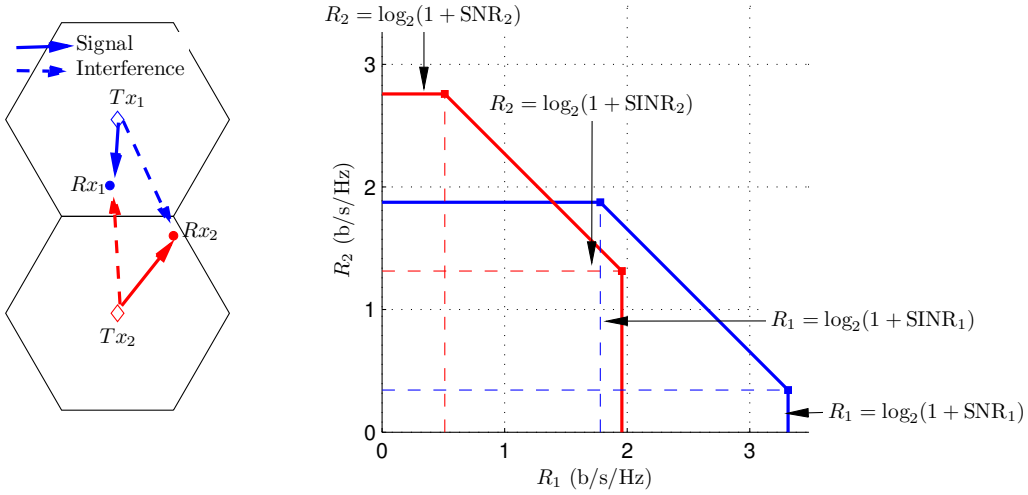

Figure 1.4: The IC formed in the downlink of two cells is decomposed in two related MACs.

1.4.3 The Interference Channel

If multiple transmitters want to communicate exclusively with a different receiver, the situation is known as the Interference Channel (IC). The capacity region for the interference channel has been for years an open problem and is known only for some special cases (cf. [48–50]). The downlink of cellular networks is an instance of the IC. For the purpose of this thesis, we point out that the IC can be decomposed in two related MACs as shown in Figure 1.4

The details and deductions obtained from this decomposition are carefully described in Chapter 4.

Part II

Coordinated Multi-Point Transmission

Chapter 2

Coordinated Multi-point transmission with limited feedback and other-cell interference

Pushed by the exponential traffic growth and the rapidly increasing demand for multimedia applications, wireless networks are compelled to evolve in order to meet the extraordinary performance requirements of future broadband networks in terms of spectral efficiency and coverage. Fundamental results from information theory [23, 51, 52] advocate for network cooperation as a promising concept, which in the cellular context could help increase multi-cell spectral efficiency and improve the coverage performance of cell-edge users. Over the last years, different network cooperation schemes in the uplink and downlink have been extensively researched [31, 53, 54] to the point that cooperation has transited from a theoretical concept to many practical techniques [24, 55, 56]. In 3GPP standardization activities, BS cooperation is referred to as coordinated multi-point transmission (CoMP) and is included in 4G wireless standards, such as LTE-Advanced.

The scope in this chapter is in downlink CoMP systems with quantized channel direction and feedback delay. A general theoretical framework is proposed in section 2.2, allowing to derive closed-form expressions and accurate approximations for the average achievable rates of

CoMP systems with QD-CSI. The analysis is based on tools from [34] and characterizes the interplay between delay and number of feedback bits. The impact of QD-CSI on the average sum rate performance of JT and CBF systems is analyzed in section 2.3. In section 2.4, a multi-mode transmission (MMT) scheme is presented, enabling to identify the optimal operating regions of each CoMP scheme depending on the average SNR, the number of feedback bits, the number of antennas and users served, and delay. This scheme adaptively switches among transmission modes in order to maximize the sum rate. Furthermore, for analytical tractability, a moment matching technique is used to approximate the interference distribution and the weighted sums of chi-squared random variables by Gamma distributions. These approximations are validated through system level simulations, evaluating different cases of pathloss asymmetry and the effect of OCI. In section 2.5 a complete review of the outage performance is obtained based on derived closed-form expressions for the outage probability of QD-CSI CoMP systems. Numerical results in section 2.6 provide design guidelines under which conditions and system operating parameters, cellular users would experience higher throughput using CoMP as compared to non-cooperative transmission techniques.

2.1 System Model and Preliminaries

Consider a network of hexagonal cells, in which a cluster of M coordinated BSs, each located at the center of its cell, is surrounded by a ring of M_{OCI} non-cooperative cells generating OCI. The total number of BSs in the system is $M + M_{\mathrm{OCI}}$. Each BS has N_t transmit antennas to serve $1 \leq U \leq N_t$ single-antenna receivers over the same time and frequency resources. Users are placed at different fixed positions anywhere in the cells and distance-dependent attenuation is considered. User selection is not considered here and the effect of shadowing is left for future work. Figure 2.1 illustrates an example of the network model, in which around $M = 2$ and 3 coordinating cells, the external ring of interfering cells has $M_{\mathrm{OCI}} = 8$ and 9 BSs, respectively.

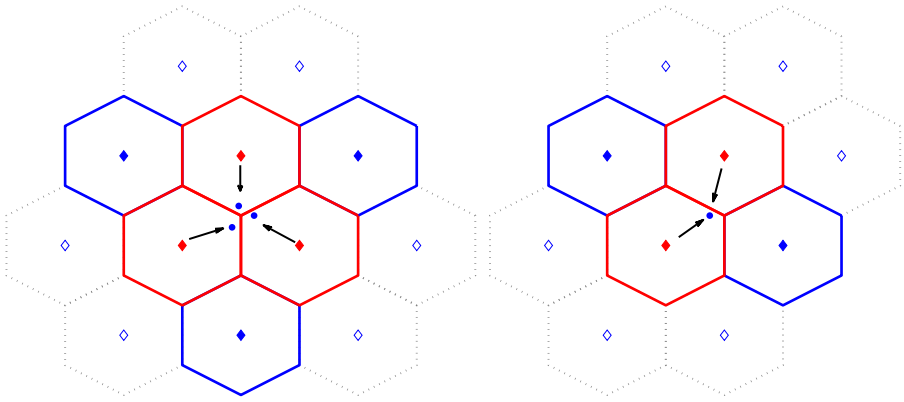

Figure 2.1: Network layout with $M = M_{\text{OCI}} = 3$ (left) and SU-JT with $M = M_{\text{OCI}} = 2$ (right).

2.1.1 Transmission modes

Two main cooperative schemes are investigated here: joint transmission and coordinated beamforming. In JT, the coordinated BSs exchange and share both data and control channel information (CSI) and under perfect CSI, it can provide multiplexing gain up to N_t and power gain of the order of $M(N_t - U + 1)$. In CBF, only control channel information (CSI) is shared among BSs to mitigate the interference inside the cooperative cluster. In theory, a spatial multiplexing gain of at most M can be achieved and the power gain is reduced (with respect to JT) to $N_t - M + 1$.

For exposition convenience, both schemes are presented below in the absence of OCI, i.e. $M_{\text{OCI}} = 0$.

- *Joint Transmission Mode (JT)*: In this transmit mode, the same $1 \leq U \leq N_t$ users are served from each BS.

  The received signal for the j-th user at time instant n is given by

$$y_j[n] = \sum_{i=1}^{M} \sum_{u=1}^{U} \sqrt{\theta_{u,i}} \mathbf{h}_{j,i}^{\text{H}}[n] \mathbf{w}_{u,i}[n] s_{u,i}[n] + z[n], \tag{2.1}$$

where $\mathbf{h}_{j,i} \in \mathbb{C}^{N_t \times 1}$ is the channel vector from the i-th BS to the j-th user, $\mathbf{w}_{u,i} \in \mathbb{C}^{N_t \times 1}$ is the precoding vector employed by the i-th BS to transmit to the u-th user, and $s_{u,i}$ is the transmitted signal with power constraint $\mathbb{E}\left[\sum_{i=1}^{M} |s_i|^2\right] = P$. Equal power allocation is assumed among all BSs and each channel vector consists of i.i.d. complex Gaussian elements $\sim \mathcal{CN}(0,1)$ (Rayleigh fading). The distance-dependent path-loss attenuation from the i-th BS to u-th user is denoted by $\theta_{u,i} = d_{u,i}^{-\alpha}$, with $d_{u,i}$ being the distance between the i-th BS and the u-th user and α is the path-loss exponent. The additive white Gaussian noise (AWGN) is $z[n] \sim \mathcal{CN}(0,1)$.

When only one user is served by all BSs ($U = 1$), the scheme is reffered as single-user joint transmission (SU-JT) and $\mathbf{w}_{u,i} \in \mathbb{C}^{Nt \times 1}$ is the eigen-beamforming vector used by the i-th BS for user u, i.e. $\mathbf{w}_{u,i} = \mathbf{h}_{u,i}$. For $U > 1$, the scheme is called multiuser joint transmission (MU-JT) and $\mathbf{w}_{u,i}$ is the zero-forcing precoding vector.

- *Coordinated Beamforming (CBF)*: In this mode, BSs serve different users exploiting knowledge of the control channel information from neighboring cells. Each BS uses the shared CSI to serve its own user nulling the interference caused to users from neighboring cells. The received signal at the u-th user served by the u-th BS at instant n is given by

$$y_u[n] = \sqrt{\theta_{u,u}}\mathbf{h}_{u,u}^{\mathrm{H}}[n]\mathbf{w}_u[n]s_u[n] + \sum_{\substack{i=1 \\ i \neq u}}^{M} \sqrt{\theta_{u,i}}\mathbf{h}_{u,i}^{\mathrm{H}}[n]\mathbf{w}_i[n]s_i[n] + z[n]. \tag{2.2}$$

For CBF, this thesis considers always $U = M$ and $\mathbf{w}_u$ is the u-th column of the zero-forcing beam-forming matrix (Moore-Penrose pseudoinverse).

2.1.2 Imperfect CSI

- *Delay CSI feedback:* The standard Gauss-Markov regular process is used to study the effect of CSI delay and to model the temporal variation of the channel state. A block fading model [57] is assumed, where $\mathbf{h}$ remains constant over each frame of length T channel uses, and evolves from frame to frame according to an ergodic stationary spatially white

jointly Gaussian process. Under the Gauss-Markov AR(1) model (i.e., auto regressive of order 1), the channel evolves in time as

$$\mathbf{h}[n] = \rho \mathbf{h}[n-1] + \mathbf{e}[n], \tag{2.3}$$

where ρ is the correlation coefficient ($0 < \rho < 1$), $\mathbf{h}[n]$ denotes the channel realization at time instant n and the error vector $\mathbf{e}[n] \in \mathbb{C}^{N_t \times 1}$ is complex Gaussian with zero mean and variance $\epsilon^2 = 1 - \rho^2$ (i.i.d. in time and independent of $\mathbf{h}[n-1]$). For the channel correlation coefficient, we use the Jakes-Clarke's model and set $\rho = J_0(2\pi f_d T_s)$, where $J_0(\cdot)$ is the zero-th order Bessel function of the first kind, f_d denotes the Doppler frequency shift and T_s the symbol time. Note that channel estimation or prediction errors can be also modeled using the above auto-regressive model, making these results more general.

- *Quantized CSI:* In FDD systems, each user reports back to its BS channel direction information (CDI) for the channels between the user and its serving and interfering BSs. This is done using a quantization codebook known at both sides. Each user employs a different codebook and the quantized channel is chosen from a codebook denoted by $\mathcal{C}_u = \{\mathbf{c}_{u,1}, \mathbf{c}_{u,2}, \ldots, \mathbf{c}_{u,L}\}$ and containing $L = 2^b$ unit norm vectors. The chosen quantization codevector is the one maximizing $|\bar{\mathbf{h}}_{u,i}^{\mathrm{H}} \mathbf{c}_{u,\ell_i}|$ and the index ℓ_i is fed back using b bits at BS i, where $\bar{\mathbf{h}}_{\mathbf{u,i}} = \frac{\mathbf{h}_{u,i}}{\|\mathbf{h}_{u,i}\|}$ is the CDI. This criterion is equivalent to minimizing the quantization error $\sin^2\phi = 1 - |\bar{\mathbf{h}}\hat{\mathbf{h}}^H|^2$ where $\hat{\mathbf{h}} = \mathbf{c}_{u,\ell_i}$ is the quantized channel direction. Since it provides a good compromise between analytical tractability and asymptotic optimality [33, 58], random vector quantization (RVQ) is used. The expected value of the cosine of the angle $\phi = \angle \bar{\mathbf{h}}\hat{\mathbf{h}}$, which is related to the quantization error, is given by [59]

$$\xi = \mathbb{E}_\phi \left[\cos^2 \phi\right] = 1 - 2^b \cdot \beta\left(2^b, \frac{N_t}{N_t - 1}\right), \tag{2.4}$$

where $\beta(\cdot,\cdot)$ is the Euler Beta function.

2.1.3 Preliminaries

Consider a heterogeneous scenario with unequal path-loss and Rayleigh fading, hence terms (signal, interference, or OCI) involving sums of χ^2 distributed random variables appear. Those

sums become weighted sums of χ^2 variates due to different distances between users and BSs. Notice that a chi-squared distribution is a special case of the Gamma distribution, such that if $aX \sim \chi^2(D)$, $aX = A$, then $A \sim Gamma(D, a)$, where D is the shape parameter and a is the scale parameter.

Exact Results

Let $A_i \sim Gamma(D_i, \theta_i)$ and $X = \sum_{i=1}^{M} A_i$. There are various closed-form solutions for the distribution of X [60,61]. The sums of Gamma random variables have scale parameters $D_i \in \mathbb{N}$ and different $\theta_i > 0$. In this case, the exact distribution for the sum of Gamma distributed r.v. is given by [62]

$$f_X(x) = K \sum_{i=1}^{M} P_i(x)\, e^{-\theta_i x}, \tag{2.5}$$

where

$$K = \prod_{i=1}^{M} \theta_i^{D_i}, \quad P_i(x) = \sum_{k=1}^{D_i} c_{i,k} x^{k-1},$$

$$c_{i,D_i} = \frac{1}{(D_i - 1)!} \prod_{\substack{j=1 \\ j \neq i}}^{M} \left(\frac{1}{\theta_j} - \frac{1}{\theta_i} \right)^{-D_j}, \; i = 1, \ldots, M, \tag{2.6}$$

and

$$c_{i,D_{i-k}} = \frac{1}{k} \sum_{j=1}^{k} \frac{(D_i - k + j - 1)!}{(D_i - k - 1)!} R(j, i, M)\, c_{i,D_i}, k = 1, \ldots, D_i - 1, i = 1, \ldots, M,$$

$$R(j, i, M) = \sum_{\substack{k=1 \\ k \neq i}}^{M} D_k \left(\frac{1}{\theta_i} - \frac{1}{\theta_k} \right)^{-j}, \; j = 1, \ldots, D_i - 1. \tag{2.7}$$

Approximate Results

One of the objectives of this work is to derive closed-form expressions for the achievable sum rate in CoMP systems, for which the pdf of the SINR distribution should be kept as simple as possible so that $\mathbb{E}[\log_2(1 + \mathrm{SINR})]$ can be reduced to an insightful expression. Using (2.5) in any of the SINR terms makes the expression for the achievable throughput intractable. For that, advantage is taken of the fact that the weighted sum of gamma distributions can be very well

approximated with another gamma distribution, and the precision of this approximation depends on the similarity of the scales of the different terms in the sum, i.e. the different distances from BSs to mobile users. The distribution of $X = \sum_{I=1}^{M} A_i$ with $A_i \sim Gamma(D_i, \theta_i)$ is approximated by a Gamma distribution by matching the first two moments (moment matching method). In other words, X is approximated by a Gamma distributed r.v. $\hat{X}$ such that the first and second moments of $\hat{X}$, $\hat{\mu}_X = \hat{D}_X \hat{\theta}_X$ and $\hat{\sigma}_X^2 = \hat{D}_X \hat{\theta}_X^2$, respectively, are equal to the sum of all first and second moments of every A_i respectively, i.e.

$$\hat{\mu}_X = \hat{D}_X \hat{\theta}_X = \sum_{i=1}^{M} D_i \theta_i, \quad \hat{\sigma}_X^2 = \hat{D}_X \hat{\theta}_X^2 = \sum_{i=1}^{M} D_i \theta_i^2.$$

Therefore, to find the scale and shape parameters for $\hat{X}$, one only needs to calculate

$$\hat{D}_X = f_D\left(\bar{D}, \bar{\theta}\right) = \frac{\left(\sum_{i=1}^{M} D_i \theta_i\right)^2}{\sum_{i=1}^{M} D_i \theta_i^2}, \quad \hat{\theta}_X = f_\theta\left(\bar{D}, \bar{\theta}\right) = \frac{\sum_{i=1}^{M} D_i \theta_i^2}{\sum_{i=1}^{M} D_i \theta_i}, \tag{2.8}$$

where $\bar{D} = [D_1 \dots D_M]$ and $\bar{\theta} = [\theta_1 \dots \theta_M]$. $(\hat{\cdot})$ is used to denote a second order approximation of a Gamma distributed r.v. and $f_D(\cdot,\cdot), f_\theta(\cdot,\cdot)$ are the functions to find the shape D (DoF in the equivalent χ^2 distribution) and scale θ parameters respectively. Consequently, the r.v. $\hat{X} \sim Gamma(\hat{D}_X, \hat{\theta}_X)$ is said to be a second order approximation of X using the moment matching method.

2.2 Average Achievable Rate Analysis

This section provides an analytic framework to calculate the average achievable rate for both JT and CBF CoMP transmissions. Considering the general case where the effect of quantization and delay on the CSI, the inherent unequal pathloss attenuations, and the impact of OCI are all included. First, we start by deriving the distribution of the SINR, which serves as a building block for calculating the average rate.

2.2.1 SINR Distribution in JT

The case of MU-JT is revised, deriving the distributions of the and interference signals as a means to calculate the SINR distribution.

Desired Signal

The desired signal for the u-th user at instant n is received from M BSs and takes on the form

$$S_{\mathrm{JT,u}} = \frac{P}{MU} \sum_{i=1}^{M} \theta_{u,i} \left| \mathbf{h}_{u,i}^{\mathrm{H}}[n] \mathbf{w}_{u,i}[n] \right|^2 . \tag{2.9}$$

Under the QD-CSI model used in this paper and described in Section II, the expression can be expanded and then simplified as shown in the following proposition.

Proposition 1. *In a JT system, the desired signal for the u-th user at instant n under quantized and delayed CSI is given by*

$$\begin{aligned} S_{\mathrm{JT,u}}^{(\mathrm{qd})} &= \overbrace{\frac{P\rho^2\xi}{MU}}^{\textit{Constant}} \sum_{i=1}^{M} \theta_{u,i} \overbrace{\|\mathbf{h}_{u,i}[n-1]\|^2 \left| \hat{\mathbf{h}}_{u,i}^{\mathrm{H}}[n-1] \mathbf{w}_{u,i}^{\mathrm{qd}}[n] \right|^2}^{\textit{Gamma r.v.}} \\ &\sim \frac{P\rho^2\xi\hat{\theta}}{MU} \hat{X} \sim \gamma_x \hat{X}, \end{aligned}$$

where all constant terms can be grouped in $\gamma_x = P\rho^2\xi\hat{\theta}/MU$ with $\hat{\theta} = f_\theta\left(N_t, [\theta_{u,1} \ldots \theta_{u,M}]\right)$, ξ is given in (2.4), and the r.v. is $\hat{X} \sim Gamma(\hat{D}, 1)$, with $\hat{D} = f_D\left(N_t, [\theta_{u,1} \ldots \theta_{u,M}]\right)$.

Proof. See Appendix A.0.2. □

Interference Term

Under quantized and delayed CSI and $U > 1$, interference is created in the downlink transmission within the cooperative cluster. The interference generated from M BSs is given by

$$I_{\mathrm{JT,u}}^{(\mathrm{qd})} = \frac{P}{MU} \sum_{i=1}^{M} \theta_{u,i} \sum_{j \neq u}^{U} \left| \mathbf{h}_{u,i}^{\mathrm{H}}[n] \, \mathbf{w}_{u,j}^{\mathrm{qd}}[n] \right|^2 . \tag{2.10}$$

Aiming to calculate the achievable rate, we simplify (2.10) in the following proposition.

Proposition 2. *In a JT system, the inter-cell interference term for the u-th user at instant n under quantized and delayed CSI is distributed as*

$$\begin{aligned} I_{\mathrm{JT,u}}^{(\mathrm{qd})} &\sim \frac{P}{MU}\sum_{i=1}^{M}\theta_{u,i}\left[\rho^2\delta Y_1+\epsilon^2 Y_2\right] \\ &\approx \gamma_{y1}\hat{Y}_1+\gamma_{y2}\hat{Y}_2, \end{aligned} \tag{2.11}$$

where $\gamma_{y1}=P\rho^2\delta\hat{\theta}/MU$, $\gamma_{y_2}=P\epsilon^2\hat{\theta}/MU$, $\hat{\theta}=f_\theta(U-1,[\theta_{u,1}\dots\theta_{u,M}])$, ρ and ϵ are given in (2.3), and $\delta=2^{-b/(N_t-1)}$. Both $\hat{Y}_1,\hat{Y}_2\sim Gamma(\hat{D},1)$ and $\hat{D}=f_D(U-1,[\theta_{u,1}\dots\theta_{u,M}])$.

Proof. See Appendix A.0.3. □

2.2.2 SINR Distribution in CBF

Considering now the case of CBF and the distribution of the desired signal and the interference term are derived accordingly.

Desired Signal

In CBF case, the desired signal arrives at the receiver from only one BS, thus eliminating the summation in (2.10) and having only one pathloss attenuation coefficient $\theta_{u,u}$ in front. In that case, similarly to Proposition 1, the desired signal is given by

$$\begin{aligned} S_{\mathrm{CBF,u}} &= \frac{P\rho^2\xi}{M}\theta_{u,u}\left\|\mathbf{h}_{u,u}[n-1]\right\|^2\left|\hat{\mathbf{h}}_{u,u}^{\mathrm{H}}[n-1]\mathbf{w}_{u,u}^{\mathrm{qd}}[n]\right|^2 \\ &\sim \gamma_x X, \end{aligned} \tag{2.12}$$

where $\gamma_x=P\rho^2\xi\theta_{u,u}/M$ and $X\sim Gamma(N_t-M+1,1)$.

Interference term

The interference in the CBF case is the summation of $M-1$ terms coming from $M-1$ BSs serving one user each. Hence, the result in 2.10 can be rewritten as

$$I_{\mathrm{CBF,u}}^{(\mathrm{qd})}=\frac{P}{MU}\sum_{\substack{i=1\\ i\neq u}}^{M}\theta_{u,i}\left|\mathbf{h}_{u,i}^{\mathrm{H}}[n]\,\mathbf{w}_{u,j}^{\mathrm{qd}}[n]\right|^2. \tag{2.13}$$

Following the same derivations as in the JT case (see Appendix A.0.3), the distribution of $I^{(\mathrm{qd})}_{\mathrm{CBF,u}}$ is given by

$$\begin{aligned} I^{(\mathrm{qd})}_{\mathrm{CBF,u}} &\sim \frac{P}{M}\sum_{\substack{i=1\\ i\neq u}}^{M}\theta_{u,i}\left[\rho^2\delta Y_1+\epsilon^2 Y_2\right] \\ &\approx \gamma_{y1}\hat{Y}_1+\gamma_{y_2}\hat{Y}_2, \end{aligned} \tag{2.14}$$

where now $\gamma_{y1}=P\rho^2\delta\hat{\theta}/M$, $\gamma_{y_2}=P\epsilon^2\hat{\theta}/M$, $\hat{\theta}=f_\theta(1,[\theta_{u,1}\ldots\theta_{u,i-1},\theta_{u,i+1}\ldots\theta_{u,M}])$. Both $\hat{Y}_1,\hat{Y}_2\sim Gamma(\hat{D},1)$ and $\hat{D}=f_D(1,[\theta_{u,1}\ldots\theta_{u,i-1},\theta_{u,i+1}\ldots\theta_{u,M}])$.

2.2.3 The effect of Other-Cell Interference

Considering M_{OCI} non-cooperative (interfering) cells and that each interfering BS transmits one single stream under the same power constraint per BS, the OCI term is given by the weighted sum of M_{OCI} gamma distributed random variables. Evidently, the pathloss attenuation is larger in the case of OCI than for the signals generated inside the cooperative cells, as the users to serve are expected to be near the cell edge. The OCI, which is considered to be the same for any transmission mode, is given by

$$\begin{aligned} \mathrm{OCI} &= \frac{P}{M}\sum_{i=1}^{M_{OCI}}\theta_{u,i}\left|\mathbf{h}_{u,i}\mathbf{w}_i\right|^2 \\ &\sim \gamma_{y_3}\hat{Y}_3, \end{aligned} \tag{2.15}$$

where $\gamma_{y_3}=P\hat{\theta}_{\mathrm{OCI}}/M$ and $\hat{Y}_3\sim Gamma(\hat{D},1)$. In this case, the gamma approximation can be used as

$$\hat{D}=f_D\left(1,[\theta_{u,\mathrm{OCI1}},\ldots,\theta_{u,\mathrm{M_{OCI}}}]\right),\text{ and }\hat{\theta}_{\mathrm{OCI}}=f_\theta(1,[\theta_{u,\mathrm{OCI1}},\ldots,\theta_{u,\mathrm{M_{OCI}}}]).$$

2.2.4 General Expressions for Average Achievable Rate

In this section, a general result is given for the average achievable rate for a general expression of SINR given as ratio of gamma distributions. This general SINR expression incorporates the

	γ_x	DoF of X D_X	γ_{y_1}	γ_{y_2}	DoF of Y_1 D_{Y_1}	DoF of Y_2 D_{Y_2}
CBF	$P\rho^2\xi\theta/M$	$N_t - U + 1$	$P\rho^2\delta\theta/M$	$P\epsilon^2\theta/M$	$U-1$	$U-1$
JT	$P\rho^2\xi\theta/MU$	$M(N_t - U + 1)$	$P\rho^2\delta\theta/MU$	$P\epsilon^2\theta/MU$	$M(U-1)$	$M(U-1)$

Table 2.1: Variables and values for CBF and JT

SINR of any of the aforementioned CoMP transmission schemes and takes on the form of

$$\mathrm{SINR}^{(\mathrm{qd})}_{\mathrm{CoMP,u}} = \frac{\gamma_x X}{1 + \gamma_{y_1} Y_1 + \gamma_{y_2} Y_2 + \gamma_{y_3} Y_3}, \tag{2.16}$$

where (qd) implies QD-CSI. This SINR expression takes a particular form for different CoMP schemes depending on the values of the parameters of the gamma distributed random variables, as given in table 2.1.

In both CBF and JT cases, $\gamma_{y_3} = P\theta_{OCI}/M$ and for the gamma distribution Y_3, $D_{Y_3} = M_{OCI}$. The values shown in Table 2.1 do not consider unequal pathloss. In the heterogeneous scenario with unequal path-loss, an approximate SINR expression is used where the parameters θ and D are replaced by the corresponding values obtained using the Gamma approximation as $\hat{\theta} = f_\theta(\bar{D}, \bar{\theta})$ and $\hat{D} = f_D(\bar{D}, \bar{\theta})$ according to (2.8).

Based on (2.16), a general expression for the average achievable per-user rate, which is valid for both CBF and JT is derived.

Theorem 1. *In JT and CBF systems with quantized and delayed CSI and OCI, the average achievable per-user rate is approximated by*

$$\begin{aligned} R^{(\mathrm{qd})}_{\mathrm{CoMP,u}} \;\approx\; & \log_2(e) \sum_{i=0}^{D_X-1} \sum_{j=1}^{3} \sum_{k=0}^{D_{Y_j}-1} \sum_{l=0}^{i} \frac{\kappa_k^{(j)} (l+k)!}{l!\,(i-l)!} \gamma_x^{l+k-i+1} \\ & \mathcal{I}\left(\frac{1}{\gamma_x}, \frac{\gamma_x}{\gamma_{y_j}}, i, l+k+1\right), \end{aligned} \tag{2.17}$$

where

$$\mathcal{I}(a,b,m,n) = \int_0^\infty \frac{x^m e^{-ax}}{(x+b)^n (x+1)}\,\mathrm{d}x. \tag{2.18}$$

Proof. See Appendix A.0.4. □

The achievable rate expression can be simplified in the high SNR regime (interference-limited region), in which $\mathrm{SINR}_{\mathrm{CoMP,u}}^{(\mathrm{qd})} \approx \gamma_x X/(\gamma_{y_1} Y_1 + \gamma_{y_2} Y_2 + \gamma_{y_3} Y_3)$.

Corollary 1. *In the high SNR regime, the average achievable per-user rate of JT and CBF systems with quantized and delayed CSI and OCI is approximated by*

$$R_{\mathrm{CoMP,u}}^{(\mathrm{qd,h-SNR})} \approx \log_2(e) \sum_{i=0}^{D_X-1} \sum_{j=1}^{3} \sum_{k=0}^{D_{Y_j}-1} \frac{\kappa_k^{(j)} (i+k)!}{i!} a^{k+1} \mathcal{I}_2\left(\frac{\gamma_x}{\gamma_{y_j}}, i, i+k+1\right), \quad (2.19)$$

where

$$\mathcal{I}_2(a,m,n) = \int_0^\infty \frac{x^m}{(x+a)^n (x+1)} \,\mathrm{d}x.$$

Proof. See Appendix A.0.5. □

2.2.5 Special Case: Single User JT

In this subsection, single-user JT systems is examined, i.e. JT mode where only one user is served, and provide simpler expressions for the average achievable rate. Since only one user is served, there is no interference coming from the cooperative cluster, and the SINR takes on the form $\gamma_x X/(1+\gamma_{y_3} Y_3)$.

Corollary 2. *In single-user JT systems with quantized and delayed CSI, the average achievable rate is approximated as*

$$R_{\mathrm{SUJT}}^{(\mathrm{qd})} \approx \log_2(e) \sum_{i=0}^{D_X-1} \sum_{j=0}^{i} \frac{(D_{Y_3}+j-1)! \gamma_x^{D_{Y_3}+j-i}}{j!\,(i-j)!\,(\gamma_{y_3}-1)! \gamma_{y_3}^{D_{Y_3}}} \times \mathcal{I}\left(\frac{1}{\gamma_x}, \frac{\gamma_x}{\gamma_{y_3}}, i, D_{Y_3}+j\right) \quad (2.20)$$

Proof. The result follows easily by applying the same derivations shown in Appendix A.0.4 and using the pdf of Y_3 in Appendix A.0.4 equation (A.5). □

Furthermore, the following simpler expression can be obtained in the high SNR regime.

Corollary 3. *In the high SNR regime, the average achievable rate in single-user JT systems with quantized and delayed CSI is approximately given by*

$$R_{\mathrm{SUJT}}^{(\mathrm{qd,h-SNR})} \approx \log_2(e) \sum_{i=0}^{D_X-1} \frac{(D_{Y_3}-1+i)!}{i!\,(\gamma_{y_3}-1)!} \left(\frac{\gamma_x}{\gamma_{y_3}}\right)^{D_{Y_3}} \times \mathcal{I}_2\left(\frac{\gamma_x}{\gamma_{y_3}}, i, D_{Y_3}+i\right). \quad (2.21)$$

Proof. The result follows easily from Corollary 2 and applying the same steps as in appendix A.0.5. □

In the absence of OCI, e.g. due to orthogonal frequency allocation among cells, the SINR is given by $\mathrm{SINR} = \gamma_x X$ and the achievable rate is given by [63]

$$R_{\mathrm{SUJT}}^{\mathrm{qd,noOCI}} \approx \log_2(e)\, e^{1/\gamma_x} \sum_{i=0}^{D_X-1} \frac{\Gamma(-i, 1/\gamma_x)}{\gamma_x^i}, \tag{2.22}$$

where $\Gamma(\alpha, x) = \int_x^\infty t^{\alpha-1} e^{-t}\, \mathrm{d}t$ is the lower incomplete gamma function.

2.3 Rate Degradation due to Quantization and Delay

In this section, the impact of quantization and delay on the average achievable rate in CoMP systems is investigated. It is also shown that if the feedback rate is scaled at the appropriate rate, a constant rate offset between the rate achievable with perfect CSI and that with QD-CSI can be maintained.

2.3.1 Quantization

First, the effect of delay is neglected and only quantized CSI is considered using RVQ. In that case, the per-user average rate loss is upper bounded as

$$\begin{aligned} \Delta R_u^{(\mathrm{q})} &= R_{\mathrm{CoMP},u} - R_{\mathrm{CoMP},u}^{(\mathrm{q})} = \mathbb{E}\left\{\log_2(1+\mathrm{SNR}_u)\right\} - \mathbb{E}\left\{\log_2(1+\mathrm{SINR}_{\mathrm{u}})\right\} \\ &\leq \log_2\left(1 + \frac{P\hat{\theta}(U-1)}{U} 2^{-\frac{b}{N_t-1}}\right), \end{aligned} \tag{2.23}$$

where for CBF, in the denominator of the above expression $U = M$ and for $U = 1$, $\Delta R_u^{(\mathrm{q})} = 0$. The following proposition gives a sufficient scaling of feedback bits to maintain a constant bounded rate offset.

Proposition 3. *To maintain a constant rate offset per-user of* $\log_2(\beta)$ *between CoMP with per-*

fect CSI and with quantized CSI, the number of feedback bits per user should scale as

$$b = (N_t - 1)\log_2\left(\frac{P\hat{\theta}(U-1)}{U}\right) - (N_t - 1)\log_2(\beta) \tag{2.24}$$

$$\approx (N_t - 1)P_{dB} + (N_t - 1)\log_2\left(\frac{\hat{\theta}(U-1)}{U}\right) - (N_t - 1)\log_2(\beta) \tag{2.25}$$

Proof. The result follows by setting the rate offset upper bound given in (2.23) equal to the maximum allowable gap of $\log_2 b$ and solving for b. The approximation comes from the fact that $\log_2 P \approx P_{dB}/3$. Note that the above result is in accordance with results in [33] for multi-user MISO broadcast channels with quantized CSI. □

2.3.2 Delay

The average rate offset is considered when only delayed CSI is taken into account. Similarly to the case of quantized CSI and (2.23), the following rate offset upper bound due to delayed CSI is given

$$\Delta R_u^{(\mathrm{d})} \leq \log_2\left(1 + \frac{P\hat{\theta}(U-1)}{U}\epsilon^2\right). \tag{2.26}$$

Since $\epsilon^2 = 1 - \rho^2$ is related to the Bessel function of the first kind, we notice that for realistic values, the product $2\pi f_d T_s < 1$ and so we can simplify the value of ϵ^2 with relative good precision as

$$\begin{aligned}
\epsilon^2 &= 1 - J_0^2(2\pi f_d T_s) = 1 - \left[\sum_{i=0}^{\infty} \frac{\left(\frac{-(2\pi f_d T_s)^2}{4}\right)^i}{(i!)^2}\right]^2 \\
&= 1 - \left[\sum_{i=0}^{1} \frac{-(\pi f_d T_s)^{2i}}{(i!)^2} - O((\pi f_d T_s)^4)\right]^2 \\
&\approx 1 - \left(1 - \frac{(\pi f_d T_s)^2}{4}\right)^2 \approx 2(\pi f_d T_s)^2.
\end{aligned} \tag{2.27}$$

In order to maintain a constant rate offset no larger than $\log_2(\beta)$, let

$$\log_2\left(1 + \frac{P\hat{\theta}(U-1)}{U}\epsilon^2\right) = \log_2(\beta). \tag{2.28}$$

Replacing (2.27) into (2.28) and solving for T_s, the following result is obtained

$$T_s = \frac{1}{\pi f_d}\sqrt{\frac{U\left(\beta-1\right)}{2P\hat{\theta}\left(U-1\right)}}. \tag{2.29}$$

This result shows a non-linear relation between the maximum delay on the feedback and the rate offset, as T_s should scale in the order of $P^{-1/2}$.

2.3.3 Quantization and Delay trade off

If the effect of both quantization and delay is taken into account, the average rate offset can be derived similarly to [13] as

$$\Delta R_u^{(\mathrm{qd})} \leq \log_2\left(1+\frac{P\hat{\theta}\left(U-1\right)}{U}\left[\rho^2\delta+\epsilon^2\right]\right), \tag{2.30}$$

where $\delta = 2^{-b/(N_t-1)}$.

In order to maintain a bounded rate offset no larger than $\log_2(\beta)$, the number of feedback bits per user and the delay spread should scale as

$$b = (N_t-1)\log_2\left(\frac{\rho^2(U-1)P\hat{\theta}}{U(\beta-1)-\epsilon^2 P\hat{\theta}(U-1)}\right) \tag{2.31}$$

$$T_s = \frac{1}{\pi f_d}\sqrt{\frac{U\left(\beta-1\right)}{2P\hat{\theta}\left(U-1\right)\left(1-\delta\right)}-\frac{\delta}{2(1-\delta)}}. \tag{2.32}$$

The tradeoff between delay and feedback resolution is shown in Figure 2.2 for $\epsilon^2 \approx \delta \approx 0.2$, $T_s = 5$ ms, and $b = 7$ bits. In this setting, a rate loss of 1 bps/Hz can be seen by either reducing by 2 bits the feedback resolution or increasing the delay by 4 ms.

2.4 Adaptive Multi-mode Transmission

In the previous average achievable rate analysis, it was shown that under imperfect CSI, there is a tradeoff between different CoMP transmission modes, i.e. CBF, SU-JT, and MU-JT, and the natural question that arises is which CoMP modes is optimal to use in each case. A crisp theoretical answer to this question seems to be hard to give as the optimal CoMP scheme depends on

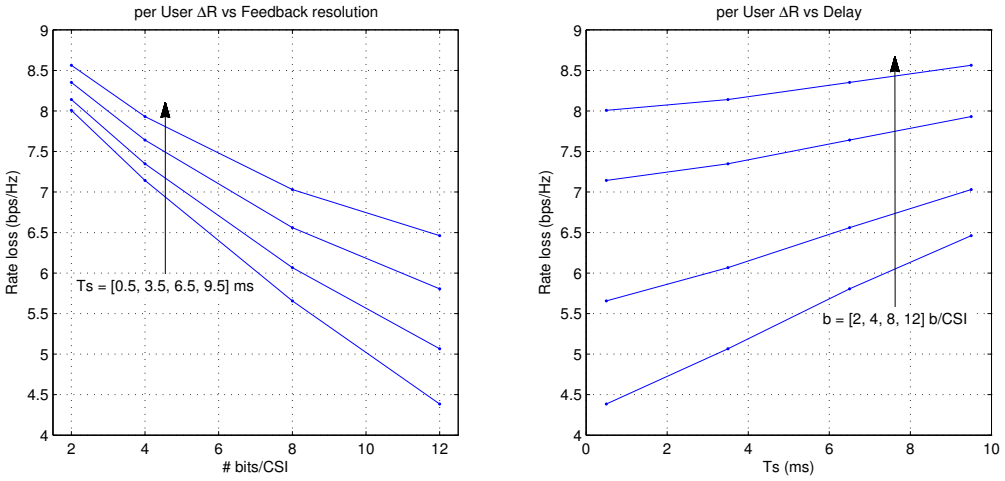

Figure 2.2: Average per user rate offset for CBF with perfect and QD-CSI in the high SNR regime (i.e. $\mathrm{SNR} = 30$ dB) for $M = 2$, $N_t = 4$, $v = 5$ km/h, and $f_c = 2.1$ GHz.

many parameters, namely path-loss, SNR operating regime, feedback resolution, delay, number of users, BSs, and antennas. For that, a set of simple rules is provided, based on the closed-form expressions and an adaptive multi-mode transmission scheme is proposed. In this policy, the achievable sum rate can be maximized by adaptively switching among different transmission modes (SU-JT, MU-JT, and CBF) as a means to balance between power gain and spatial multiplexing gain. Under MMT, the active transmission mode m^* is selected as

$$m^* = \arg\max_{m} R(m) \tag{2.33}$$

where

$$R(m) = \begin{cases} \sum_{u=1}^{M} R_{\mathrm{CBF}}^{(\mathrm{qd})} & : m = 0 \\ \sum_{u=1}^{U} R_{\mathrm{JT,u}}^{(\mathrm{qd})} & : m = U \end{cases}$$

To build further intuition, an approximate framework in order to analytically find the switching points for the proposed MMT scheme is presented. For that, expressions for the difference between the rates of different CoMP modes along all SNR regimes were found. Following

previous notation, the rate difference is in general defined as

$$\Delta R := R - R' = U\mathbb{E}\left\{\log_2\left(1+\frac{aX}{1+\sum_i b_i Y_i}\right)\right\} - U'\mathbb{E}\left\{\log_2\left(1+\frac{a'X'}{1+\sum_i b'_i Y'_i}\right)\right\}. \tag{2.34}$$

Proposition 4. *In the low to moderate SNR regime, the rate difference between two CoMP transmission modes without OCI is approximated by*

$$\Delta R^{(\text{mod.SNR})} \approx \log_2\left(\frac{\left(ae^{U\psi(D_X)}\right)}{\left(a'e^{U'\psi(D_{X'})}\right)}\right), \tag{2.35}$$

where $\psi(\cdot)$ is the digamma function.

Proof. See Appendix A.0.6. □

Proposition 5. *In the high SNR regime, the rate difference between two CoMP transmission modes without OCI is approximated by*

$$\Delta R^{(\text{high SNR})} \approx \log_2\left(\frac{\left[\eta e^{\psi(D_X)-\psi(D_Y)}\right]^U}{\left[\eta' e^{\psi(D_{X'})-\psi(D_{Y'})}\right]^{U'}}\right), \tag{2.36}$$

where η is defined in Appendix A.0.7.

Proof. See Appendix A.0.7. □

Tighter approximations can be obtained by defining the following rate differences

$$\Delta R_1 := R^{(\text{qd})}_{\text{SUJT}} - R^{(\text{qd})}_{\text{MUJT}} \tag{2.37}$$

$$\Delta R_2 := R^{(\text{qd})}_{\text{SUJT}} - R^{(\text{qd})}_{\text{CBF}}. \tag{2.38}$$

Using these rate differences and based on Propositions 4 and 5 the following corollaries are obtained as indicated in [63].

Corollary 4. *In the low to moderate SNR regime, the rate difference between SU mode and MU mode in JT and CBF transmission is approximated by*

$$\Delta R_1 = \Delta R_2 \approx \log_2\left(\frac{1+aD_X}{\left(a'e^{\psi(D_{X'})}\right)^{U'}}\right). \tag{2.39}$$

Proof. The proof follows easily along with the elements of Appendix A.0.6 replacing $R(1) = R_{\mathrm{JT},1}^{(qd)}$ and $R'(U) = \sum_u^U R_{\mathrm{JT,u}}^{(qd)}$ for ΔR_1 and $R'(0) = R_{\mathrm{CBF}}^{(qd)}$ for ΔR_2. □

Corollary 5. *In the high SNR regime, the rate gap between between SU mode and MU mode in JT and CBF transmission is*

$$\Delta R_1 = \Delta R_2 \approx \log_2 \left(\frac{aD_X}{\left[\eta' e^{(\psi(D_{X'}) - \psi(D_{Y'}))}\right]^{U'}} \right). \tag{2.40}$$

Proof. The proof is based on Appendix A.0.7, replacing $R(1) = R_{\mathrm{JT},1}^{(qd)}$ and $R'(U) = \sum_u^U R_{\mathrm{JT,u}}^{(qd)}$ for ΔR_1 and $R'(0) = R_{\mathrm{CBF}}^{(qd)}$ for ΔR_2. □

In the presence of OCI, the above approximations become looser, the reason being the inclusion of additional gamma distributions with different scale and shape parameters. In Figure 2.3, the rate differences obtained with the analytic framework derived in section 2.2.4 are shown on the upper graph. In the bottom, the approximations for ΔR indicate a minor shift of the order of $2 - 3$ dB for both high and moderate SNR regimes.

2.5 Success Probability Analysis

As shown in the previous sections, the SINR for the main CoMP transmission modes, can be written as the ratio of gamma functions (2.16). This result gives the possibility of deriving the success probability for each case, analyzing how the different modes and the analytic approximations impact the performance. The success probability is defined as the probability that the received SINR at the u-th user, is greater than a predefined threshold β; or equivalently, the probability that the user is not in outage, i.e.:

$$\begin{aligned} \mathbb{P}_{\mathrm{succ}}^{(u)} &= 1 - \mathbb{P}_{\mathrm{out}}^{(u)} \\ &= 1 - \mathbb{P}\left\{\mathrm{SINR}_u \leq \beta\right\} \\ &= 1 - F_{\mathrm{SINR}_u}(\beta), \end{aligned} \tag{2.41}$$

where F_{SINR_u} is the CDF of the random variable SINR_u.

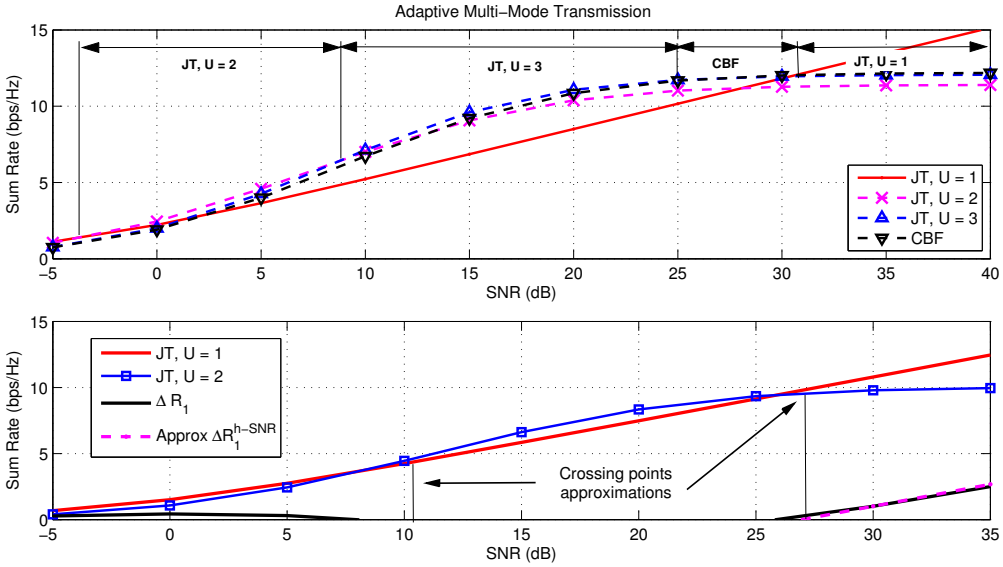

Figure 2.3: Top: Adaptive Multi-mode Transmission for CoMP. $M = 3$, $N_t = 4$ and $b = 4$. Bottom: ΔR approximations and crossing points. $M = 3$, $N_t = 2$ and $b = 6$. Both graphs use $v = 5$ km/h, $T_s = 1$ ms, and $f_c = 2.1$ GHz.

2.5.1 Single User Joint Transmission

Starting from the simplest case, the SINR for a single user served on JT by M stations is $\text{SINR} = \gamma_x \sum_{i=1}^{M} X_i$, where $X_i \sim Gamma(N_t, \theta_i)$. Accordingly, the expression for the CDF of the sum of multiple Gamma distributed r.v. is used in order to write the success probability as

$$\begin{aligned} \mathbb{P}_{\text{succ}}^{(u)} &= 1 - F_{\text{SINR}_u}(\beta) \\ &= K \sum_{i=1}^{M} P_i^*(\beta) e^{-\beta/\theta_i}, \end{aligned} \tag{2.42}$$

where

$$K=\prod_{i=1}^{M}1/\theta_i^{D_i},\quad P_i^*\left(x\right)=\sum_{k=1}^{D_i}c_{i,k}(k-1)!\sum_{j=0}^{k-1}\frac{\theta_i^{k-j}x^j}{j!},$$
$$c_{i,D_i}=\frac{1}{(D_i-1)!}\prod_{\substack{j=1\\j\neq i}}^{M}\left(\frac{1}{\theta_j}-\frac{1}{\theta_i}\right)^{-D_j},\ i=1,\ldots,M,$$

and

$$c_{i,D_{i-k}}=\frac{1}{k}\sum_{j=1}^{k}\frac{(D_i-k+j-1)!}{(D_i-k-1)!}R\left(j,i,M\right)c_{i,D_i-(k-j)},$$
$$k=1,\ldots,D_i-1,i=1,\ldots,M,$$
$$R\left(j,i,M\right)=\sum_{\substack{k=1\\k\neq i}}^{M}D_k\left(\frac{1}{\theta_i}-\frac{1}{\theta_k}\right)^{-j},\ j=1,\ldots,D_i-1.$$

If the SINR includes any exact distribution of sums of Gamma random variables the success probability expression is intractable. It is possible to appeal to the moment matching approximation proposed in (2.8).

SU-JT without Interference

Finding a good approximation for the sum of Gamma r.v. as $\hat{X}\approx\sum_{i=1}^{M}X_i$ where $\hat{X}\sim Gamma(\hat{D},N_t)$, facilitates the analysis because $\mathrm{SINR}=\gamma_x\hat{X}$ and the success probability is easily obtained as

$$\mathbb{P}_{\mathrm{succ}}^{(u)}=e^{-\beta/\hat{\theta}_X}\sum_{i=0}^{\hat{D}_X-1}\frac{\left(\beta/\hat{\theta}_X\right)^i}{i!}. \tag{2.43}$$

SU-JT with OCI

If OCI is taken into account, based on $\mathrm{SINR}=\theta_{\hat{X}}\hat{X}/(1+\theta_{\hat{Y}}\hat{Y})$, where $\theta_{\hat{Y}}\hat{Y}$ represents the OCI, following the proof in A.0.8 then (2.43) is simplified as

$$\mathbb{P}_{\mathrm{succ}}^{(u)}=e^{-\beta/\theta_{\hat{X}}}\sum_{i=0}^{D_{\hat{X}}-1}\sum_{j=0}^{i}\binom{i}{j}\frac{\left(\beta/\theta_{\hat{X}}\right)^i}{i!}\frac{\partial^j\mathcal{L}_{\hat{Y}}\left(\beta/\theta_{\hat{X}}\right)}{\partial\left(\beta/\theta_{\hat{X}}\right)^j}, \tag{2.44}$$

where

$$\frac{\partial^j \mathcal{L}_{\hat{Y}}\left(\beta/\theta_{\hat{X}}\right)}{\partial\left(\beta/\theta_{\hat{X}}\right)^j} = \left(-\theta_{\hat{Y}}\right)^j \frac{\left(D_{\hat{Y}}-1+j\right)!}{\left(D_{\hat{Y}}-1\right)!}\left(1+\frac{\theta_{\hat{Y}}}{\theta_{\hat{X}}}\beta\right)^{-D_{\hat{Y}}-j}$$

as shown in (2.50).

SU-JT high-SNR regime

In the high-SNR regime, where the system is interference limited, the Gamma approximation yields a simpler expression: $\mathrm{SINR} = \theta_{\hat{X}}\hat{X}/(\theta_{\hat{Y}}\hat{Y})$ and the success probability is

$$\mathbb{P}_{\mathrm{succ}}^{(u)} = e^{-\beta/\theta_{\hat{X}}} \sum_{i=0}^{D_{\hat{X}}-1} \frac{\left(\beta/\theta_{\hat{X}}\right)^i}{i!} \frac{\partial^i \mathcal{L}_{\hat{Y}}\left(\beta/\theta_{\hat{X}}\right)}{\partial\left(\beta/\theta_{\hat{X}}\right)^i}. \tag{2.45}$$

2.5.2 Multi-user CoMP modes

Based on the single-user case in (2.43), the analysis for any CoMP transmission mode serving multiple users is extended; either for MU-JT or CBF.

Success Probability for multi-user CoMP

As shown in section 2.2 in the more general case with M cooperative BSs and M_{OCI} interfering BSs the $\mathrm{SINR} = \sum_{j=0}^{M}\theta_j X_j/(1+\sum_{k=1}^{M_{OCI}} = \theta_k Y_k)$. Using a Gamma approximation only on the signal term $\mathrm{SINR} = \theta_{\hat{X}}\hat{X}/(1+\sum_{k=1}^{M_I} = \theta_k Y_k)$, the following result on the success probability is obtained.

Theorem 2. *The success probability under CoMP with QD-CSI and OCI, in which the u-th user is served by M BSs and receives interference from M_{OCI} BSs, is given by*

$$\mathbb{P}_{\mathrm{succ}}^{(u)} = e^{-\beta/\theta_{\hat{X}}} \sum_{i=0}^{D_{\hat{X}}-1} \sum_{j=0}^{i} \binom{i}{j} \frac{\left(\beta/\theta_{\hat{X}}\right)^i}{i!} \frac{\partial^j \prod_{k=1}^{M_{OCI}} \mathcal{L}_{Y_k}\left(\beta/\theta_{\hat{X}}\right)}{\partial\left(\beta/\theta_{\hat{X}}\right)^j}, \tag{2.46}$$

where $\mathcal{L}_{Y_k}$ is the Laplace transform of each interfering term.

Proof. See Appendix A.0.8. □

Simplified Success Probability for multi-user CoMP

The above result may not be easy to calculate as one needs to find high-order derivatives of the product of M_I Laplace transforms. In both CBF and MU-JT, the most important interference terms are due to quantization and OCI. Hence to provide a simpler expression, the delayed CSI term is neglected and the SINR takes the form $\mathrm{SINR} = \hat{X}/(1+\hat{Y}_1+\hat{Y}_2)$.

Theorem 3. *The success probability under CoMP with Q-CSI and OCI, in which the u-th user is served by M BSs and receives interference from M_{OCI} BSs, is given by the success probability for a multi-user CoMP transmission and can be written as*

$$\mathbb{P}_{\mathrm{succ}}^{(u)} = e^{-s} \sum_{i=0}^{D_{\hat{X}}-1} \sum_{j=0}^{i} \sum_{k=0}^{j} \frac{s^i}{i!} \binom{i}{j} \binom{j}{k} \mathcal{L}_{\hat{Y}_1}(s)^{(j-k)} \mathcal{L}_{\hat{Y}_2}(s)^{(k)}, \tag{2.47}$$

where $\mathcal{L}_{\hat{Y}_1}(s)^{(j)}$ is the j-th derivative of the Laplace transform of $\hat{Y}_1(s)$.

Proof. See Appendix A.0.9. □

Moment Generating functions

As stated previously, the Laplace transform can be calculated by means of the MGF. For any Gamma distributed random variable $X \sim Gamma(D,\theta)$, the MGF is $M_X(x) = (1-x\theta)^{-D}$ and therefore

$$\mathcal{L}_X(x) = M_X(-x) = (1+x\theta)^{-D}. \tag{2.48}$$

For each of the interference terms $\hat{Y}_i \sim Gamma(D_{\hat{Y}_i}, \theta_{\hat{Y}_i})$ the (zero order derivative) Laplace transform is

$$\mathcal{L}_{Y_i}^{(0)}(\beta/\theta_{\hat{X}}) = \left(1+\frac{\theta_{\hat{Y}_i}}{\theta_{\hat{X}}}\beta\right)^{-D_{\hat{Y}_i}}. \tag{2.49}$$

The j-th derivative is obtained as

$$\begin{aligned}
\mathcal{L}_{Y_i}^{(j)}(\beta/\theta_{\hat{X}}) &= \theta_{\hat{Y}_i}^{j}(-D_{\hat{Y}_i})(-D_{\hat{Y}_i}-1)\ldots(-D_{\hat{Y}_i}-j+1)\left(1+\frac{\theta_{\hat{Y}_i}}{\theta_{\hat{X}}}\beta\right)^{-D_{\hat{Y}_i-j}} \\
&= (-\theta_{\hat{Y}_i})^j(D_{\hat{Y}_i})(D_{\hat{Y}_i}+1)\ldots(D_{\hat{Y}_i}+j-1)\left(1+\frac{\theta_{\hat{Y}_i}}{\theta_{\hat{X}}}\beta\right)^{-D_{\hat{Y}_i-j}} \\
&= (-\theta_{\hat{Y}_i})^j\frac{(D_{\hat{Y}_i}+j-1)!}{(D_{\hat{Y}_i}-1)!}\left(1+\frac{\theta_{\hat{Y}_i}}{\theta_{\hat{X}}}\beta\right)^{-D_{\hat{Y}_i-j}}
\end{aligned} \tag{2.50}$$

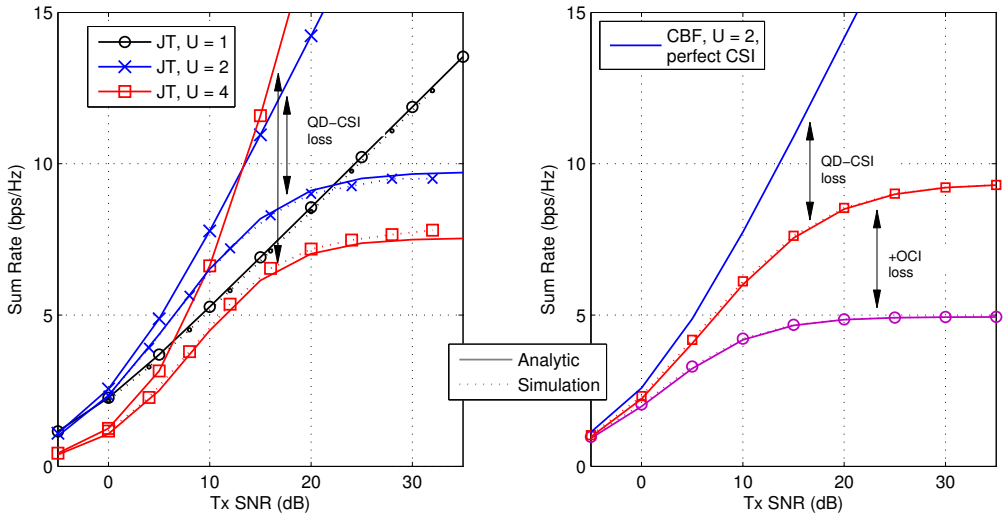

Figure 2.4: Left: Achievable rates for JT with perfect and QD-CSI. $M = 3$, $Nt = 4$, $b = 10$, and $v = 10$ km/h. Right: Achievable rates for CBF including perfect CSI, QD-CSI and the effect of OCI. $M = 2$, $Nt = 4$, $b = 8$, and $v = 5$ km/h.

the above results may finally be used to evaluate the system performance in terms of the so called transmission capacity [64] or equivalently the spectral efficiency of a transmission scheme that operates with no link adaptation mechanism, supposing the use of capacity achieving coding and modulation. A system with U users has a transmission capacity in the form

$$C = \sum_{u=1}^{U} \log\left(1 + \beta_u\right) \mathbb{P}_{\text{succ}}^{(u)} \tag{2.51}$$

2.6 Numerical Results

In this section, the performance analysis and the analytical expressions and approximations derived in Section 2.2.4 are validated. First, the approximation for the achievable rate with equal pathloss (homogeneous scenario) is verified. Unless otherwise stated, $T_s = 1$ ms and $f_c = 2.1$ GHz. In Figure 2.4, the analytical expressions derived above with simulations are compared. The graph on the left shows the number of users U served in JT to maximize the sum rate for

an increasing SNR, however the achievable sum rate of MU-JT exhibits a ceiling effect due to imperfect CSI. On the right-hand graph, a similar result is obtained for CBF, showing the significant impact of quantization and delay on the sum rate, while OCI reduces the sum rate by almost 50% in the high SNR regime. Second, in Figure 2.5, the gamma distribution approximations considered in the heterogeneous scenario with unequal pathloss are verified. Its is observed that the analytical expressions, which also use the moment matching approximation method, provide an accurate approximation in all cases, i.e. CoMP with QD-CSI when approximations are taken on the signal and interference terms, and CoMP with OCI where an additional approximation is used in the denominator of the SINR. The figure also shows the rate degradation due to quantization and delay and the additional degradation incurred for OCI. Moreover, in Figure 2.6, the results based on RVQ are compared with the performance using standardized LTE codebooks [65] for CBF without OCI. As expected, if the number of antennas (or BSs) increase, RVQ exhibits a performance very close to codebooks used in real systems.

In Figure 2.7, it is shown the number of feedback bits required to obtain a rate gain by adding one more BS in the cooperative cluster no larger than 0.5 bps/Hz for different CoMP modes. It can be observed that adding a BS in the cooperative cluster, e.g. going from 2 to 3 BSs, requires a feedback rate of around 7 bits per user per BS, which is larger that the resolution used in current LTE systems.

Furthermore, the case when it is beneficial from an average sum rate point of view to perform CoMP transmission as compared to a non-cooperative transmission is evaluated. In the latter, it is assumed that each of M BSs transmits independently to its user using eigen-beamforming (also known as maximal ratio combining at the transmitter (MRT)). Determining whether CoMP transmission is beneficial is dominated by the distance (path-loss) of the user(s) to the possible CoMP BSs. In Figure 2.8, it is seen that as the feedback resolution increases, the region where CoMP outperforms MRT is extended. If a set of users is placed in any point inside that region, the respective CoMP mode under QD-CSI and OCI performs better than MRT under the same operating conditions. If all users are outside the region, performing non-cooperative transmission achieves higher sum rate compared to CoMP. We also see that CBF has a broader region than JT, however in terms of sum rate, JT has larger gains over MRT than CBF. Finally, for

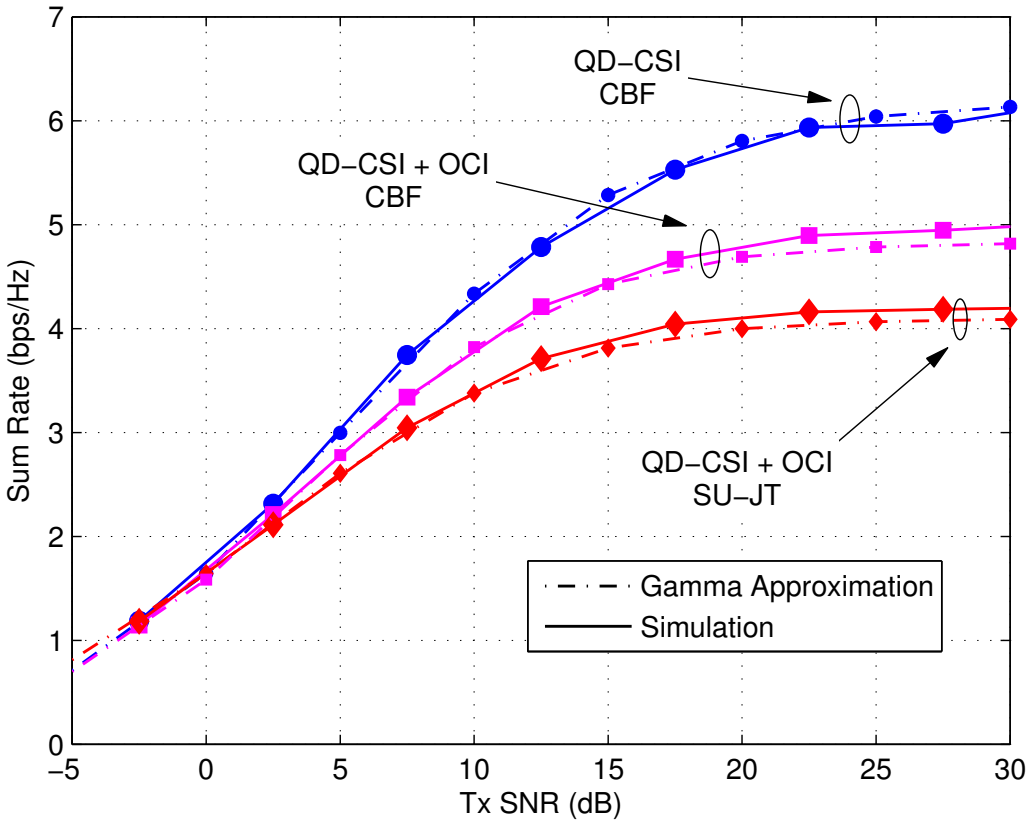

Figure 2.5: Gamma approximations on the signal term, the interference terms and the OCI term. Users are randomly placed around the cell-edge. $M = 2$, $N_t = 4$, $b = 4$ bits.

$M = 3$ and $b = 4$, there is no cell area in the cluster for which CoMP is beneficial.

The performance of the different transmission modes compared to MRT for 2 BSs having 4 antennas is shown in Figure 2.9. Different feedback resolution and delay values are evaluated as the SNR increases. Both users have been placed near the cell-edge. MU-JT is not shown as its results are only marginally better than CBF which does not implies sharing data among BSs. In the low SNR regime, MRT dominates both graphics. SU-JT is the best mode for low feedback resolution, but the addition of OCI gives to CBF a wider region over SU-JT. Finally CBF provides superior performance in a large portion of both graphics but important gains are seen only from the medium resolution, low delay and medium SNR regimes combined.

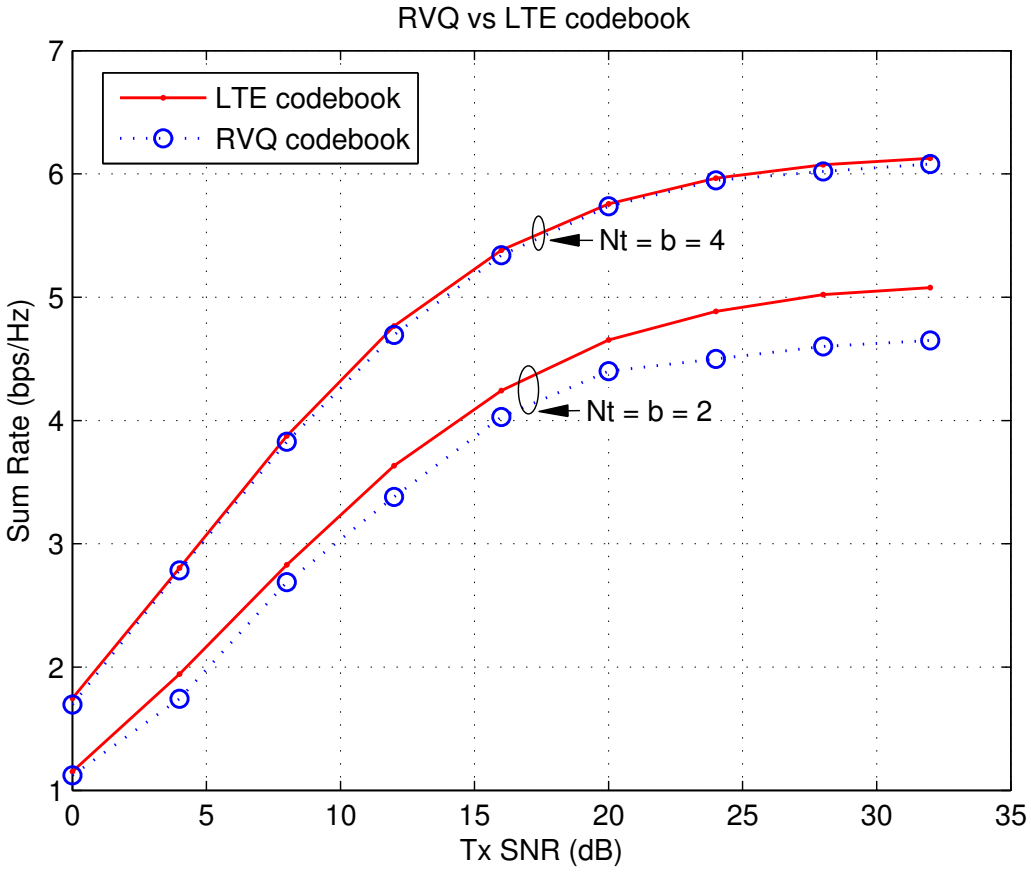

Figure 2.6: Average Sum Rate of CBF systems without OCI for $M = 2$, $N_t = 4$, and $v = 5$ km/h.

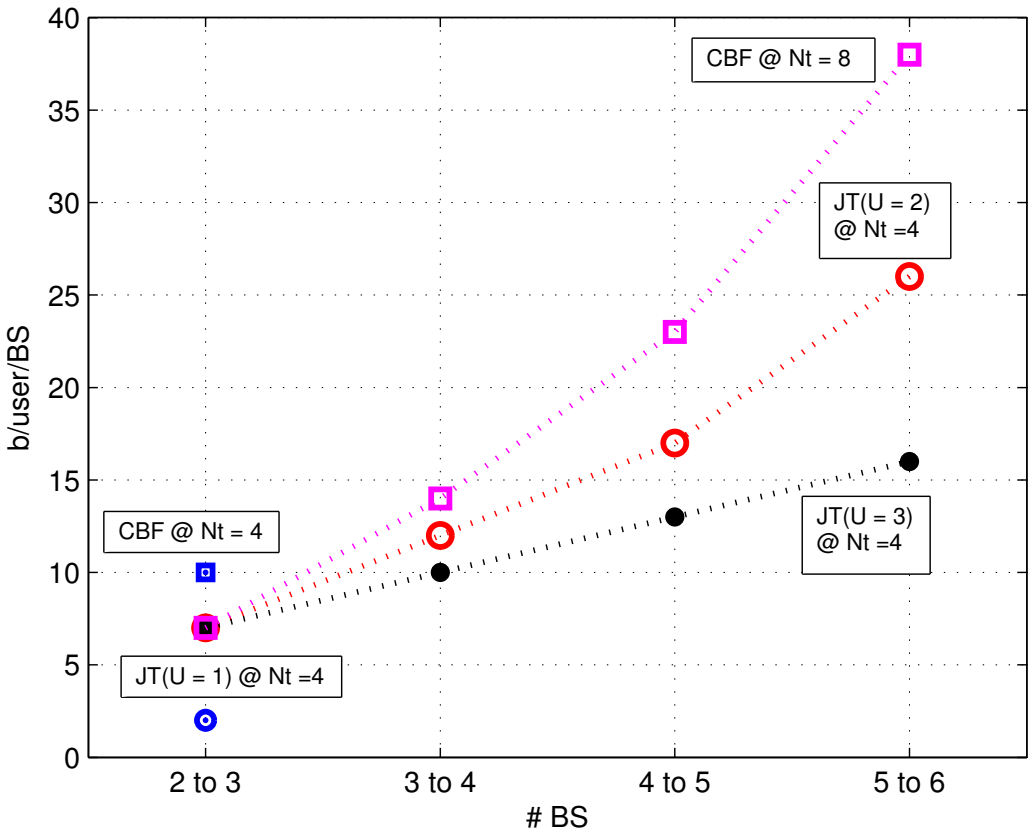

Figure 2.7: Number of CSI bits needed to ensure a sum rate gain of 0.5 bps/Hz, by increasing the number of BS.

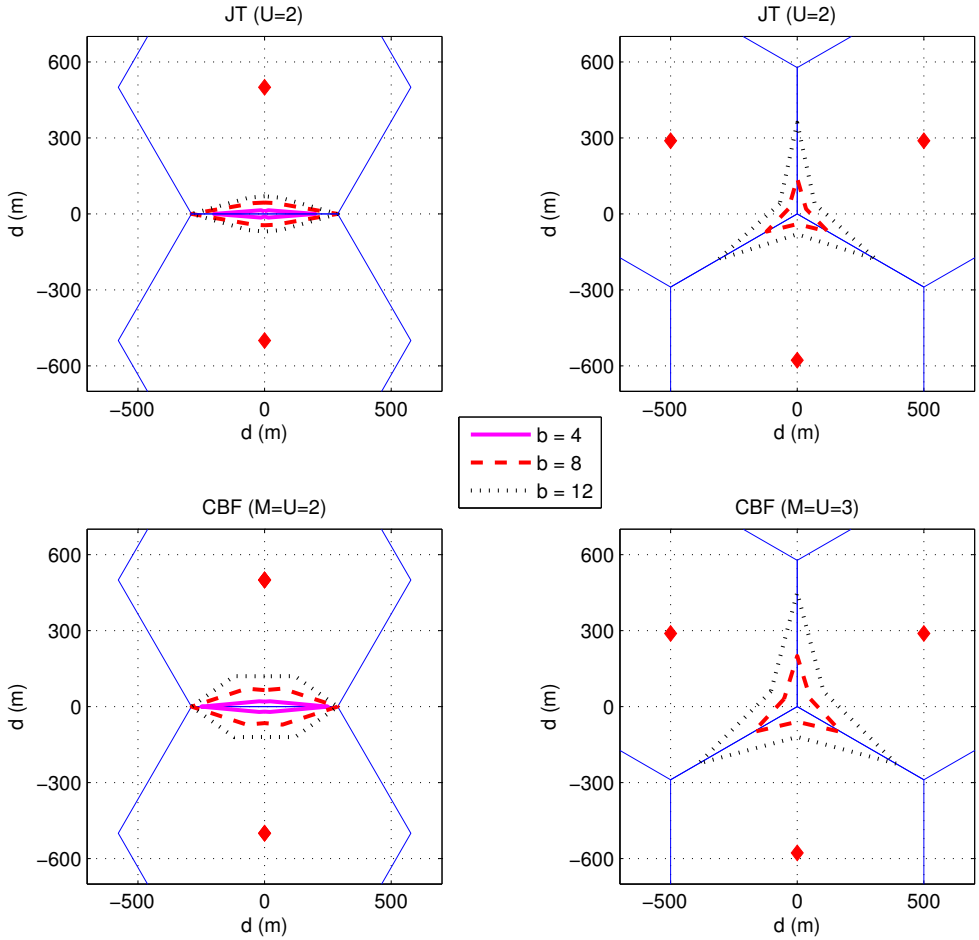

Figure 2.8: Cell regions comparing the sum rate of CoMP vs. Non Cooperation (MRT) for different number of feedback bits b, and $N_t = 4$, $v = 5$ km/h, $T_s = 1$ ms, $f_c = 2.1$ GHz.

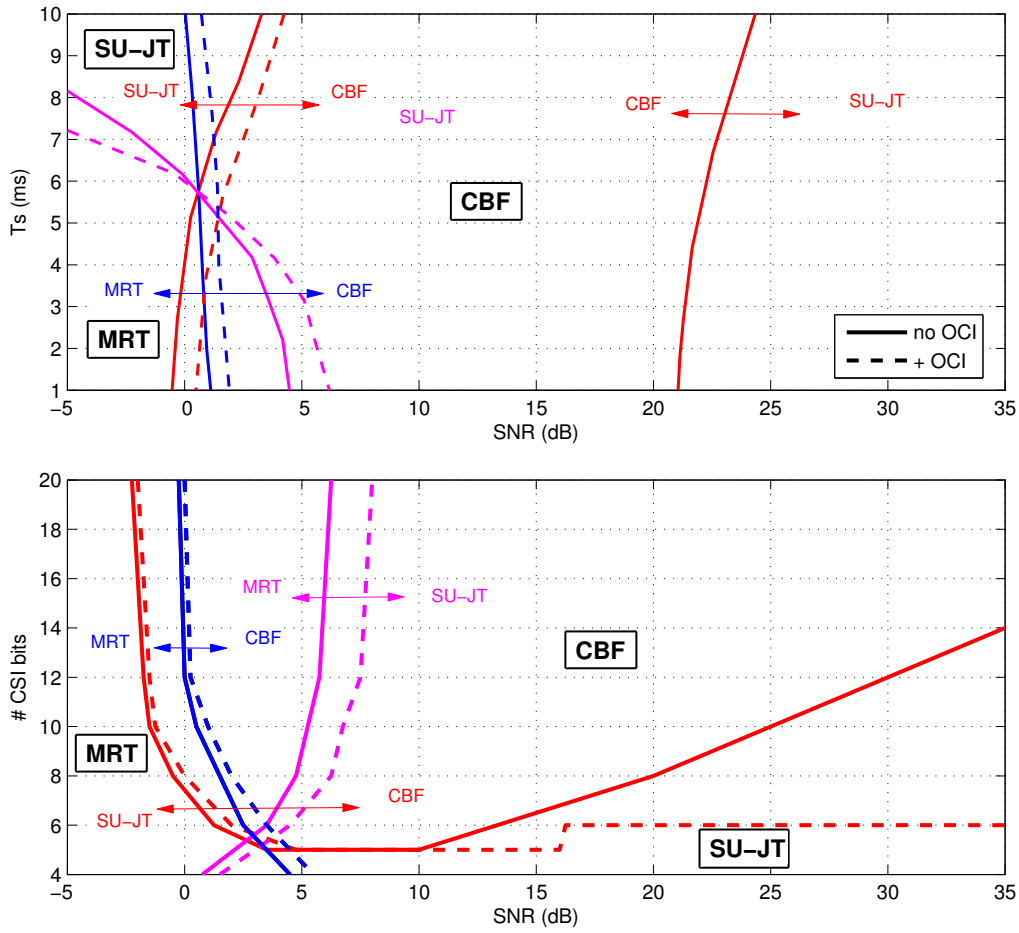

Figure 2.9: Operating regions for different transmit modes with delayed and quantized CSI, M = 2, Nt = 4, v = 10 km/h. Top: Delay changes with $b = 8$. Bottom: Resolution changes with $T_s = 1$ ms.

Appendices

Appendix A

Appendix A

A.0.1 Lemma A.0.1

The ergodic capacity can be expressed as

$$R = \mathbb{E}_X \left[\log(1+X)\right] = \int_0^\infty \log(1+x)\mathrm{d}F(x) = -\int_0^\infty \log(1+x)\frac{\mathrm{d}(1-F(x))}{\mathrm{d}x}\mathrm{d}x.$$

Integrating by parts then

$$R = \mathbb{E}_X \left[\log(1+X)\right] = -\left[\log(1+x)(1-F(x))\right]_0^\infty + \int_0^\infty \frac{1-F(x)}{1+x}\mathrm{d}x.$$

Since the first term vanishes evaluating in the integral limits we get

$$R = \mathbb{E}_X \left[\log(1+X)\right] = \int_0^\infty \frac{1-F_X\left(x\right)}{x+1}\,\mathrm{d}x. \tag{A.1}$$

A.0.2 Proof of Proposition 1

Starting from (2.9) and applying the delay model as described in (2.3), the received signal is given by

$$\begin{aligned}
S_{\mathrm{JT,u}}^{(\mathrm{qd})} &= \frac{P}{MU}\sum_{i=1}^{M}\theta_{u,i}\left|\left(\rho\mathbf{h}_{u,i}[n-1]+\mathbf{e}_u[n]\right)^{\mathrm{H}}\mathbf{w}_{u,i}^{\mathrm{qd}}[n]\right|^2 \\
&\overset{(a)}{=} \frac{P}{MU}\sum_{i=1}^{M}\theta_{u,i}\left|\rho\mathbf{h}_{u,i}^{\mathrm{H}}[n-1]\mathbf{w}_{u,i}^{\mathrm{qd}}[n]\right|^2 \\
&= \frac{P}{MU}\sum_{i=1}^{M}\theta_{u,i}\rho^2\left\|\mathbf{h}_{u,i}[n-1]\right\|^2\left|\bar{\mathbf{h}}_{u,i}^{\mathrm{H}}[n-1]\mathbf{w}_{u,i}^{\mathrm{qd}}[n]\right|^2 \\
&\overset{(b)}{=} \frac{P}{MU}\sum_{i=1}^{M}\theta_{u,i}\rho^2\left\|\mathbf{h}_{u,i}[n-1]\right\|^2\left|\left(\cos\phi\hat{\mathbf{h}}_{u,i}[n-1]+\sin\phi\hat{\mathbf{g}}_{u,i}[n-1]\right)^{\mathrm{H}}\mathbf{w}_{u,i}^{\mathrm{qd}}[n]\right|^2 \\
&\overset{(c)}{=} \frac{P}{MU}\sum_{i=1}^{M}\theta_{u,i}\rho^2\cos^2\phi\left\|\mathbf{h}_{u,i}[n-1]\right\|^2\left|\hat{\mathbf{h}}_{u,i}^{\mathrm{H}}[n-1]\mathbf{w}_{u,i}^{\mathrm{qd}}[n]\right|^2, \qquad \text{(A.2)}
\end{aligned}$$

where in (a), $\mathbf{e}_u[n]$ is neglected as it is small compared to $\rho\mathbf{h}_{u,i}^{\mathrm{H}}[n-1]\mathbf{w}_{u,i}^{\mathrm{qd}}[n]$; (b) shows the vector decomposition of the channel direction $\bar{\mathbf{h}}_{u,i}$ and (c) is the result of the orthogonality of $\hat{\mathbf{g}}_{u,i}[n-1]$ and $\mathbf{w}_{u,i}^{\mathrm{qd}}[n]$. The term $\left\|\mathbf{h}_{u,i}[n-1]\right\|^2\left|\hat{\mathbf{h}}_{u,i}^{\mathrm{H}}[n-1]\mathbf{w}_{u,i}^{\mathrm{qd}}[n]\right|$ is distributed as $\chi^2_{2(N_t-U+1)}$ [13]. Noticing that every term in the summation is weighted with its pathloss attenuation, the gamma approximation using moment matching is applied with $\bar{\theta}=[\theta_{u,1},\ldots,\theta_{u,M}]$ and $\bar{D}=[D_1,\ldots,D_M]$. Finding $\hat{\theta}=f_\theta(\bar{D},\bar{\theta})$ and $\hat{D}=f_D(\bar{D},\bar{\theta})$, the signal term is reduced to (2.10), which concludes the proof.

A.0.3 Proof of Proposition 2

The interference term in (2.10) can be written as

$$\begin{aligned}
I_{\mathrm{JT,u}}^{(\mathrm{qd})} &= \frac{P}{MU}\sum_{i=1}^{M}\theta_{u,i}\sum_{j\neq u}^{U}\left|\mathbf{h}_{u,i}^{\mathrm{H}}[n]\,\mathbf{w}_{u,j}^{\mathrm{qd}}[n]\right|^2 \\
&= \frac{P}{MU}\sum_{i=1}^{M}\theta_{u,i}\sum_{j\neq u}^{U}\left|\left(\rho\mathbf{h}_{u,i}^{\mathrm{H}}[n-1]+\mathbf{e}_{u,i}^{\mathrm{H}}[n]\right)\mathbf{w}_{u,j}^{\mathrm{qd}}[n]\right|^2 \\
&\overset{(a)}{\approx} \frac{P}{MU}\sum_{i=1}^{M}\theta_{u,i}\sum_{j\neq u}^{U}\left[\rho^2\left|\mathbf{h}_{u,i}^{\mathrm{H}}[n-1]\,\mathbf{w}_{u,j}^{\mathrm{qd}}[n]\right|^2+\left|\mathbf{e}_{u,i}^{\mathrm{H}}[n]\,\mathbf{w}_{u,j}^{\mathrm{qd}}[n]\right|^2\right]. \qquad \text{(A.3)}
\end{aligned}$$

where (a) is obtained by neglecting the term containing both $\mathbf{h}_{u,i}[n-1]$ and $\mathbf{e}_{u,i}[n]$, which is normally insignificant as compared to the others. The distribution of the above terms is

$$\sum_{j\neq u}^{U}\left|\mathbf{h}_{u,i}^{\mathrm{H}}\left[n-1\right]\mathbf{w}_{u,j}^{\mathrm{qd}}\left[n\right]\right|^{2}\sim\delta Y_{1}$$
$$\sum_{j\neq u}^{U}\left|\mathbf{e}_{u,i}^{\mathrm{H}}\left[n\right]\mathbf{w}_{u,j}^{\mathrm{qd}}\left[n\right]\right|^{2}\sim\epsilon^{2}Y_{2}, \tag{A.4}$$

where $\left|\mathbf{h}_{u,i}^{\mathrm{H}}\left[n-1\right]\mathbf{w}_{u,j}^{\mathrm{qd}}\left[n\right]\right|^{2}$ and $\left|\mathbf{e}_{u,i}^{\mathrm{H}}\left[n\right]\mathbf{w}_{u,j}^{\mathrm{qd}}\left[n\right]\right|^{2}$ follow an exponential distribution [13], which is equivalent to $Gamma(1,1)$, and therefore, $\delta Y_1 \sim Gamma(U-1,\delta)$ and $\epsilon^2 Y_2 \sim Gamma(U-1,\epsilon^2)$. Since both sums are weighted by the pathloss in (A.3), each of them further simplifies to the result in (2.11) using gamma approximation.

A.0.4 Proof of Theorem 1

As seen in section 2.2, the SINR takes on the general form in (2.16) and can be simplified as

$$\mathrm{SINR}=\frac{aX}{1+b_1Y_1+b_2Y_2+b_3Y_3}=\frac{aX}{1+Y},$$

where $Y=b_1Y_1+b_2Y_2+b_3Y_3$ with pdf given by [62]

$$f_Y\left(y\right)=\sum_{j=1}^{3}\sum_{k=0}^{D_{Y_j}-1}\kappa_k^{(j)}y^k e^{-y/b_j}, \tag{A.5}$$

where $\kappa_k^{(j)}$ can be found using (2.6) and (2.7). Denote $\mathrm{SINR}=S$, the cdf of S is given by

$$\begin{aligned}F_S\left(s\right) &= \mathbb{P}\left(\frac{aX}{1+Y}\leq s\right)\\ &= \int_0^\infty F_{X|Y}\left(\frac{s}{a}\left(1+y\right)\right)f_Y\left(y\right)\,\mathrm{d}y.\end{aligned} \tag{A.6}$$

Replacing the CDF of X and the PDF of Y into (A.6), we get

$$\begin{aligned}
F_S(s) &= \int_0^\infty \left[1 - e^{\left(\frac{s}{a}(1+y)\right)} \sum_{i=0}^{D_X-1} \frac{\left(\frac{s}{a}(1+y)\right)^i}{i!}\right] \sum_{j=1}^{3} \sum_{k=0}^{D_{Y_j}-1} \kappa_k^{(j)} y^k e^{-y/b_j} \,\mathrm{d}y \\
&= 1 - e^{-s/a} \int_0^\infty \sum_{i=0}^{D_X-1} \sum_{j=1}^{3} \sum_{k=0}^{D_{Y_j}-1} \frac{\left(\frac{s}{a}(1+y)\right)^i}{i!} \kappa_k^{(j)} y^k e^{-y/b_j} e^{-y(s/a)} \,\mathrm{d}y \\
&\overset{(a)}{=} 1 - e^{-s/a} \int_0^\infty \sum_{i=0}^{D_X-1} \sum_{j=1}^{3} \sum_{k=0}^{D_{Y_j}-1} \sum_{l=0}^{i} \binom{i}{l} y^l \frac{(s/a)^i}{i!} \kappa_k^{(j)} y^k e^{-y/b_j} e^{-y(s/a)} \,\mathrm{d}y \\
&= 1 - e^{-s/a} \sum_{i=0}^{D_X-1} \sum_{j=1}^{3} \sum_{k=0}^{D_{Y_j}-1} \sum_{l=0}^{i} \binom{i}{l} \frac{(s/a)^i}{i!} \kappa_k^{(j)} \int_0^\infty y^{l+k} e^{-y(s/a+1/b_j)} \,\mathrm{d}y \\
&\overset{(b)}{=} 1 - e^{-s/a} \sum_{i=0}^{D_X-1} \sum_{j=1}^{3} \sum_{k=0}^{D_{Y_j}-1} \sum_{l=0}^{i} \binom{i}{l} \frac{(s/a)^i}{i!} \kappa_k^{(j)} (l+k)! \left(\frac{s}{a} + \frac{1}{b_j}\right)^{-(l+k+1)} \qquad \text{(A.7)}
\end{aligned}$$

where (a) is obtained using the binomial expansion for $(1+y)^i$ and (b) comes from the identity $\int_0^\infty y^M e^{\alpha y} \mathrm{d}y = M! \alpha^{-(M+1)}$. Then, by Lemma A.0.1, the average achievable rate is expressed as

$$R_{\mathrm{CoMP,u}}^{(\mathrm{qd})} = \mathbb{E}_S\left[\log(1+S)\right] = \int_0^\infty \frac{1 - F_S(s)}{s+1} \,\mathrm{d}s. \qquad \text{(A.8)}$$

Replacing (A.7) into (A.8) and rearranging, we obtain

$$\begin{aligned}
R_{\mathrm{CoMP,u}}^{(\mathrm{qd})} &= \log_2(e) \int_0^\infty e^{-s/a} \sum_{i=0}^{D_X-1} \sum_{j=1}^{3} \sum_{k=0}^{D_{Y_j}-1} \sum_{l=0}^{i} \frac{(l+k)! \kappa_k^{(j)}}{l!(i-l)!} a^{l+k-i+1} \frac{s^i \left(s + a/b_j\right)^{-(l+k+1)}}{s+1} \,\mathrm{d}s \\
&= \log_2(e) \sum_{i=0}^{D_X-1} \sum_{j=1}^{3} \sum_{k=0}^{D_{Y_j}-1} \sum_{l=0}^{i} \frac{(l+k)! \kappa_k^{(j)}}{l!(i-l)!} a^{l+k-i+1} \int_0^\infty \frac{s^i e^{-s/a}}{(s+1)\left(s + a/b_j\right)^{-(l+k+1)}} \,\mathrm{d}s.
\end{aligned}$$

Finally, using the integral notation of (2.18), the proof is completed.

A.0.5 Proof of Corollary 1

In the high SNR regime, the SINR distribution is approximated as

$$\mathrm{SINR} \approx \frac{aX}{b_1 Y_1 + b_2 Y_2 + b_3 Y_3} \sim \frac{aX}{Y},$$

Following the same derivations as in Appendix A.0.4, the CDF of S is calculated as

$$\begin{aligned} F_S(s) &= \int_0^\infty \left[1 - e^{-sy/a} \sum_{i=0}^{D_X-1} \frac{(sy/a)^i}{i!}\right] \sum_{j=1}^{3} \sum_{k=0}^{D_{Y_j}-1} \kappa_k^{(j)} y^k e^{-y/b_j} \, \mathrm{d}y \\ &= 1 - \sum_{i=0}^{D_X-1} \sum_{j=1}^{3} \sum_{k=0}^{D_{Y_j}-1} \frac{(s/a)^i}{i!} \kappa_k^{(j)} \int_0^\infty y^{i+k} e^{-y(s/a+1/b_j)} \, \mathrm{d}y \\ &= 1 - \sum_{i=0}^{D_X-1} \sum_{j=1}^{3} \sum_{k=0}^{D_{Y_j}-1} \frac{(s/a)^i}{i!} \kappa_k^{(j)} (i+k)! \left(\frac{s}{a} + \frac{1}{b_j}\right)^{-(i+k+1)}. \end{aligned} \tag{A.9}$$

Replacing (A.9) into (A.8) and rearranging terms, Corollary 1 is proved. Note that the resulting integral can be expressed in terms of the Appell hypergeometric series F_1 as

$$\mathcal{I}_2(a, m, n) = \int_0^\infty \frac{x^m}{(x+a)^n (x+1)} \, \mathrm{d}x = \frac{x^{m+1}}{a^n (m+1)} F_1(m+1, n, 1, m+2, -x/a, -x).$$

A.0.6 Proof of Proposition 4

First, the expected value of the rate is approximated as

$$R_u = \mathbb{E}\left\{\log_2\left(1 + \frac{aX}{1 + \sum_i b_i Y_i}\right)\right\} \approx \log_2\left(1 + \frac{A}{B}\right) = \log_2(B + A) - \log_2(B), \tag{A.10}$$

where A and B denote the mean value of the signal and the interference-plus-noise terms, respectively, both being functions of P (cf. Section 2.2). In the low to moderate SNR regime, i.e. $P \approx [0,\ 8]$ dB, we have that the average value A is of the order of $B/(B-1)$, i.e. aD_X is approximately equal to $\frac{1+\sum_i b_i D_{Y_i}}{\sum_i b_i D_{Y_i}}$, which implies that $R_u \approx \log_2 A$. Thus, the sum rate can be approximated as

$$\begin{aligned} R &\approx U\mathbb{E}\left\{\log_2(aX)\right\} = \mathbb{E}\left\{\log_2(a) + \log_2(X)\right\} \\ &= U\left[\log_2(a) + \log_2(e)\mathbb{E}\left\{\log(X)\right\}\right] \\ &= U\left[\log_2(a) + \log_2(e)\left(\psi(D_X) + \log(1)\right)\right] \\ &= U \log_2\left(a e^{\psi(D_X)}\right). \end{aligned} \tag{A.11}$$

Applying the same procedure to a second rate R', we can approximate the rate difference in the low to moderate SNR regime as

$$\Delta R \approx \log_2 \left(\frac{\left(ae^{\psi(D_X)}\right)^U}{\left(a'e^{\psi(D_{X'})}\right)^{U'}} \right). \tag{A.12}$$

Note that the range of validity of this approximation is in the SNR range for which $A \approx \frac{B}{B-1}$.

A.0.7 Proof of Proposition 5

The rate difference is written as

$$\Delta R = U\mathbb{E}\left\{\log_2\left(1+\frac{aX}{1+\sum_i b_i Y_i}\right)\right\} - U'\mathbb{E}\left\{\log_2\left(1+\frac{a'X'}{1+\sum_i b'_i Y'_i}\right)\right\}, \tag{A.13}$$

which in turn is approximated by

$$\Delta R \approx U\mathbb{E}\left\{\log_2\left(\frac{aX}{\sum_i b_i Y_i}\right)\right\} - U'\mathbb{E}\left\{\log_2\left(\frac{a'X'}{\sum_i b'_i Y'_i}\right)\right\}. \tag{A.14}$$

Since b_1 and b_2 are similar (see Table 2.1) and $Y_1 = Y_2$, we use $b_1 + b_2 = b$ and $Y = Y_1 = Y_2$ so that

$$\Delta R \approx U\mathbb{E}\left\{\log_2\left(\frac{aX}{bY}\right)\right\} - U'\mathbb{E}\left\{\log_2\left(\frac{a'X'}{b'Y'}\right)\right\}. \tag{A.15}$$

Finally, using $\log_2(X) = \log_2(e^{\psi(D_X)})$, where $X \sim Gamma(D_X, 1)$, we obtain

$$\Delta R = \log_2 \left(\frac{\left[\eta e^{\psi(D_X)-\psi(D_Y)}\right]^U}{\left[\eta' e^{\psi(D_{X'})-\psi(D_{Y'})}\right]^{U'}} \right), \tag{A.16}$$

where $\eta = a/b$ and $\eta' = a'/b'$.

A.0.8 Proof of Theorem 2

The success probability defined in terms of the target SNR is

$$\mathbb{P}_{\text{succ}}^{(u)} = \mathbb{P}\left\{\text{SINR}_u > \beta\right\} = 1 - \mathbb{P}\left\{\hat{X} < \beta\left(1+Y\right)\right\}.$$

Then, using a binomial expansion and the cdf of the received signal, the probability is expressed in terms of the pdfs of the interfering signals as

$$\mathbb{P}_{\text{succ}}^{(u)} = e^{-\beta/\theta_{\hat{X}}} \sum_{i=0}^{D_{\hat{X}}-1} \sum_{j=0}^{i} \frac{\left(\beta/\theta_{\hat{X}}\right)^i}{i!} \binom{i}{j} \int_0^{\infty} y^j e^{-\beta y/\theta_{\hat{X}}} \sum_{k=1}^{M_I} f_{Y_k}(y) dy.$$

Note that $\int_0^{\infty} e^{-\beta y/\theta_{\hat{X}}} f_{Y_k}$ is the Laplace transform of every interference source $\mathcal{L}_{Y_k}\left(\beta/\theta_{\hat{X}}\right)$, then.

$$\int_0^{\infty} y^j e^{-\beta y/\theta_{\hat{X}}} f_{Y_k} = \frac{\partial^j \mathcal{L}_{Y_k}\left(\beta/\theta_{\hat{X}}\right)}{\partial \left(\beta/\theta_{\hat{X}}\right)^j}.$$

Using the definition of the moment generating function (MGF) for a Gamma distributed r.v. we know that $\mathcal{L}_{Y_k}\left(\beta/\theta_{\hat{X}}\right) = M_{Y_k}(-x) = \left(1+\theta_{\hat{X}} x\right)^{-\hat{D}_{\hat{X}}}$. Finally, since the pdf of the sum of the interference terms is the convolution of the individual pdfs, the MGF of the sum is nothing but the product of every individual $M_{Y_k}(-x)$ and

$$\int_0^{\infty} y^j e^{-\beta y/\theta_{\hat{X}}} \sum_{k=1}^{M_I} f_{Y_k}(y) dy = \frac{\partial^j \prod_{k=1}^{M_I} \mathcal{L}_{Y_k}\left(\beta/\theta_{\hat{X}}\right)}{\partial \left(\beta/\theta_{\hat{X}}\right)^j},$$

which concludes the proof.

A.0.9 Proof of Theorem 3

Replacing $Y = \hat{Y}_1 + \hat{Y}_2$, then the success probability can be calculated as

$$\mathbb{P}_{\text{succ}}^{(u)} = \mathbb{P}\left\{\text{SINR}_u > \beta\right\} = 1 - \mathbb{P}\left\{\hat{X} < \beta\left(1+Y\right)\right\}.$$

Using the cdf of $\hat{X}$ and the law of total probability on Y then

$$\begin{aligned}
\mathbb{P}_{\text{succ}}^{(u)} &= 1 - \int_0^{\infty} F_{\hat{X}}\left(\beta(1+y)\right) f_Y(y)\, \mathrm{d}y \\
&= \int_0^{\infty} e^{-\beta(1+y)/\theta_{\hat{X}}} \sum_{i=0}^{D_{\hat{X}}-1} \frac{\left(\beta(1+y)/\theta_{\hat{X}}\right)^i}{i!} f_Y(y) \mathrm{d}y \\
&= e^{-\beta/\theta_{\hat{X}}} \sum_{i=0}^{D_{\hat{X}}-1} \sum_{j=0}^{i} \frac{\left(\beta/\theta_{\hat{X}}\right)^i}{i!} \binom{i}{j} \int_0^{\infty} y^j e^{-\beta y/\theta_{\hat{X}}} f_Y(y) \mathrm{d}y,
\end{aligned}$$

and introducing the variable $s = \beta/\theta_{\hat{X}}$ the expression simplifies to

$$\mathbb{P}_{\text{succ}}^{(u)} = e^{-s} \sum_{i=0}^{D_{\hat{X}}-1} \sum_{j=0}^{i} \frac{s^i}{i!} \binom{i}{j} \int_0^\infty y^j e^{-sy} f_Y(y) \mathrm{d}y. \tag{A.17}$$

The term $\mathcal{L}_Y(s) = \int_0^\infty e^{-sy} f_Y(y) \mathrm{d}y$ is the Laplace transform of the function $f_Y(s)$, and its j-th derivative is obtained as

$$\int_0^\infty y^j e^{-sy} f_Y(y) \mathrm{d}y = \frac{\partial^j \mathcal{L}_Y(s)}{\partial (s)^j}. \tag{A.18}$$

The expression above can be presented into more detail given that the Laplace transform is closely related to the moment generating function (MGF) as $\mathcal{L}_Y(s) = M_Y(-x)$. Being $Y = \hat{Y}_1 + \hat{Y}_2$, the pdf $f_Y(y)$ is the convolution $f_{\hat{Y}_1} * f_{\hat{Y}_2}$. In consequence $M_Y(-x)$ is the product of each MGF $M_{\hat{Y}_1}(-x) M_{\hat{Y}_2}(-x)$ or equivalently, the product of the Laplace transforms as follows

$$\int_0^\infty y^j e^{-sy} f_Y(y) \mathrm{d}y = \frac{\partial^j \left(\mathcal{L}_{\hat{Y}_1}(s) \mathcal{L}_{\hat{Y}_2}(s) \right)}{\partial (s)^j}.$$

Next, the general Leibniz rule can be applied to obtain the j-th derivative of a product

$$\left(\mathcal{L}_{\hat{Y}_1}(s) \mathcal{L}_{\hat{Y}_2}(s) \right)^{(j)} = \sum_{k=0}^{j} \binom{j}{k} \mathcal{L}_{\hat{Y}_1}(s)^{(j-k)} \mathcal{L}_{\hat{Y}_2}(s)^{(k)},$$

hence, replacing in (A.17) the proof is completed.

Chapter 3

Adaptive Feedback Bit Allocation for Coordinated Multi-Point Transmission

3.1 Introduction

The performance of CoMP significantly depends on the CSI availability. In frequency division duplexing (FDD) systems, a closed-loop feedback mechanism is needed to send the CSI from the user back to the BS. The most common approach is codebook-based channel information quantization and feedback. In this case, the user estimates the channel using pilot symbols and feeds back the index of the closest codeword to its channel direction. Random vector quantization (RVQ) [59], which is asymptotically optimal, is usually assumed for analytical tractability. If the CSI is inaccurate and outdated, the performance gains of CoMP are diminished due to the interference. The delay and quantization error, which are inherent to the feedback mechanism, set a major bottleneck for CoMP transmission and their impact in CoMP systems has been studied, for instance in [38, 40, 63, 66].

In CoMP transmission systems with M cooperative BSs, a user sends b bits to report each CSI index to its serving BS using a total of bM bits. How to allocate these bM bits among different channels is referred to as the feedback bit allocation problem and is the main topic of this work. Intuitively, more feedback bits should be given to channels suffering from lower

attenuation, shorter delays or for which increasing the feedback resolution will increase the average rate. This problem was first introduced in [67], then investigated in more detail in [68,69] specifically for CBF and [70] for a multi-user JT case. Their approach consists of finding a bound for the rate loss due to limited CSI with respect to perfect CSI, and then minimizing this bound under a given bit budget constraint (bM). However, existing solutions to the problem of adaptive feedback allocation usually provide high gains for large number of cells, which may not be feasible in CoMP systems. The common approach is to decouple the desired signal and interference term to simplify and solve the feedback allocation problem, yielding suboptimal solutions. In this chapter, two different techniques for adaptive feedback allocation are proposed. Specifically, the main contributions of this new approach are:

- The feedback allocation problem is formulated and solved in CBF systems without decomposing the solution into two parts (desired signal and interference) as known in the literature. This approach is shown to provide significant sum rate improvement.
- In single-user JT systems, important gains are observed for cell-edge users through adaptive feedback allocation even with few BSs. In particular, our simulation results show that significant gains over existing schemes or equal bit allocation can be achieved even with only two or three cooperating base stations.

3.2 System Model

3.2.1 Network Layout

Similar as in chapter 2, a grid of M hexagonal cells is used, where a BS is placed at the cell center. Other Cell Interference (OCI) is not considered, since it does not fundamentally change the allocation results. Each BS has N_t antennas to serve single-antenna users and operates in the same transmission modes JT and CBF that are briefly revisited here.

- *Joint Transmission:* In JT, only one user is served and data and CSI are shared among all BSs via the backhaul connection. Using eigen-beamforming (often referred to as MRT),

the received signal at instant n is

$$y[n] = \sum_{i=1}^{M} \sqrt{\theta_i} \mathbf{h}_i^{\mathrm{H}}[n] \mathbf{w}_i[n] s_i[n] + z[n], \tag{3.1}$$

where $\mathbf{h}_i$ and $\mathbf{w}_i$ are the $\mathbb{C}^{N_t \times 1}$ channel and precoding vectors from the i-th BS, respectively. Equal power allocation is assumed with $\mathbb{E}\left[\sum_{i=1}^{M} |s_i|^2\right] = P$, and $z[n] \sim \mathcal{CN}(0,1)$ is the complex additive white Gaussian noise. The path-loss attenuation is a function of the distance as $\theta_i = d_i^{-\alpha}$.

- *Coordinated Beamforming:* CBF serves one user per cooperative BS and shares only CSI among BSs. The received signal at the u-th user takes the form

$$\begin{aligned} y_u[n] =& \sqrt{\theta_u} \mathbf{h}_{u,u}^{\mathrm{H}}[n] \mathbf{w}_u[n] s_u[n] \\ &+ \sum_{\substack{i=1 \\ i \neq u}}^{M} \sqrt{\theta_i} \mathbf{h}_{u,i}^{\mathrm{H}}[n] \mathbf{w}_i[n] s_i[n] + z[n], \end{aligned} \tag{3.2}$$

where the beamforming vector $\mathbf{w}_u$ is the u-th column of the zero-forcing precoding matrix.

3.2.2 Quantized and Delayed CSI Feedback

The effect of quantization and delay on CSI feedback is considered again as in chapter 2, using Random Vector Quantization (RVQ) (2.4) and the Gauss-Markov regular processes (2.3).

Random Vector Quantization

In RVQ, the quantization error expressed as $\sin^2 \phi = 1 - |\bar{\mathbf{h}}^{\mathrm{H}} \hat{\mathbf{h}}|^2$ where $\bar{\mathbf{h}} = \mathbf{h}/||\mathbf{h}||$, $\phi = \angle \hat{\mathbf{h}}, \bar{\mathbf{h}}$, and $\hat{\mathbf{h}}$ is the quantized channel direction. Its expected value is given by [59]

$$\tilde{\xi} = \mathbb{E}_{\phi}\left[\sin^2 \phi\right] = 2^b \cdot \beta\left(2^b, \frac{N_t}{N_t - 1}\right), \tag{3.3}$$

where $\beta(\cdot,\cdot)$ is the Euler Beta function. A useful and tight bound for the quantization error is given by [33]

$$2^{-\frac{b}{N_t-1}} \leq 2^b \cdot \beta\left(2^b, \frac{N_t}{N_t-1}\right). \tag{3.4}$$

Gauss-Markov Process

The Gauss-Markov block regular process is used to model the signal correlation and error caused by the delayed CSI. One symbol remains unchanged during its whole period and successive symbols are related as

$$\mathbf{h}[n] = \rho\mathbf{h}[n-1] + \mathbf{e}[n]. \tag{3.5}$$

The channel correlation using Clarke's model is given by $\rho = J_0(2\pi f_d T_s)$, where $J_0(\cdot)$ is the zero-th order Bessel function of the first kind, T_s is the symbol duration and f_d is the Doppler spread. The error vector, denoted $\mathbf{e}[n]$, has i.i.d. normally distributed elements with zero mean and variance ϵ^2 and is independent of $\mathbf{h}[n-1]$.

3.3 Adaptive Feedback Allocation

Using JT and CBF transmission modes implies that each user should feedback M indices using $B = bM$ bits, where b is the number of bits used to feed back one CSI index. Since B bits are the total feedback used and not all the channel gains are equal, the adaptive bit allocation aims at increasing the average rate by finding the best bit allocation $\bar{b} = [b_1, \ldots b_M]$ such that $\sum_{i=1}^{M} b_i = B$.

Formally, the problem can be stated as follows:

$$\bar{b}^* = \arg\max_{\bar{b}} \mathbb{E}\left\{\log_2(1 + \mathrm{SINR}(\bar{b}))\right\}. \tag{3.6}$$

The optimal allocation vector $\bar{b}^* = [b_1^*, \ldots b_M^*]$ can be found by calculating first the expression $\mathbb{E}\left\{\log_2(1 + \mathrm{SINR}(\bar{b}))\right\}$.

3.3.1 Adaptive Feedback for SU-JT

The received SNR under quantized and delayed CSI is given by [63]

$$\mathrm{SNR}_{\mathrm{JT}} = \frac{P}{M}\sum_{i=1}^{M}\xi_i\rho_i^2\theta_i\left\|\mathbf{h}_i[n-1]\right\|^2, \tag{3.7}$$

where $\xi_i = 1-\tilde{\xi}_i$ (see (3.3)). Since in SU-JT mode only one user is served and in the no OCI case $\mathrm{SINR} \equiv \mathrm{SNR}$.

Although it is possible to calculate the achievable rate as shown in (2.17), the expression is involved and does not allow solving the optimization problem. For that, the achievable rate is first bounded using Jensen's inequality, i.e.

$$\mathbb{E}\left\{\log_2(1+\mathrm{SNR}(\bar{b}))\right\} \leq \log_2(1+\mathbb{E}\left\{\mathrm{SNR}(\bar{b})\right\}). \tag{3.8}$$

The expected value of SNR is easy to calculate, knowing that $\sum_{i=1}^{M}\left\|\mathbf{h}_i[n-1]\right\|^2 \sim \chi^2_{2(MN_t)}$, i.e.

$$\mathbb{E}\left\{\mathrm{SNR}(\bar{b})\right\} = \frac{PN_t}{M}\sum_{i=1}^{M}\rho_i^2\theta_i\left(1-2^{b_i}\cdot\beta\left(2^{b_i},\frac{N_t}{N_t-1}\right)\right). \tag{3.9}$$

Finally, using $\tilde{\theta}_i = \rho_i^2\theta_i$ and the bounds in (3.4) and (3.8)

$$\begin{aligned}\mathbb{E} \quad & \left\{\log_2(1+\mathrm{SINR}(\bar{b}))\right\} \\ \leq \quad & \log_2\left(1+\frac{PN_t}{M}\sum_{i=1}^{M}\tilde{\theta}_i\left(1-2^{-\frac{b_i}{N_t-1}}\right)\right).\end{aligned} \tag{3.10}$$

Theorem 4. *The optimal number of bits that maximizes the upper bound on the single-user JT achievable rate (eq. (3.10)) is given by*

$$b_i^* = \frac{B}{M} + (N_t-1)\log_2\left(\frac{\tilde{\theta}_i}{[\prod_{i=1}^{M}\tilde{\theta}_i]^{1/M}}\right), \tag{3.11}$$

and consequently the optimal bit allocation is $\bar{b}^* = [b_1^* \ldots b_M^*]$.

Proof. Due to the concavity of the logarithmic function, the problem (3.6) can be reduced into maximizing the expected value of the SNR as

$$\begin{aligned}\bar{b}^* \quad = \quad & \arg\max_{\bar{b}}\sum_{i=1}^{M}\tilde{\theta}_i\left(1-2^{\frac{-b_i}{N_t-1}}\right) \\ & \text{s.t.}\sum_{i=1}^{M}b_i = B.\end{aligned} \tag{3.12}$$

Introducing now a new variable $x_i = 2^{-b_i/(N_t-1)}$ and rewriting the above problem as

$$\begin{aligned} \bar{b}^* &= \arg\min_{\bar{b}} \sum_{i=1}^{M} \tilde{\theta}_i x_i \\ &\quad \text{s.t.} \prod_{i=1}^{M} x_i = 2^{-B/(N_t-1)}, \end{aligned} \tag{3.13}$$

the optimal bit allocation can be found using the Arithmetic Mean Geometric Mean (AM-GM) inequality, i.e. GM $\leq$ AM. The inequality provides a minimum value for any summation of M numbers, such that the product of any summation is equal to a constant. This is exactly the problem stated in (3.13). Hence,

$$\frac{1}{M} \sum_{i=1}^{M} \tilde{\theta}_i x_i \geq \left[\prod_{i=1}^{M} \tilde{\theta}_i x_i \right]^{1/M}. \tag{3.14}$$

Since equality (i.e. the minimum) in the AM-GM inequality holds if and only if $\tilde{\theta}_1 x_1 = \tilde{\theta}_2 x_2 = \ldots = \tilde{\theta_M} x_M$, we have

$$\tilde{\theta}_i \left(2^{-\frac{b_i}{N_t-1}} \right) = \left[2^{-B/(N_t-1)} \prod_{i=1}^{M} \tilde{\theta}_i \right]^{1/M}. \tag{3.15}$$

Finally, solving (3.15) for b_i the optimal number of bits in (3.11) is obtained. □

3.3.2 Adaptive Feedback for Coordinated Beamforming

In the CBF mode, a similar procedure as in the JT case is used for the SINR expression, which is given by [66]

$$\mathrm{SINR}_{\mathrm{CBF,u}} = \frac{\frac{P\rho_u^2}{M} \theta_u \left| \mathbf{h}_{u,u}^{\mathrm{H}} \mathbf{w}_u^{\mathrm{qd}} \right|^2}{1 + \frac{P}{M} \sum\limits_{\substack{i=1 \\ i \neq u}}^{M} \theta_i \left[\rho_i^2 \left| \mathbf{h}_{u,i}^{\mathrm{H}} \mathbf{w}_i^{\mathrm{qd}} \right|^2 + \left| \mathbf{e}_{u,i}^{\mathrm{H}} \mathbf{w}_i^{\mathrm{qd}} \right|^2 \right]}.$$

For analytical convenience, the term $\left| \mathbf{e}_{u,i}^{\mathrm{H}} \mathbf{w}_i^{\mathrm{qd}} \right|^2$ is neglected as it is not a function of the feedback quantization and does not fundamentally affect the resulting $\bar{b}^*$. Then the expected value of the

SINR is calculated as

$$\begin{aligned}\mathbb{E}\left\{\mathrm{SINR}_{\mathrm{CBF,u}}\right\} &= \mathbb{E}\left\{\frac{P\rho_u^2}{M}\theta_u\left|\mathbf{h}_{u,u}^{\mathrm{H}}\mathbf{w}_u^{\mathrm{qd}}\right|^2\right\}\times\mathbb{E}\left\{\frac{1}{1+\frac{P}{M}\sum_{\substack{i=1\\i\neq u}}^{M}\rho_i^2\theta_i\left|\mathbf{h}_{u,i}^{\mathrm{H}}\mathbf{w}_i^{\mathrm{qd}}\right|^2}\right\}\\ &\overset{(a)}{\geq} \frac{\frac{P\rho_u^2}{M}(N_t-M+1)\theta_u\xi_u}{1+\frac{P}{M}\sum_{\substack{i=1\\i\neq u}}^{M}\rho_i^2\theta_i\delta_i},\end{aligned} \tag{3.16}$$

knowing that $\left|\mathbf{h}_{u,u}^{\mathrm{H}}\mathbf{w}_u^{\mathrm{qd}}\right|^2 \sim \chi^2_{2(N_t-M+1)}$ and $\left|\mathbf{h}_{u,i}^{\mathrm{H}}\mathbf{w}_i^{\mathrm{qd}}\right|^2 \sim \delta_i\chi_2^2$ where $\delta_i = 2^{-b_i/(N_t-1)}$ and (a) results from the fact that $1/(1+X)$ is convex. Having used an upper bound (3.8) followed by a lower bound (3.16), the expression on the average achievable rate is an approximation, where ξ_u is replaced by $1-\delta_u$ and the constant terms are regrouped as $(P\rho_u^2/M)(N_t-M+1)\theta_u = \tilde{\theta}_u$ and $(P\rho_i^2/M)\theta_i = \tilde{\theta}_i$ to get

$$\mathbb{E}\left\{\log_2(1+\mathrm{SINR}_{\mathrm{CBF,u}})\right\} \approx \log_2\left(1+\frac{\tilde{\theta}_u(1-\delta_u)}{1+\sum_{\substack{i=1\\i\neq u}}^{M}\tilde{\theta}_i\delta_i}\right). \tag{3.17}$$

In spite of the approximation, the above expression allows to find an efficient bit allocation policy as shown in the following section.

The adaptive bit allocation optimization problem is cast in the form of maximizing the approximate average SINR under a fixed budget of total feedback bits, i.e.

$$\begin{aligned}\bar{b}^* &= \arg\max_{\bar{b}} \frac{\tilde{\theta}_u\left(1-2^{-\frac{b_u}{N_t-1}}\right)}{1+\sum_{\substack{i=1\\i\neq u}}^{M}\tilde{\theta}_i 2^{-\frac{b_i}{N_t-1}}}\\ &\quad \text{s.t.}\sum_{i=1}^{M} b_i = B.\end{aligned} \tag{3.18}$$

Theorem 5. *The optimal number of bits that maximizes the approximate average rate of CBF transmission is given by*

$$b_i^* = (N_t-1)\log_2(x_i^*), \tag{3.19}$$

where u is used as the sub-index of the signal term, and x_u^* is the solution to the equation

$$x_u^* - \left[\frac{\mathcal{C}}{x_u^*\prod_{\substack{i=1\\i\neq u}}^{M}\tilde{\theta}_i}\right]^{\frac{1}{M-1}} = M, \tag{3.20}$$

otherwise, if the sub-index corresponds to interference terms, x_k^* is given by

$$x_k^* = \left[\frac{\tilde{\theta}_k^{M-2} \mathcal{C}}{x_u^* \prod_{\substack{i=1 \\ i \neq k,u}}^{M} \tilde{\theta}_i} \right]^{\frac{1}{M-1}} . \tag{3.21}$$

Where $b_i^* = (N_t - 1)\log_2(x_i^*)$, determines the optimal bit allocation $\bar{b}^*$.

Proof. See Appendix B.0.1. □

Analytical solutions for (A.4) and (3.21) can be found only for $M \leq 3$, while numerical methods are required for $M > 3$. The above expressions do find though a solution for the optimal bit allocation problem in CBF transmission systems.

Note that in both cases (JT and CBF), since b_i^* is not necessarily a natural number, a rounding operation for $\bar{b}^*$ should be carried out in order to select the best rounded solution. Furthermore, $b_i^* < 0$ means that the i-th BS will not receive any feedback bits and hence the allocation should be performed over the other BSs.

3.4 Simulation Results

Simulations were performed on a hexagonal cell grid layout. Users are placed in positions where it is beneficial to perform BS cooperation rather than any non-cooperative transmission, i.e. near the cell edge, according to the zones shown in Figure 2.8. The obtained results are averaged over 50 different user locations. Results are presented for $M = 2$ and $M = 3$ and compare with the performance of state of the art bit allocation (BA) methods. Splitting BA denotes the method where the solution is found separating the desired signal and interference to solve the optimization problem. The optimal BA is found using exhaustive search over all possible combinations of $\bar{b}$ such that $\sum_i b_i = B$.

Fig. 3.1 shows on the left the single-cell average rate for CBF for two different settings with two and three BSs. On the right hand side the gain with respect to equal BA is shown for the corresponding BA methods. The gains increase with $M > 3$ but it can be observed that in most of the cases only 2 or 3 BSs receive all the allocated bits, while other BSs are much further thus having a minor contribution in the rate.

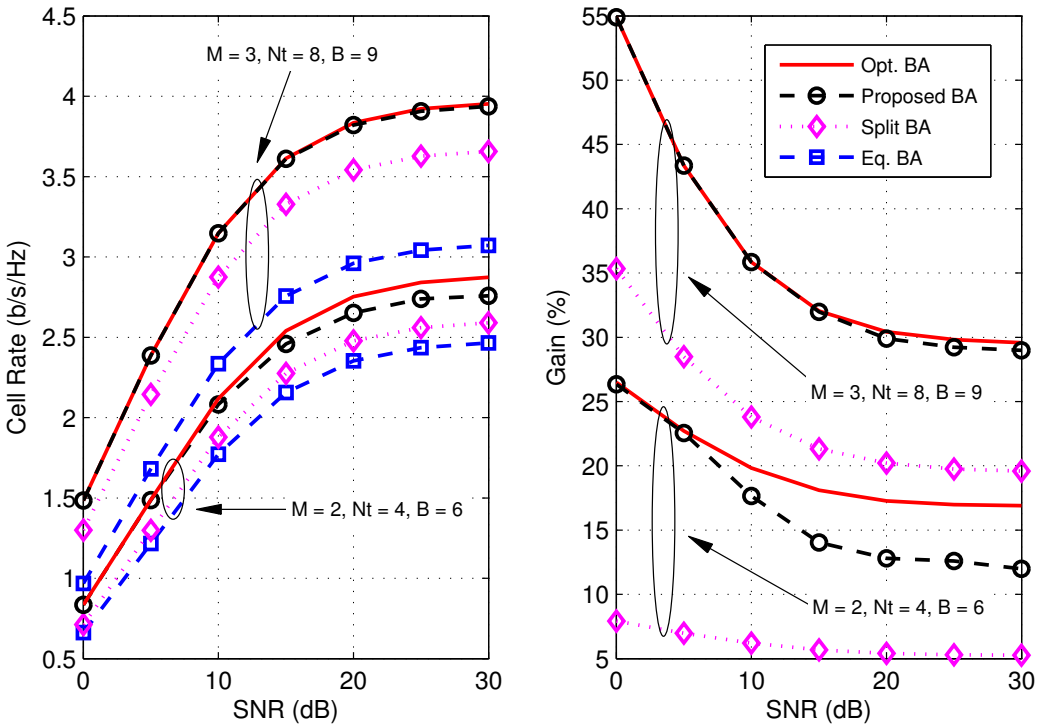

Figure 3.1: Left: Single-cell rates for CBF. Right: Gains with respect to Equal BA.

In Fig. 3.2, the gains with respect to Equal BA are shown for JT with $M = 3$ at 0 and 5 dB. Note that as the total number of bits B grows, the performance gain is decreased, showing that low feedback resolution has higher gain potential. Similarly, if the number of antennas increases, more bits are required to reduce the quantization error and the gain potential increases.

In Fig. 3.3, a comparison between the optimal BA (Opt. BA) that provides the highest gain and the gains obtained with the proposed algorithm for CBF is shown. Any circle in the graphic placed on the diagonal dashed line, represents a configuration where the proposed BA reaches the optimal. When the feedback resolution is increased (i.e. as the circles get bigger), the relative gain (in percentage) is reduced. In contrast, the total rate of the system is increasing due to a better quantization, but the potential for unequal bit allocation gets reduced. Additionally, the difference between the optimal BA and the proposed scheme reduces when

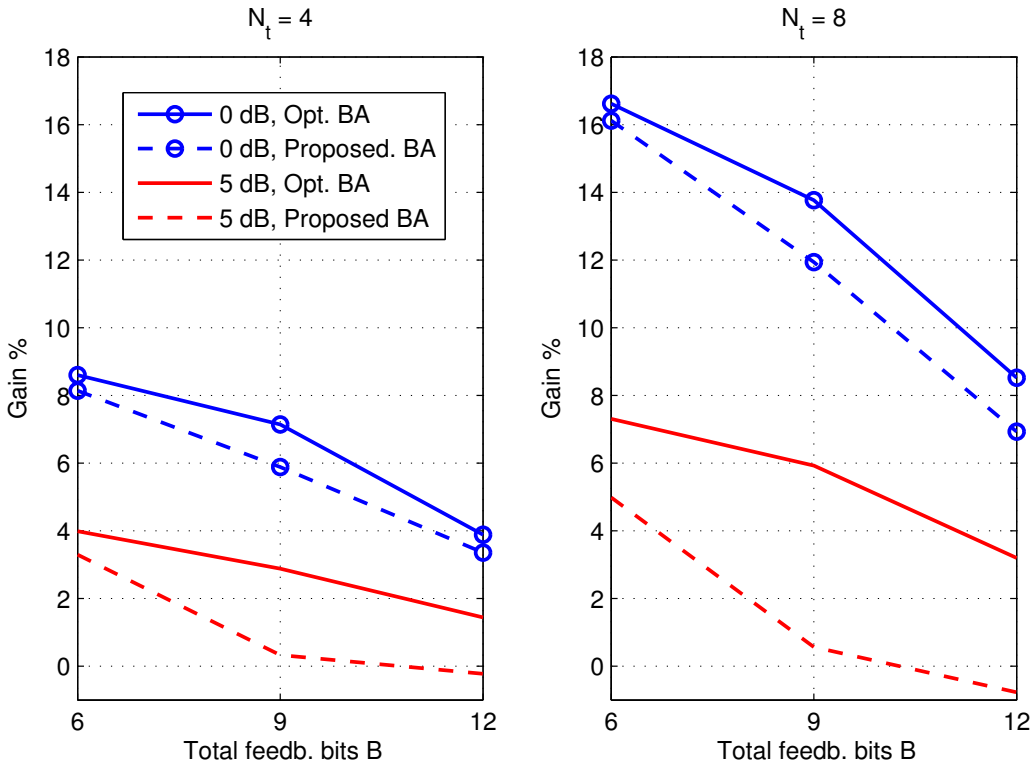

Figure 3.2: Gains w.r.t. Equal BA for JT with $M = 3$.

the number of antennas increases, proving that the approximations taken for the bit allocation solutions in Theorems 4 and 5 are relaxed for large N_t values. On the left graph where $M = 2$, gains are difficult to find for $N_t = 2$ while for $N_t = 4, 6$, the gains with respect to equal BA may reach 30%. On the right hand-side graphic, for $M = 3$ the gains approach 50%. Finally, although not seen in the figure, it is worth noting that the net gains with respect to equal BA, are normally greater as the rates increase, that is, as N_t or b increase or similarly, as the SNR increases, as can be seen in Figure 3.1.

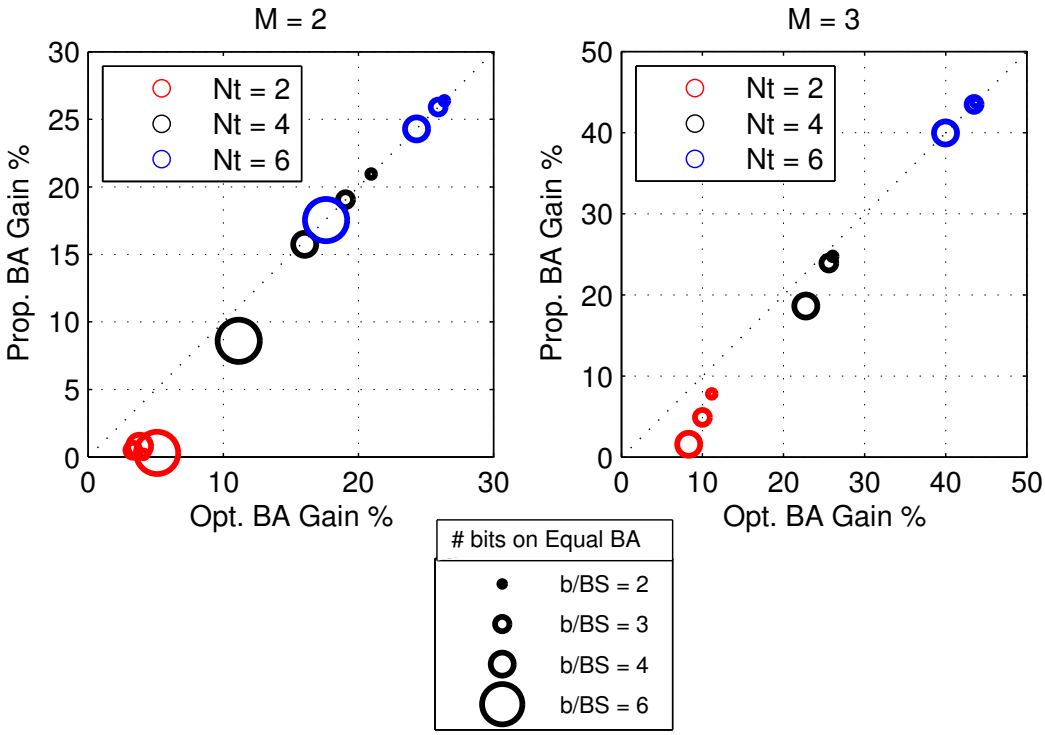

Figure 3.3: Optimal BA vs. Proposed BA gain for CBF at $\mathrm{SNR} = 0$ dB.

Appendices

Appendix B

Appendix B

B.0.1 Proof of Theorem 5

With change of variable $x_i = 2^{b_i/(N_t-1)}$, the problem in (3.17) can be written as

$$\begin{aligned} \bar{b}^* &= \arg\max_{\bar{b}} \frac{\tilde{\theta}_u \left(1 - \frac{1}{x_u}\right)}{1 + \sum_{\substack{i=1 \\ i \neq u}}^{M} \frac{\tilde{\theta}_i}{x_i}} \\ &\quad \text{s.t.} \prod_{i=1}^{M} x_i = 2^{B/(N_t-1)}. \end{aligned} \tag{B.1}$$

The problem is now composed of a convex objective function and a convex equality constraint, and can be solved using Lagrange multipliers. The Lagrange function and its respective partial derivatives are defined as

$$\Lambda(x_1, \ldots x_M, \lambda) = \frac{\tilde{\theta}_u \left(1 - 1/x_u\right)}{1 + \sum_{\substack{i=1 \\ i \neq u}}^{M} \tilde{\theta}_i / x_i} - \lambda \left[\prod_{i=1}^{M} x_i - \mathcal{C} \right],$$

$$
\begin{aligned}
\frac{\partial \Lambda}{\partial x_u} &= \frac{\tilde{\theta}_u / x_u^2}{1 + \sum_{\substack{i=1 \\ i \neq u}}^{M} \tilde{\theta}_i / x_i} - \lambda \prod_{\substack{i=1 \\ i \neq u}}^{M} x_i, \\
\frac{\partial \Lambda}{\partial x_k} &= \frac{\tilde{\theta}_u \left(1 - 1/x_u\right) \tilde{\theta}_k / x_k^2}{\left(1 + \sum_{\substack{i=1 \\ i \neq u}}^{M} \tilde{\theta}_i / x_i\right)^2} - \lambda \prod_{\substack{j=1 \\ j \neq k}}^{M} x_j, \ \forall k \neq u, \\
\frac{\partial \Lambda}{\partial \lambda} &= -\prod_{j=1}^{M} x_j + \mathcal{C}, \qquad \text{(B.2)}
\end{aligned}
$$

where $\mathcal{C} = 2^{B/(N_t - 1)}$. Setting $\vec{\nabla} \Lambda = \mathbf{0}$ and solving for λ, we have

$$
\lambda = \frac{\tilde{\theta}_u / x_u^2}{\left(1 + \sum_{\substack{i=1 \\ i \neq u}}^{M} \tilde{\theta}_i / x_i\right) \prod_{\substack{i=1 \\ i \neq u}}^{M} x_i} \qquad \text{(B.3)}
$$

$$
\lambda = \frac{\tilde{\theta}_u \left(1 - 1/x_u\right) \tilde{\theta}_k / x_k^2}{\left(1 + \sum_{\substack{i=1 \\ i \neq u}}^{M} \tilde{\theta}_i / x_i\right)^2 \prod_{\substack{j=1 \\ j \neq k}}^{M} x_j}. \qquad \text{(B.4)}
$$

Note that (B.4) is consistent for all x_k where $k \neq u$. Then, taking for instance two values $x_l, x_k \neq x_u$ and equalizing their respective partial derivatives as (B.4), then

$$
\tilde{\theta}_k / x_k = \tilde{\theta}_l / x_l. \qquad \text{(B.5)}
$$

Furthermore, setting (B.3) = (B.4), results in

$$
\begin{aligned}
x_u &= \frac{1 + \sum_{\substack{i=1 \\ i \neq u}}^{M} \tilde{\theta}_i / x_i}{\left(1 - 1/x_u\right) \tilde{\theta}_k / x_k} \\
&= \frac{1 + \sum_{\substack{i=1 \\ i \neq u}}^{M} \tilde{\theta}_i / x_i}{\tilde{\theta}_k / x_k} + 1 \\
&\overset{(a)}{=} \frac{1 + (M-1) \tilde{\theta}_k / x_k}{\tilde{\theta}_k / x_k} + 1 \\
&= x_k / \tilde{\theta}_k + M, \qquad \text{(B.6)}
\end{aligned}
$$

where (a) comes from replacing every x_i for $x_k \tilde{\theta}_i / \tilde{\theta}_k$ as indicated in (B.5).

On the other hand, the equation $\partial \Lambda / \partial \lambda = 0$ allows to write

$$
x_k = \frac{\mathcal{C}}{\prod_{\substack{i=1 \\ i \neq k}}^{M} x_i}. \qquad \text{(B.7)}
$$

Replacing (B.5) into (B.7), the optimal value is found for

$$\begin{aligned} x_k^* &= \frac{\mathcal{C}}{x_u \prod_{\substack{i=1 \\ i\neq k,u}}^{M} \tilde{\theta}_i (x_k^*/\tilde{\theta}_k)^{M-2}} \\ &= \left[\frac{\tilde{\theta}_k^{M-2}\mathcal{C}}{x_u \prod_{\substack{i=1 \\ i\neq k,u}}^{M} \tilde{\theta}_i} \right]^{\frac{1}{M-1}}, \end{aligned} \tag{B.8}$$

and finally, replacing (B.8) in (B.6) yields the following expression where the optimal value for x_u is given by

$$x_u^* = \left[\frac{\mathcal{C}}{x_u \prod_{\substack{i=1 \\ i\neq u}}^{M} \tilde{\theta}_i} \right]^{\frac{1}{M-1}} + M. \tag{B.9}$$

Part III

Successive Interference Cancellation

Chapter 4

Cooperative Successive Interference Cancellation in Wireless Networks

In the firsts chapters, network coordination techniques were evaluated under the impact of realistic feedback mechanisms. All the previous presented CoMP techniques take place at the transmitter side and all the analysis is made for MISO channels. In particular, dealing with interference on the transmitter side is the most favorable scenario from the network operator perspective in terms of controlling the traffic and carefully managing its resources; yet, it can also be the most expensive solution, as most of the complexity and the actions to obtain CSI are carried on the network equipments. Nonetheless, is fair to say that a large portion of the actual practical and theoretical interference mitigation techniques, take place at the receiver side. In cellular networks, the first diversity techniques such as rake receivers exploits multipath channels using parallel receiver chains with a single antenna. The use of multiple antennas in portable equipments is seriously restricted due to a necessary minimum antenna separation related to the signal's wave-length. If the separation is not met the multiple antennas tend to act as a single antenna and the possible gains are spoiled. This physical impediment although does not ban multiple antennas, limits its usability in the downlink of cellular networks. However, multiple antennas is not the only strategy to fight interference. In particular, the second part of this thesis is devoted to exploring the use of network cooperation to enable a capacity achieving

technique for the Multiple Access Channel known for years as Successive Interference Cancellation.

In this chapter, SIC is used in the downlink of cellular networks and in a broader perspective the results here derived apply to wireless networks in general. The downlink of a wireless network does not exactly corresponds to a MAC but to an Interference Channel (IC). Nevertheless, it will be shown that SIC receivers have an important potential to increase the system capacity.

Without cooperation, a cellular network is an instance of an IC for which the capacity region is in general not known, except in certain special regimes [49, 50, 71]. Recent work [72] has also reveal the role of SIC in large interference-limited networks. Furthermore, SIC has gained attention in different contexts, e.g. hard or soft decision SIC receiver design [73], joint SIC usage in OFDM systems [74], performance of SIC receivers in wireless ad hoc networks [75].

Despite the various theoretical results, SIC is far from being a mature and reliable technique to be incorporated in real-world wireless networks and standards. The theoretically promised gains may not be easily achievable in realistic scenarios [76] and enhanced link adaptation schemes leave marginal possibilities to the use of SIC. A fundamental obstacle hindering the use of SIC in wireless networks is the lack of a complete characterization of the spatial distribution of the SINR. In fact, the SINR spatial distribution in a network can be mapped into weak or strong interference regimes and is ultimately determinant to realize the favorable or ideal conditions usually assumed in information theoretic approaches. In this regard, recent results have analyzed the performance of SIC using stochastic geometry [77], [78]. A different approach is taken in [79], where the authors describe the cell areas in which different SIC orders are feasible. In [80], the authors provided system-level simulations for the use of SIC receivers in downlink LTE networks, proving that there is still room for gains by applying SIC in a cellular context. In line with this result, ongoing 3GPP discussions on interference cancellation advanced receivers show that SIC is being seriously considered as an interference mitigation solution in future broadband networks

In this chapter, cooperation between the base stations (BSs) is considered and aim at finding practical techniques for enabling SIC receivers in downlink cellular networks. First, a cooperative SIC scheme for a two-cell network is propose , in which the user in one cell performs SIC

and receives its data at the single-user capacity (without interference), whereas the transmit rate in the other cell is properly adapted to maximize the sum rate. The main intuition behind this scheme is to enforce the system to operate in the corner points of the MAC capacity region of the user performing SIC, while sacrificing the least from other user' rate. For that, conditions for which using SIC increases the sum rate as compared to treating interference as noise (IaN) are derived initially for the 2-Tx case in section 4.2, then generalized to the N-Tx case in section 4.2.3. Furthermore, the case for flexible user association is visited in section 4.3, where users that not necessarily receive the largest SNR from the serving BS use SIC to increase both the sum rate and the system fairness. The impact of small-scale fading is considered in section 4.4. Finally, a centralized scheduling algorithm is presented in section 4.5 for implementing the proposed cooperative SIC in large multi-cell networks. Numerical results confirm that using SIC receivers in the dowlink of wireless networks, bring significant sum rate gains, especially for cell-edge users.

4.1 Network Model

This chapter focuses on the downlink of SISO wireless networks. Several transmitters intend to communicate with their respective receivers simultaneously. Each transmitter will use a power $\hat{P}$ where $P = \hat{P}/\sigma^2$ and σ^2 is the noise power. All propagation phenomena are comprised in the following expression where the received SNR from the j-th transmitter (Tx_j) to the i-th receiver (Rx_i) is

$$P_{ji} = P\kappa_{ji}d_{ji}^{-\alpha}, \tag{4.1}$$

$\alpha > 2$ is the path-loss exponent and d_{ji} is the distance from Tx_j to Rx_i and κ_{ji} accounts for any kind of fading, either long term propagation factors such as shadowing, or small-scale fading as will be presented in section 4.4.

The basic network is an instance of an Interference Channel, where two juxtaposed hexagonal cells are the coverage area of two transmitters and two respective receivers as observed in Figure 4.1. In particular, the minimum received SNR is called p and is obtained at any of

the hexagon's corners. When the network is extended for a general number of cells $N > 2$, transmitters are placed in an hexagonal grid. Since the analysis is mainly intended to evaluate the performance of SIC, MIMO configurations are avoided with single-antenna transmitters and receivers. Similarly, the problem of scheduling is not considered and networks include the same number of receivers and transmitters.

4.2 SIC Coordination in a Cellular Context

The term *cellular* refers to the fact that any user receives more power from its serving transmitter than from any other. Equivalently, this means that each user is associated with its strongest transmitter as in cellular networks. For ease of exposition, in the sequel $P_i = P_{ii} = P\kappa_{ii}d_{ii}^{-\alpha}$ is the received SNR at the i-th user from its serving transmitter. Hence, the cellular context is formally stated as

$$\text{Cellular context: } \Rightarrow \boxed{P_i > P_{ji},\ \forall i.}$$

Note however that since the cells are hexagons (not circles), P_i may be less than P_{ij}, meaning that a user outside a given cell may receive more power from that cell transmitter than the user inside the cell thus, it may happen that $P_i < P_{ij}$. Additionally, transmitters and receivers are denoted whit the shortcut Tx and Rx respectively.

4.2.1 Cooperative SIC in 2-cells

The downlink of two Tx-Rx pairs is analyzed. In Figure 4.1 the users are deliberately placed near the cell edge.

The IC in Figure 4.1 can be decomposed in two MAC channels. These two MACs are dependent: the desired signal source in Rx_1 is the interference source in Rx_2 and vice versa. Without using SIC, both Rxs will be served at the same time-frequency resource, and the system's total

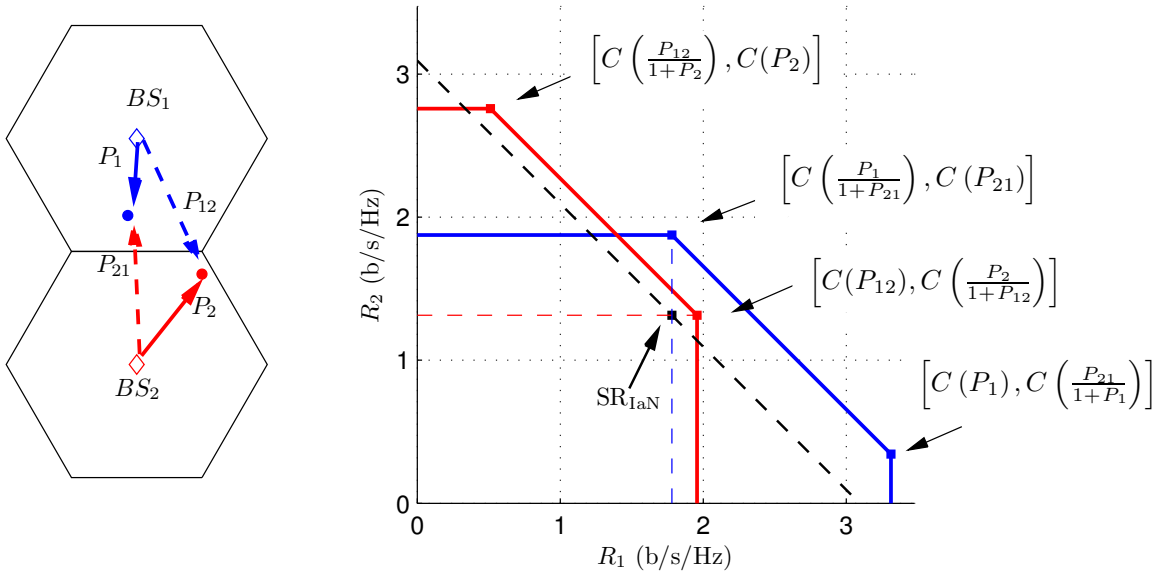

Figure 4.1: A 2x2 IC decomposed in 2 MACs.

achievable spectral efficiency, called sum rate in the sequel, is

$$\begin{aligned} \mathrm{SR}_{\mathrm{IaN}} &= C\left(\mathrm{SINR}_1\right) + C\left(\mathrm{SINR}_2\right), \\ &= C\left(\frac{P_1}{1+P_{21}}\right) + C\left(\frac{P_2}{1+P_{12}}\right), \end{aligned} \tag{4.2}$$

where $C(x) = \log_2(1+x)$ denotes the achievable rate function in (b/s/Hz). The subindex IaN refers to the fact that receivers treat *Interference as Noise*. Using SIC receivers will probably lead to important gains in the sum rate as the interference term P_{ji} disappears, still, several fundamental questions arise: Can any of the Rxs decode its interference? If both, which Rx should perform the SIC? or can they both perform SIC simultaneously? If the interference rate is not decodable can it be reduced so that SIC is possible? To answer these questions some hints are shown in Figure 4.1 which illustrates the capacity regions for both MACs superposed in the same axes. The black dashed diagonal represents all points achieving the same sum rate $\mathrm{SR}_{\mathrm{IaN}}$. Both MACs have corners beyond the IaN line. These corner points can be achieved using SIC, but the rates received at one user are not both desired signals. Recalling that the goal is not to perform SIC thoughtlessly but to use this technique in order to increase the system capacity, the

following result proves that there is a condition guaranteeing that SIC can provide throughput gains in the IC.

Proposition 6. *The following conditions are necessary and sufficient to perform SIC at Rx_i in order to increase the total sum rate with respect to using IaN receivers in a two-cell network:*

$$P_{ji} > \frac{P_j}{1+P_{ij}} \tag{4.3a}$$

$$R_j = \min\left\{C\left(\frac{P_{ji}}{1+P_i}\right), C\left(\frac{P_j}{1+P_{ij}}\right)\right\} \tag{4.3b}$$

Proof. The pair of rates $[C(P_1), C(P_{21}/(1+P_1))]$ is a corner in the capacity region of the MAC formed by the signals from Tx_1 and Tx_2 at Rx_1. It means that if the system transmits at

$$\begin{aligned} R_1 &= C(P_1) \\ R_2 &= C\left(\frac{P_{21}}{1+P_1}\right), \end{aligned} \tag{4.4}$$

Rx_1 can decode R_2, suppress it and then, decode R_1 free of interference. But to maximize the sum rate, Rx_2 must also be able to decode R_2. Therefore, R_2 should be constrained to

$$R_2 = \min\left\{C\left(\frac{P_{21}}{1+P_1}\right), C\left(\frac{P_2}{1+P_{12}}\right)\right\}. \tag{4.5}$$

To ensure that the network will increase its capacity the following inequality should be verified

$$\begin{aligned} \text{SR}_{\text{SIC}^1} &> \text{SR}_{\text{IaN}} \\ C(P_1) + \min\left\{C\left(\frac{P_{21}}{1+P_1}\right), C\left(\frac{P_2}{1+P_{12}}\right)\right\} &> C\left(\frac{P_1}{1+P_{21}}\right) + C\left(\frac{P_2}{1+P_{12}}\right) \end{aligned} \tag{4.6}$$

So in the first case, let the minimum in (4.5) be $C(P_2/(1+P_{12}))$. Then

$$\begin{aligned} \text{SR}_{\text{SIC}^1} &> \text{SR}_{\text{IaN}} \\ C(P_1) + C\left(\frac{P_2}{1+P_{12}}\right) &> C\left(\frac{P_1}{1+P_{21}}\right) + C\left(\frac{P_2}{1+P_{12}}\right) \\ C(P_1) &> C\left(\frac{P_1}{1+P_{21}}\right). \end{aligned}$$

The above inequality always holds true. In other words, the use of SIC yields gains in sum rate. Otherwise, if the the minimum in (4.5) is $C(P_{21}/(1+P_1))$, then (4.7) can be reduced to

$$\begin{aligned}
\mathrm{SR}_{\mathrm{SIC}^1} &> \mathrm{SR}_{\mathrm{IaN}} \\
C\left(P_1\right) + C\left(\frac{P_{21}}{1+P_1}\right) &> C\left(\frac{P_1}{1+P_{21}}\right) + C\left(\frac{P_2}{1+P_{12}}\right) \\
\left(1+P_1\right)\left(1+\frac{P_{21}}{1+P_1}\right) &> \left(1+\frac{P_1}{1+P_{21}}\right)\left(1+\frac{P_2}{1+P_{12}}\right) \\
\left(1+P_1\right)\left(\frac{1+P_1+P_{21}}{1+P_1}\right) &> \left(\frac{1+P_1+P_{21}}{1+P_{21}}\right)\left(1+\frac{P_2}{1+P_{12}}\right) \\
\Rightarrow P_{21} &> \frac{P_2}{1+P_{12}},
\end{aligned} \tag{4.7}$$

Clearly, (4.7) is a particular form of (4.3a) hence, completing the proof. □

Note that the condition (4.3a) is necessary to define a region where SIC gain could happen, while fixing the rate for Rx_j as (4.3b) inside the region defined by (4.3a) is sufficient to guarantee the gain. The reasoning behind this transmission strategy is that one user can decode and suppress its interference to achieve a larger rate, while the other user receives the minimum possible rate in order to increase the sum rate.

If Other Cell Interference (OCI) is present, the received SNR from OCI at Rx_i is P_{Oi} and the same derivations lead to the following conditions

$$\begin{aligned}
\frac{P_{ji}}{1+P_{Oi}} &> \frac{P_j}{1+P_{ij}+P_{Oj}} \\
R_j &= \min\left\{C\left(\frac{P_{ji}}{1+P_i+P_{Oi}}\right), C\left(\frac{P_j}{1+P_{ij}+P_{Oj}}\right)\right\}
\end{aligned} \tag{4.8}$$

Figure 4.1 helps understanding inequality (4.3a) named ***SIC gain condition*** in the sequel. The IaN line will be under the MAC diagonal if the SIC gain condition holds true. Reading the condition inequality, if the received SNR from the interferer is greater than the neighbor's SINR then is worth doing SIC from one user, as the gains of the SIC receiver will compensate for the possibly small rate transmitted for the user using a IaN receiver. To take advantage of the SIC gain condition, a new transmission strategy is proposed called ***Cooperative SIC:*** When the SIC

gain condition is verified, the transmitting rates should be

$$\begin{aligned} R_i &\leq C\left(P_i\right), \\ R_j &\leq \min\left\{C\left(\frac{P_j}{1+P_{ij}}\right), C\left(\frac{P_{ji}}{1+P_i}\right)\right\}. \end{aligned} \tag{4.9}$$

In summary, Rx_i uses its SIC capability to decode its data at the single-user capacity (without interference) while Rx_j decodes the highest rate for which reliable communication is still possible from Tx_j to both users. Since the IC is composed by two MACs, there are two SIC gain conditions. The notation to identify these conditions in the rest of this chapter is:

$$\text{SIC gain condition at } \mathrm{Rx}_1\text{: } P_{21} > \frac{P_2}{1+P_{12}} \Rightarrow \boxed{\mathrm{SIC}^1 :\ P_{21} > \mathrm{SINR}_2}$$

$$\text{SIC gain condition at } \mathrm{Rx}_2\text{: } P_{12} > \frac{P_1}{1+P_{21}} \Rightarrow \boxed{\mathrm{SIC}^2 :\ P_{12} > \mathrm{SINR}_1}$$

Both conditions are clearly related, but there are no implications from any of them: none, one, or both can hold at a given situation. In particular, the conditions determine the spatial regions where only SIC^1 holds, only SIC^2 holds or where both conditions hold, as will be seen in the next section.

4.2.2 SIC Gain Cell Regions

Evaluating the SIC gain conditions, the exact regions where the use of SIC receivers improves the system's capacity can be determined. For this purpose, a two-hexagonal cell network is considered: Rx_2 will be fixed and Rx_1 will move all over its cell to evaluate the SIC gain condition. Figure 4.2 shows the superposition of the MAC capacity regions as seen from the user perspective. The red user (Rx_2) is assumed to be fixed, hence its capacity region remains the same. The blue user (Rx_1) is depicted in four different positions. On each case where a user is inside the gain region depicted in the cells, the diagonal line of its MAC capacity region surpasses the IaN line. In the case 3), both conditions are satisfied however, the network should decide to operate in one of the indicated external corners.

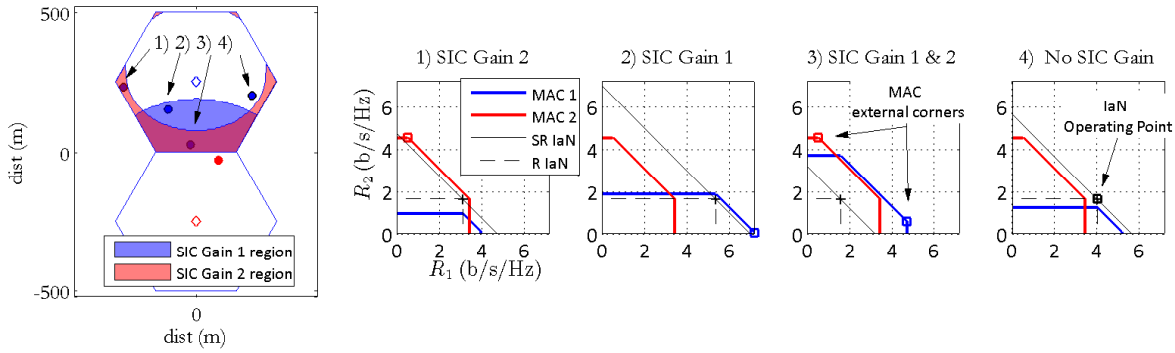

Figure 4.2: SIC Gain regions: user 2 is fixed and user 1 is placed in four different positions.

The common side to both hexagons is the region of strongest interference and will be called the *celledge*. In particular, two points are of special interest for the SIC gain condition. Point A (pt.A), is the point where P_{ji} is maximum. It is located in the middle of the line that joins both transmitters. Point B (pt.B), is the point where the $\mathrm{SINR}_i = P_i/(1 + P_{ji})$ is the minimum, and is located at any of the celledge corners. These two points (pt.A and pt.B) are equal for both receivers and lay in the celledge.

Figure 4.3 shows four examples of the SIC gain regions found for different network layouts. On the center and right-hand side axes, the receivers are placed in points A and B including OCI (bottom) and without OCI (top). The SIC gain regions largely cover important portions of the hexagon. The effect of OCI is evident: the gain regions shrink and both the sum rates and relative gain values decrease. Additionally on the left-hand side, the sum rates in function of Rx_1 position are depicted for the two cases where Rx_2 is placed in pt.B. The magenta surface is $\mathrm{SR}_{\mathrm{SIC}} = \max\left(\mathrm{SR}_{\mathrm{SIC}^1}, \mathrm{SR}_{\mathrm{SIC}^2}\right)$ and shows how the cooperative SIC strategy considerably improves $\mathrm{SR}_{\mathrm{IaN}}$ specially when the interference is stronger, i.e. close to the celledge.

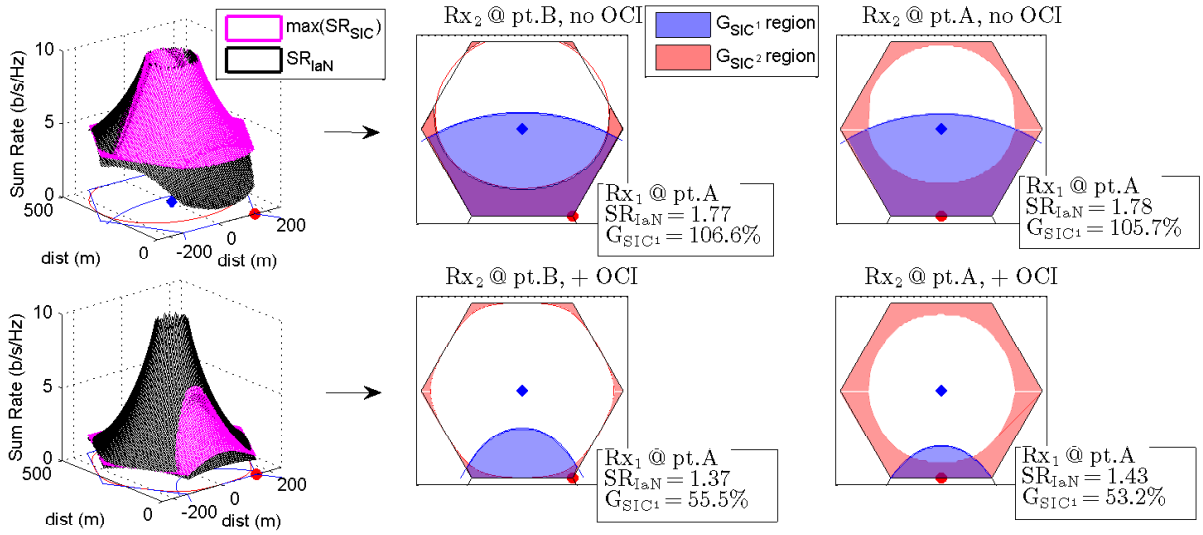

Figure 4.3: Regions for SIC gain conditions. Rx_2 fixed, Rx_1 moves all over cell 1. Minimum received SNR $p = 5$ dB.

Maximum SIC Gain values

After characterizing the SIC gain regions, it is also important to quantify the SIC gain. Based on simple observations it is possible to find an upper bound for the SIC gain as follows. If Rx_1 is at pt.A P_{21} is maximum. Moreover if Rx_2 is at pt.B SINR_2 is minimum and therefore the margin in the SIC gain condition $\mathrm{SIC}^1 : P_{21} > \mathrm{SINR}_2$ is maximized over all possible positions of both receivers. Therefore, evaluating the network with this layout will give an upper bound on the SIC gain. Initially, considering the case without OCI, a rate with the form $C(P_i)$ is achieved and the network sum rate grows indefinitely as the transmitted power increases. To observe how the gains will behave in more realistic scenarios, it is necessary to quantify OCI. Its value may broadly change in real networks depending on the user location, the propagation conditions and the frequency reuse pattern. To fix a value for the received OCI SNR, i.e. P_{Oi} some typical values are considered: the pathloss exponent $\alpha = 3.75$, the cell radius $r = 250$, the received SNR from one OCI cell assuming a user placed in pt. A. is $p_O = P(3r/(2\cos(\pi/6)))^{-\alpha}$ and

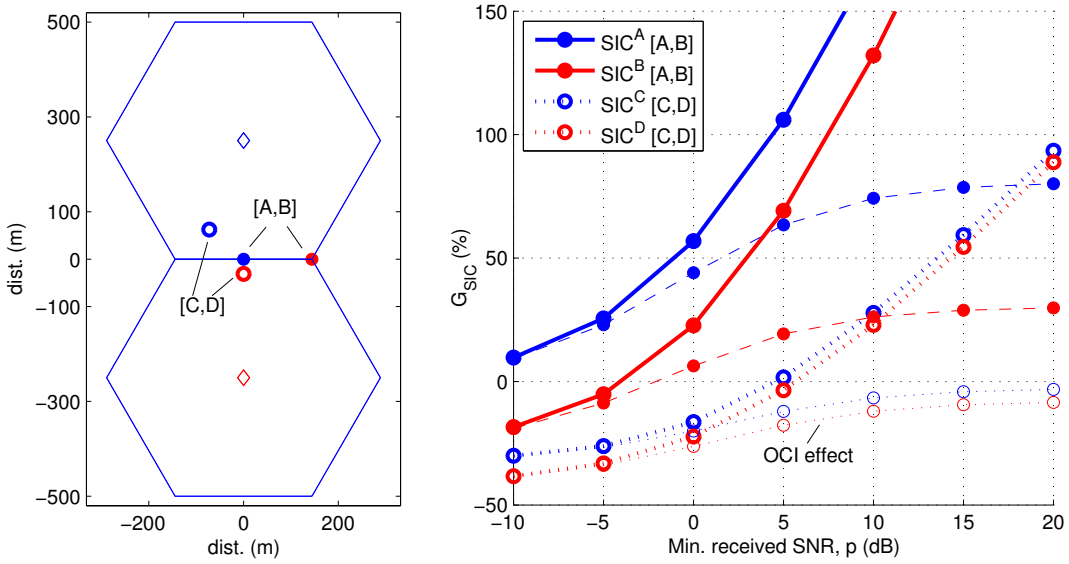

Figure 4.4: SIC gain upper bound and effect of OCI.

can be approximated as $p_O \approx p/5$. Additionally, four OCI cells are considered. Consequently, the average OCI SNR is fixed to $P_{Oi} = 4p/5$ where $p = P(r/\cos(\pi/6))^{-\alpha}$ is the minimum value for P_i received at any hexagon corner (e.g. pt.B). Figure 4.4 illustrates the wide range of values that SIC gain could take. In the best case $[A, B]$, gains are found even for the low-SNR regime, followed by a slope of 100% gain per decade in the high-SNR regime. The huge benefits are deemed in presence of OCI, where gains may oscillate from 30% to 80%. In a less favorable situation where users are not so close to the cell edge (points $[C, D]$), the gain values are moderate in the high SNR regime, and completely fade out under the effect of OCI.

Size of the SIC gain region

Finally, to have a better understanding of the SIC gain region, although its size and shape depends on the position of both receivers and the transmitted power, one of the users will be fixed conveniently at pt. B, while changing the power changes the size of the SIC gain region. To describe the relation between the transmitted power and the size of the SIC gain region the

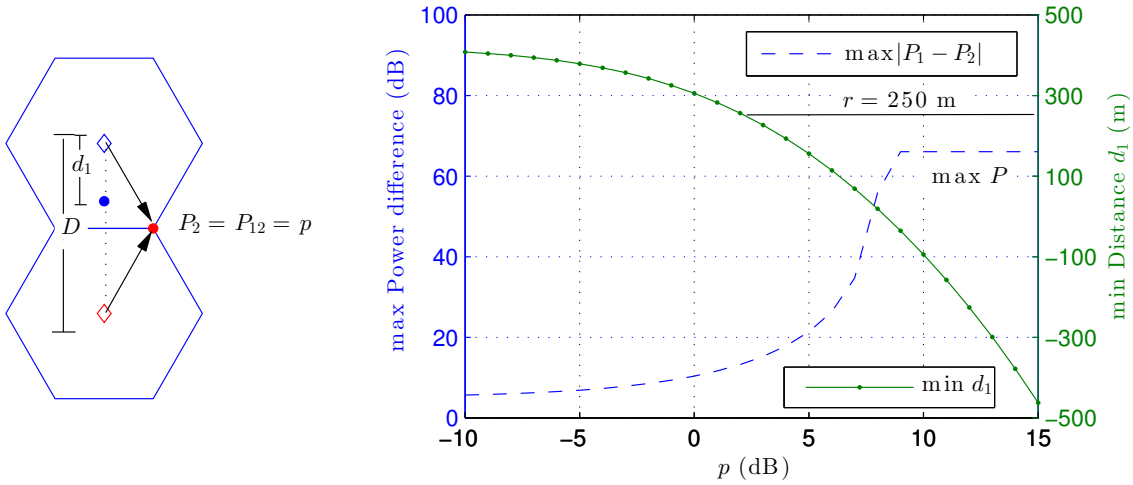

Figure 4.5: Minimum distance and maximum power difference for SIC Gain in two hexagonal cells. $D = 500$ m

following problem is solved: What is the maximum difference in desired signal powers such that the SIC user is inside the SIC gain region?. That is $\max_{P_i} |P_1 - P_2|$ subject to $P_{21} > P_2/(1 + P_{12})$. Let $\beta_1 P_1 = P_{21}$ and $\beta_2 P_2 = P_{12}$ to properly write the optimization problem as

$$\begin{aligned} &\max_{P_i} |P_1 - P_2| \\ \text{s.t.} \quad &\beta_1 P_1 > \frac{P_2}{1 + \beta_2 P_2}, \end{aligned} \tag{4.10}$$

Note that $\beta_1 = f_1(P_1)$ and $\beta_2 = f_2(P_2)$, but these functions cannot be written explicitly in closed form. However, according to the upper bound derived in the previous section, Rx_2 is placed in pt. B. while Rx_1 moves inside its cell on the line between the two Txs. The system configuration is illustrated in Figure 4.5.

The system configuration implies $P_2 = p$ and a line to move Rx_1 hence, the problem in (4.10) can be solved finding initially the minimum distance d_1 from Tx_1, where Rx_1 can be

placed while the SIC gain condition is active:

$$\min_{d_1} \left| P d_1^{-\alpha} - p \right|$$
$$\text{s.t.} \quad P(D - d_1)^{-\alpha} > \frac{p}{1+p}, \tag{4.11}$$

where $D = 2r$ is the distance between both transmitters. Solving (4.11) for d_1

$$d_1 = D - \left(\frac{p}{P(1+p)} \right)^{-1/\alpha}, \tag{4.12}$$

and finally $P_1 = P d_1^{-\alpha}$. The results are shown in Figure 4.5. Observing the low SNR regime, the minimum distance d_1 reaches the celledge ($r = 250$ m) from $p = 2$ dB. When $d_1 = 0$ m, an additional distance is included to simulate the transmitter height and therefore the maximum power difference stagnates at that point. Negative values for d_1 mean that the SIC gain region extends beyond the position of Tx_1.

4.2.3 Cooperative SIC in N-cells

The SIC gain condition can be extended to the general IC with N transmitters and N receivers. In the case where a user receives N signals, $N-1$ of which are interference that might be decoded and suppressed successively, it is also possible to find a condition guaranteeing that the use of a SIC receiver leads to a gain in the total rate of the system. Initially, only one of the N receivers uses its SIC capability. This user will suppress all the $N-1$ interference sources to decode its desired signal at the interference-free rate. In contrast, the rest of the $N-1$ users should adapt their rates to be decodable at the user doing SIC and decodable to themselves. The result is explained in the following theorem.

Theorem 6. *The following conditions are necessary and sufficient to increase the sum rate with respect to IaN by performing SIC in the u-th receiver in an N-cell network:*

$$1 + \sum_{j \neq u}^{N} P_{ju} > \prod_{i \neq u}^{N} (1 + \mathrm{SINR}_i) \tag{4.13a}$$

$$R_{k \neq u} = \min \left\{ C \left(\frac{P_{ku}}{1 + \sum_{j=1}^{k-1} P_{ju}} \right), C\left(\mathrm{SINR}_k\right) \right\} \tag{4.13b}$$

Proof. Since Rx_u receives N signals, there are N rates forming a corner of the capacity region of the MAC at Rx_u. These rates are

$$\left[C\left(P_u\right), C\left(\frac{P_{1u}}{1+P_u}\right), \ldots C\left(\frac{P_{Nu}}{1+\sum_{j\neq N}^{N} P_{ju}}\right)\right],$$

and can be achieved using SIC. Following the same argument as in (4.9), the network operating rates with N Tx-Rx pairs in the ***Cooperative SIC*** strategy are

$$R_u = C(P_u),\ R_{k\neq u} \ = \ \min\left\{C\left(\frac{P_{ku}}{1+\sum_{j=1}^{k-1} P_{ju}}\right).C\left(\text{SINR}_k\right)\right\} \tag{4.14}$$

The sum of these rates is again denoted as SR_{SIC}. In the worst possible case for SIC gain, where the sum of the SIC rates is very close to SR_{IaN}, all the receivers $k \neq u$ get the IaN rates $R_{k\neq u} = C\left(\text{SINR}_k\right)$. However, the SIC gain condition holds true since

$$\begin{aligned}
\text{SR}_{\text{SIC}} \ &> \ \text{SR}_{\text{IaN}} \\
C\left(P_u\right) + C\left(\text{SINR}_1\right) \ldots + C\left(\text{SINR}_N\right) \ &> \ \sum_{i=1}^{N} C\left(\text{SINR}_i\right) \\
\text{Always true} \Rightarrow &\boxed{C\left(P_u\right) \ > \ C\left(\text{SINR}_u\right)}.
\end{aligned} \tag{4.15}$$

Yet, the largest difference in $\text{SR}_{\text{SIC}} > \text{SR}_{\text{IaN}}$ will be obtained if all rates are equal to the maximum decodable rate according to the MAC channel formed by the N signals arriving at Rx_u and achievable using a SIC receiver. From (4.14), this implies that $R_{k\neq u} = C\left(P_{ku}/(1+\sum_{j=1}^{k-1} P_{ju})\right)$. In that case, the SIC gain condition can be expanded as

$$\begin{aligned}
C\left(P_u\right) + C\left(\frac{P_{1u}}{1+P_u}\right) \ldots + C\left(\frac{P_{Nu}}{1+\sum_{j\neq N}^{N} P_{ju}}\right) \ &> \ \sum_{i=1}^{N} C\left(\text{SINR}_i\right) \\
(1+P_u)\left(\frac{1+P_u+P_{1u}}{1+P_u}\right) \ldots \left(\frac{1+\sum_{j=1}^{N} P_{ju}}{1+\sum_{j\neq N}^{N} P_{ju}}\right) \ &> \ \prod_{i=1}^{N}\left(1+\text{SINR}_i\right) \\
1+\sum_{j=1}^{N} P_{ju} \ &> \ \left(1+\frac{P_u}{1+\sum_{j\neq u}^{N} P_{ju}}\right)\prod_{i\neq u}^{N}\left(1+\text{SINR}_i\right) \\
1+\sum_{j=1}^{N} P_{ju} \ &> \ \left(\frac{1+\sum_{j=1}^{N} P_{ju}}{1+\sum_{j\neq u}^{N} P_{ju}}\right)\prod_{i\neq u}^{N}\left(1+\text{SINR}_i\right) \\
N\text{-cell SIC gain condition: } \Rightarrow &\boxed{1+\sum_{j\neq u}^{N} P_{ju} \ > \ \prod_{i\neq u}^{N}\left(1+\text{SINR}_i\right),}
\end{aligned}$$

which concludes the proof. □

Theorem 6 proves a condition ensuring that one of the N receivers will be able to perform $N-1$ loops of SIC to get an interference-free rate (the largest possible) while the rest of $N-1$ users will either get their IaN rate or smaller rate that is decodable at Rx_u.

4.2.4 Superposition of MAC capacity regions

The IC formed by N Tx-Rx pairs can be divided into N MACs. Any N-user MAC has a known capacity region: a polyhedron in $\mathbb{R}^N$ composed of 2^N-1 hyperplanes formed by all conditions of the type

$$\sum_{i\in\mathcal{S}} R_i < C\left(\sum_{i\in\mathcal{S}} P_i\right), \tag{4.16}$$

where $\mathcal{S}$ is any non-empty subset of the set of all users $[1\dots N]$. The resulting polyhedron has $N!$ corners representing all the possible decoding orders of the received signals that can be obtained using SIC.

The use of SIC for the IC with N Tx-Rx pairs can also be understood superposing the N polyhedra corresponding to the N MACs (as shown in Figure 4.1 for $N=2$). This superposition creates a complex polyhedron $\in \mathbb{R}^N$ from which is possible to obtain a region of achievable rates for the IC by means of cooperative SIC. Note that this achievable region is by no means proved to be the IC capacity region in an information theory context. The N superposed polyhedra follow interesting mathematical properties as the received power changes. This variations may be reflected on the coverage area in a wireless network and its understanding provides key insights for the use of cooperative SIC strategies. With this purpose, it is necessary to formulate the following definitions. The $NN!$ corners of the N polyhedra obtained from an NxN-IC, can be classified as:

Definition 1. *Internal corner: A set of rates $\in \mathbb{R}^N$ decoded with SIC such that the first rate decoded is the one transmitted by the serving transmitter, i.e.*

$$\left[C\left(P_{1i}\right), C\left(\frac{P_{2i}}{1+P_{1i}}\right), \dots C\left(\frac{P_i}{1+\sum_{j\neq i}^{N} P_{ji}}\right)\right] \tag{4.17}$$

Note that the first rate to be decoded here is $R_i = C\left(P_i/(1+\sum_{j\neq i}^{N} P_{ji})\right)$ and the decoding order is $i, \ldots, 2, 1$.

Definition 2. *Ordinary corner: A set of rates $\in \mathbb{R}^N$ decoded with SIC such that the rate transmitted by the serving transmitter is neither the first nor the last rate to be decoded, i.e.*

$$\left[C\left(P_{1i}\right), \ldots C\left(\frac{P_i}{1+\sum_{j\neq i}^{i-1} P_{ji}}\right), \ldots C\left(\frac{P_{Ni}}{1+\sum_{j=1}^{N-1} P_{ji}}\right)\right] \tag{4.18}$$

Definition 3. *External corner: A set of rates $\in \mathbb{R}^N$ decoded with SIC such that the rate transmitted by the serving transmitter is last rate (interference-free) to be decoded, i.e.*

$$\left[C\left(P_i\right), C\left(\frac{P_{2i}}{1+P_i}\right), \ldots C\left(\frac{P_{Ni}}{1+\sum_{j=1}^{N} P_{ji}}\right)\right] \tag{4.19}$$

These three denominations of the polyhedron corners are not only exhaustive but non overlapping. It is also important to remember that all corners belong to the hyperplane where $\sum_{i=1}^{N} R_i = C(\sum_{i=1}^{N} P_i)$ and consequently, all corners (as all points in the hyperplane) have the same sum rate.

Regarding the cooperative SIC transmission scheme proposed in (4.14), the MAC corners can either be *feasible* or *degraded*.

Definition 4. *Corner feasibility: A corner is said to be feasible if every rate decoded by the u-th receiver with SIC, is also decodable by the respective receiver to which the symbols were transmitted. This implies that for all $k \neq u$*

$$C\left(\frac{P_{ku}}{1+\sum_{j=1}^{k-1} P_{ju}}\right) < C\left(\mathrm{SINR}_k\right) \tag{4.20}$$

Definition 5. *Corner degradation: A corner is said to be degraded to denote the interior point in a polyhedron where a non feasible corner is shifted to guarantee the feasibility of the N rates at the respective N receivers. Hence, a corner needs to be degraded if at least one rate for the k-th user $k \neq u$ is*

$$C\left(\frac{P_{ku}}{1+\sum_{j=1}^{k-1} P_{ju}}\right) > C\left(\mathrm{SINR}_k\right) \tag{4.21}$$

Based on these simple definitions and resting inside the cellular context where $P_i > Pji$, $\forall i$, the result in (4.15) can be rephrased as follows.

Proposition 7. *Any external corner provides sum rate gains if it belongs to a polyhedron where the SIC gain condition holds true.*

The proof of this proposition is precisely (4.15), where the "worst case" refers to the case of corner degradation: the $N-1$ SIC rates are shifted to the corresponding IaN rates. Even if the corner (external by definition) is unfeasible, after degradation the SIC gain is preserved.

Regarding internal corners, although they are closer to the point of maximum fairness, where each Rx will get a similar rate, they present no interest for the use of one SIC receiver, as shown in the following proposition.

Proposition 8. *Any internal corner is unfeasible under the SIC gain condition. Furthermore, if it is degraded, the sum rate gain vanishes.*

Proof. See Appendix C.0.3 □

In summary, the cooperative SIC strategy seeks at operating at the external corners of MAC capacity regions where the SIC gain condition holds true. The internal corners although closer to the point of maximum fairness, cannot be reached without loosing the sum rate gains. Ordinary corners take some importance as will be explained later in section 4.2.6.

4.2.5 MAC levels

We will use the term *level* to denote the number of transmitters in a given MAC. In a MAC of N Tx-Rx pairs, there are $N-1$ signals that can be decoded and suppressed with SIC. In regard of the different MAC levels, the IC formed by N Tx-Rx pairs, not only contains N MACs of level N but also $\binom{N}{n}$ MACs of level n, with $2 \leq n \leq N-1$. Increasing the MAC level, shrinks the area where the SIC gain condition is valid, but it also increases the amounts of net and relative gains in sum rate with respect to IaN. In this section, the relation between the different SIC levels presented in the NxN-IC is established as well as the form of the general SIC gain condition that should verify all conditions for each individual MAC.

Proposition 9. *A necessary and sufficient condition to guarantee that the sum rate of a feasible corner of level $n+1$ is greater than the sum rate of a feasible corner of level n is*

$$P_{vu} > \frac{P_v}{1+\sum_{j\neq v}^{n+1} P_{jv}}, \tag{4.22}$$

where v denotes the additional link in the MAC of level $n+1$.

Proof. The proof follows easily after some algebraic manipulation of the inequality comparing the sum rate of the system operating in a MAC corner of level $n+1$ versus the same system operating in a MAC corner of level n subject to the fact that in both cases the SIC gain condition of the same user holds true. Let $\mathrm{SR}_{\mathrm{SIC^u}}^{(\mathrm{n+1})}$ be the sum rate of the $(n+1)$-level MAC at Rx_u. The inequality comparing both levels is

$$\begin{aligned}
\mathrm{SR}_{\mathrm{SIC^u}}^{(\mathrm{n+1})} &> \mathrm{SR}_{\mathrm{SIC^u}}^{(\mathrm{n})} + C(\mathrm{SINR}_{vu}) \\
\sum_{i=1}^{n+1} C\left(\frac{P_{iu}}{1+\sum_{j=1}^{i-1} P_{ji}+P_{vu}}\right) &> \sum_{i=1}^{n} C\left(\frac{P_{iu}}{1+\sum_{j=1}^{i-1} P_{ji}+P_{vu}}\right) + C\left(\frac{P_v}{1+\sum_{j=1}^{n} P_{jv}}\right) \\
\Rightarrow P_{vu} &> \frac{P_v}{1+\sum_{j\neq v}^{n+1} P_{jv}}.
\end{aligned} \tag{4.23}$$

□

The above result can be further clarified noticing that the SIC gain condition of level n requires that the $(n+1)$-th link is treated as OCI and hence, equation (4.8) is used. The n-level SIC gain condition where v denotes the OCI link is

$$\begin{aligned}
1+\frac{\sum_{j\neq u}^{n} P_{ju}}{1+P_{vu}} &> \prod_{i\neq u}^{n}\left(1+\frac{P_i}{1+\sum_{j\neq i}^{n} P_{ji}+P_{vi}}\right) \\
1+P_{vu}+\sum_{j\neq u}^{n} P_{ju} &> \prod_{i\neq u}^{n}\left(1+\frac{P_i}{1+\sum_{j\neq i}^{n} P_{ji}+P_{vi}}\right)(1+P_{vu}).
\end{aligned} \tag{4.24}$$

Then, replacing (4.22) in the right-hand side of (4.24), yields

$$1+\sum_{j\neq u}^{n+1} P_{ju} > \prod_{i\neq u}^{n+1}\left(1+\frac{P_i}{1+\sum_{j\neq i}^{n+1} P_{ji}}\right), \tag{4.25}$$

which is precisely the $(n+1)$-level SIC gain condition at Rx_u.

As the number of possibilities for SIC gains grows with the number of links, in order to perform the best cooperative SIC scheme, a network with N Tx-Rx pairs should verify if any of the sum rates corresponding to all the feasible corners per MAC per level is indeed greater than $\mathrm{SR}_{\mathrm{IaN}}$. The total number of possible SIC sum rates is

$$\#\mathrm{SR} = \sum_{n=2}^{\overbrace{N}^{\text{levels}}} \underbrace{\binom{N}{n}}_{\text{MACs}} (\overbrace{n!}^{\text{corners}} - \underbrace{(n-1)!}_{\text{Int. cor.}}). \tag{4.26}$$

Consequently, a general SIC gain condition spanning all the sum rates achievable by cooperative SIC in the N-MACs superposed is stated in the following lemma.

Lemma 1. *There are $\sum_{n=2}^{N} n\binom{N}{n}$ different SIC gain conditions in a network with N Tx-Rx pairs. The logical union of all of them, determines the general SIC gain condition on the IC as follows*

$$\bigcup_{n=2}^{N} \bigcup_{m=1}^{\binom{N}{n}} \bigcup_{u=1}^{n} \mathrm{SIC}^{u}_{[m](n)} \tag{4.27}$$

where (n) is the MAC level, $[m]$ is an index for $\mathcal{S}_n$ the set of all MACs of level n and $u \in \mathcal{S}_n(m)$ is the index for the receiver doing SIC. Then, the individual SIC gain condition is defined as the logical value

$$\mathrm{SIC}^{u}_{[m](n)} := \left[\frac{1 + \sum_{j \neq u}^{n} P_{ju}}{1 + \sum_{\substack{k=n+1 \\ k \neq u}}^{N} P_{ku}} > \prod_{i \neq u}^{n} \left(1 + \frac{P_i}{1 + \sum_{l \neq i}^{N} P_{li}} \right) \right] \tag{4.28}$$

Figure 4.6 illustrates the different MAC levels found in the 3x3-IC formed by the cells depicted in the upper-left corner. For the 2-level conditions the third link produces a strong OCI preventing their validity. However each of the 3-level conditions holds true as shown in the three upper-right insets where the MAC capacity regions are individually highlighted. The bottom-right graphic shows in a dark gray plane, the region of all points that can be achieved by time sharing the rates obtained in the external corners. For the system to achieve such rates, one of the external corners of each MAC should be feasible without degradation. The advantage of the time sharing strategy is the ability to achieve the SIC gains and provide the rate allocation with maximum fairness among the N users.

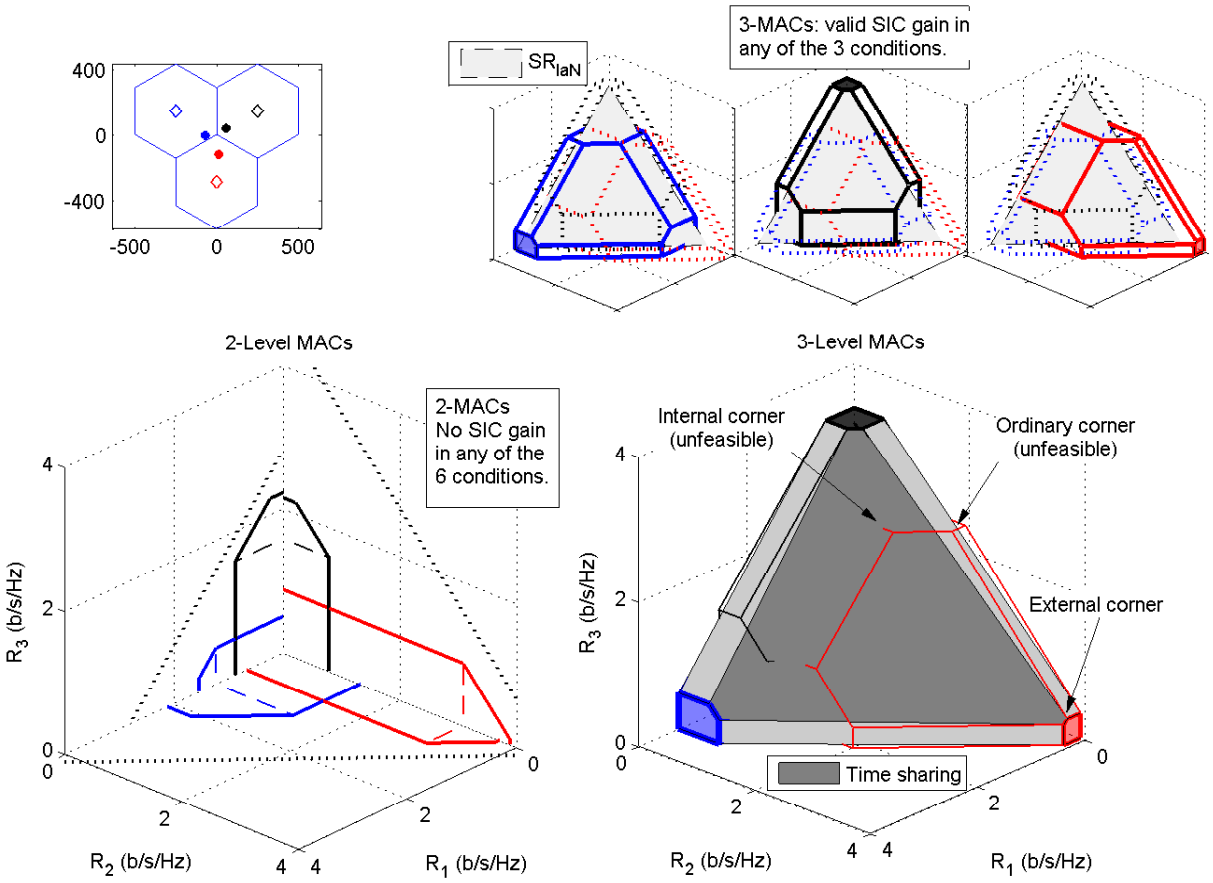

Figure 4.6: MAC levels in a 3 Tx-Rx pairs network.

4.2.6 Simultaneous SIC in NxN-IC

All results presented so far take place in a network where only one receiver uses its SIC capability at the same time-frequency resource allocation. If the rates used to satisfy SIC at a given receiver are not achievable at the respective receivers, they should be reduced to guarantee the achievability at both the victim (i.e. the user doing SIC) and the intended user, in an operation named corner degradation described in (4.21). However, degradation can be avoided, i.e. the feasibility of ordinary or internal corners can be obtained by using SIC at multiple users in the same resource slot. However, the IC for $N = 2$ is a particular case where there are no ordinary

corners (corners are either internal or external), and in the cellular context $P_i > P_{ji},\ \forall i$, any unfeasible corner cannot be feasible by means of simultaneous SIC. Let us revisit the case where a SIC gain condition holds (for Rx_i) and the external corner is unfeasible:

$$P_{ji} > \frac{P_{ji}}{1+P_i} > \frac{P_j}{1+P_{ij}}. \tag{4.29}$$

Rx_i will decode both rates if the system operates in its external corner $[R_i = C(P_i), R_j = C(P_{ji}/(1+P_i))]$, meanwhile Rx_j will be unable to decode its rate $R_j = C(P_{ji}/(1+P_i))$ and cannot use its SIC capability because the interference rate ($C(P_i)$) is greater than the Shannon capacity of the interference link i.e. $C(P_i) > C(P_{ij}/(1+P_j))$. Outside the cellular context, there may be some cases where the IC for $N = 2$ is prone for the use of simultaneous SIC as will be shown in section 4.3.1. In this section, the simultaneous SIC is treated for the IC with $N > 2$.

An example of a successful use of simultaneous SIC is presented as follows. Assume a given condition $\mathrm{SIC}^1_{(N)}$ is valid, and Rx_1 is initially the only user performing SIC at the external corner

$$[R_1, R_2, \ldots R_N] = \left[C\left(P_1\right), C\left(\frac{P_{21}}{1+P_1}\right), \ldots C\left(\frac{P_{N1}}{1+\sum_{j=1}^{N-1} P_{j1}}\right)\right]. \tag{4.30}$$

If the corner is feasible, all rates are achievable at the respective users i.e. $R_i < C(\mathrm{SINR}_i), \forall i \neq 1$). But not being the case, for instance if $R_2 > C(\mathrm{SINR}_2)$; the corner degradation makes the new point feasible $R_2 = C(\mathrm{SINR}_2)$ reducing the sum rate as the new operating point will be

$$[R_1, R_2, \ldots R_N] = \left[C\left(P_1\right), C\left(\frac{P_2}{1+\sum_{j\neq 2}^{N} P_{j2}}\right), \ldots C\left(\frac{P_{N1}}{1+\sum_{j=1}^{N} P_{j1}}\right)\right] \tag{4.31}$$

Even though, the degradation of R_2 can be avoided as soon as Rx_2 is able to get $R_2 = C(P_{21}/(1+P_1))$ using SIC. This requires that all the signals decoded in the corner (4.30) before R_2 should be decodable at Rx_2 i.e.

$$\begin{aligned} R_N &= C\left(\frac{P_{N1}}{1+\sum_{j=1}^{N-1} P_{j1}}\right) < C\left(\frac{P_{N2}}{1+\sum_{j=1}^{N-1} P_{j2}}\right) \\ &\ldots \\ R_3 &= C\left(\frac{P_{31}}{1+P_1+P_{21}}\right) < C\left(\frac{P_{32}}{1+P_{12}+P_2}\right), \end{aligned}$$

which leads the system to operate at the largest sum rate possible in the external corner by using SIC at Rx_1 suppressing $N-1$ signals and using SIC at Rx_2 suppressing $N-2$ signals. This result is generalized in the following proposition.

Proposition 10. *If a corner is unfeasible due to a set of rates* $\mathcal{U}_R = [R_\alpha \dots R_\omega]$ *with* $\alpha > 1$ *and* $1 < \omega \leq N-1$*; its feasibility can be achieved using SIC if*

$$\frac{P_{i1}}{1+\sum_{j=1}^{i-1} P_{j1}} < \frac{P_{ik}}{1+\sum_{j=1}^{i-1} P_{jk}} \quad \forall i,\ k+1 \leq i \leq N \text{ and } \forall k,\ \alpha \leq k \leq \omega \tag{4.32}$$

A conclusion can be drawn from Proposition 10: simultaneous SIC may avoid corner degradation for external, ordinary or internal corners. However only one of the users doing SIC is imposing rates on the other links. The other users should verify that they can achieve the imposed rates using the SIC capability. Furthermore if the system operates in a external corner of the polyhedron having the largest SIC gain and this corner is already feasible, the sum rate cannot be further increased using several SIC receivers at operating in a different corner. Still, the simultaneous SIC conditions may lead the system to operate in a non-external corner and henceforth increasing the system fairness.

Finally this section is closed with two important remarks.

Remark 1*: Not all conditions in Proposition 10 may happen in a cellular context.* Consider an ordinary corner for SIC at Rx_1 with the form

$$[R_1, R_2, \dots R_N] = \left[C\left(P_{21}\right), C\left(\frac{P_1}{1+P_{21}}\right), \dots C\left(\frac{P_{N1}}{1+\sum_{j=1}^{N-1} P_{j1}}\right)\right]. \tag{4.33}$$

If $R_2 \in \mathcal{U}_R$, simultaneous SIC at Rx_2 could be used to avoid degradation. Therefore, Rx_2 should be able to decode the signal from Tx_1 after having erased all previous signals in the corner's order $[N, \dots 1, 2]$ to get $C(P_{21})$. The final condition is

$$\frac{P_1}{1+P_{21}} < \frac{P_{12}}{1+P_2}, \tag{4.34}$$

which is impossible in a cellular context where $P_i > P_{ji},\ \forall i$.

Remark 2*: Several cooperative SIC rate allocations may take place simultaneously.* Different from several users performing SIC simultaneously, this remark implies that several users

where SIC gain conditions hold true may impose several rates to the same user as the result of multiple cooperative SIC rate allocations. As an example, take a 3x3-IC and suppose that SIC gain conditions are valid for $\mathrm{Rx}_{1,2}$ over Tx_3, which means that both users have a corner where the signal from Tx_3 is eliminated yielding a larger sum rate than $\mathrm{SR}_{\mathrm{IaN}}$. These two corners can be expressed as

$$\text{SIC}^1\text{:}\quad [R_1, R_2, R_3] = \left[C\left(\frac{P_1}{1+P_{21}}\right), C\left(\mathrm{SINR}_2\right), C\left(\frac{P_{31}}{1+P_1+P_{21}}\right)\right] > \mathrm{SR}_{\mathrm{IaN}}$$
$$\text{SIC}^2\text{:}\quad [R_1, R_2, R_3] = \left[C\left(\mathrm{SINR}_1\right), C\left(\frac{P_2}{1+P_{12}}\right), C\left(\frac{P_{32}}{1+P_{12}+P_2}\right)\right] > \mathrm{SR}_{\mathrm{IaN}}.$$

Then, the system can take R_1 from SIC^1, R_2 from SIC^2 to take advantage of the SIC gains. However, to guarantee that Rx_3 will receive an achievable rate then

$$R_3 = C\left(\min\left\{\frac{P_{31}}{1+P_1+P_{21}}, \frac{P_{32}}{1+P_{12}+P_2}, \mathrm{SINR}_3\right\}\right), \tag{4.35}$$

and hence, the SIC gains may get lost guaranteeing that R_3 is decodable at every user. To ensure that both cooperative SIC allocations guarantee a larger sum rate that $\mathrm{SR}_{\mathrm{IaN}}$ the scheduling entity should verify that the sum of net gains is larger than the possible loss incurred in (4.35).

4.3 SIC Coordination in Wireless Networks

The use of SIC can be extended beyond cellular networks. Different types of wireless network may include SIC receivers as means to increase its spectral efficiency. When multiple users require to be served in the same cell, i.e. being inside the range of coverage of the same transmitter, SIC may have an important role. A non cellular network may not be able to use feedback loops to determine the best multi-antenna transmission mode, or may simply not have a transmitter with multiple antennas, or even more, may be already using all of its antennas to spatially separate some of its users. Even at this point, networks could cooperate to serve more users in the same time-frequency resource using SIC receivers. In this section the cellular context is abandoned in the sense that P_{ji} may or not be greater than P_i.

4.3.1 Using both SIC receivers in 2-cells

In this section we revisit the initial setting where two transmitters and two receivers form an IC which can be decomposed on two MACs. In the cellular context described in section 4.2.1, if the SIC condition holds, one of the users will activate SIC to increase its rate while the other will get the largest rate possible under some constraints. Dropping the cellular context, in this section both users can be placed anywhere in both cells. In particular the case where Rx_i is located inside cell j and vice-versa, leads into the following proposition.

Proposition 11. *In an interference channel, both receivers can perform SIC so that the sum rate is increased compared to* $\mathrm{SR}_{\mathrm{IaN}}$ *if*

$$P_1 \leq \frac{P_{12}}{1+P_2} \;\; \textit{and} \;\; P_2 \leq \frac{P_{21}}{1+P_1}, \tag{4.36}$$

and

$$P_1(1+P_2) < P_{12} \;\; \textit{and} \;\; P_2(1+P_1) \leq P_{21}. \tag{4.37}$$

Proof. The initial conditions to decode the interference messages at each user are

$$\mathrm{R}_1 \leq C\left(\frac{P_{12}}{1+P_2}\right) \;\; \text{and} \;\; \mathrm{R}_2 \leq C\left(\frac{P_{21}}{1+P_1}\right). \tag{4.38}$$

Next, after interference cancellation the desired message can be successfully decoded, satisfying the following conditions

$$\mathrm{R}_1 \leq C\left(P_1\right) \;\; \text{and} \;\; \mathrm{R}_2 \leq C\left(P_2\right). \tag{4.39}$$

□

This proposition states a well known result: In the very strong-interference regime, the interference channel achieves the capacity region when both users perform SIC [48]. In the wireless network context, this conditions can only happen if each user lays inside the coverage region of the other cell receiving a very strong interference signal, or in simple terms, being very close to its interference transmitter.

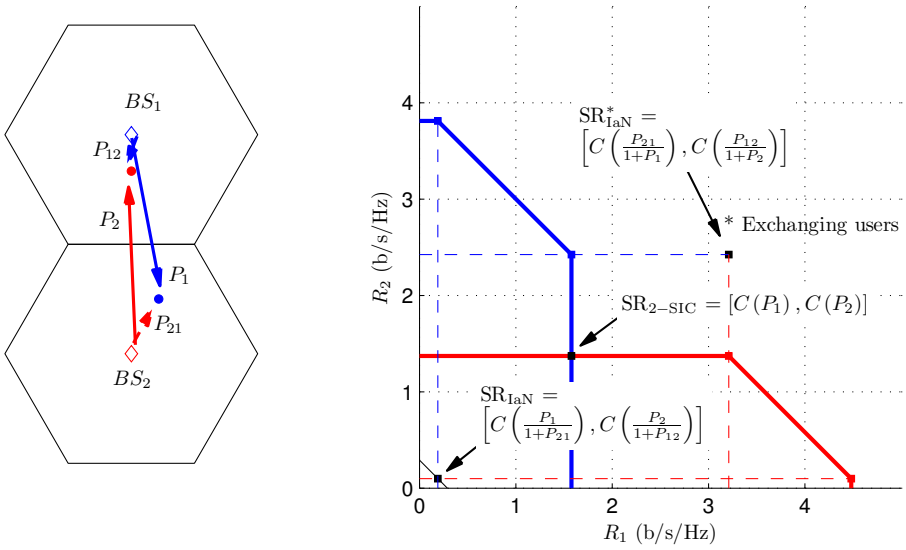

Figure 4.7: Capacity regions for two MAC superposed on a strong interference IC.

A feasible situation for Proposition 11 is drawn in Figure 4.7. Three important sum rate points are carefully described. For IaN receivers, if each transmitter serves its user, the maximum possible rates are extremely marginal. Performing SIC at each receiver both rates can be significantly lifted. However, the best possible sum rate is achieved if both Txs cooperate, serving each-other's user with no need for SIC. This result takes the analysis into the subject of flexible user association schemes.

4.3.2 Flexible User Association

Regarding the final result in section 4.3.1, if N transmitters serve an equal number of users (each Tx serves only one Rx), randomly placed inside the whole area of the network's coverage, it is not straightforward to find which transmitter should serve which receiver in order to maximize the sum rate. Strictly, the solution can be found by exhaustively searching the $N!$ association possibilities. However, as will be shown in this section, when SIC is used, the optimal association may be different from the one optimizing the network rate without SIC.

Without loss of generality, consider a system where $\mathrm{SR}_{\mathrm{SIC}^1} > \mathrm{SR}_{\mathrm{SIC}^2} > \mathrm{SR}_{\mathrm{IaN}}$. Moreover, the MAC capacity region of user 2 is fully inside the capacity region of user 1. To maximize the sum rate, following the cooperative SIC technique proposed in section 4.2.1, the system will operate in the external corner $[C(P_1), C(P_{21}/(1+P_1))]$ degraded to $[C(P_1), C(P_1/(1+P_{21}))]$. Likewise, the internal corner is $[C(P_{21}), C(P_1/(1+P_{21}))]$ but degraded, it boils down to the IaN operating point $[C(P_1/(1+P_{21})), C(P_2/(1+P_{12}))]$ (which is unfeasible by definition). Yet, if the system transmits the rates of the internal corner

$$\mathrm{SR}_{\mathrm{SIC}^1}^{[12]} = C(P_{21}) + C\left(\frac{P_1}{1+P_{21}}\right). \tag{4.40}$$

Rx_1 can decode both rates thus, in a flexible user association perspective, it could be served by Tx_2, releasing Tx_1 that could then serve Rx_2 with the maximum rate decodable at both Rxs, that is

$$\begin{aligned} R_{21} &\leq C\left(P_{21}\right) \\ R_{12} &\leq \min\left\{C\left(\frac{P_1}{1+P_{21}}\right), C\left(P_{12}\right)\right\} \overset{(a)}{=} C\left(\frac{P_1}{1+P_{21}}\right), \end{aligned} \tag{4.41}$$

where (a) is explained from the fact that the SIC gain conditions hold true. In summary, even if the system can operate in the external corner, the degraded internal corner constitutes another feasible operating point if a non-conventional user association is used, where Tx_1 serves Rx_2 and vice-versa.

Intuitively, scenarios where users are placed in neighboring cells are prone to require flexible user associations and may eventually activate the cooperative SIC scheme with flexible user association (cf (4.41)). Surprisingly, even if each user remains inside its hexagonal cell range, there is a region where the inverse Tx-Rx pairing using SIC as described in (4.41) reaches larger sum rates than the normal pairing where each transmitter serves the closest user with IaN receivers. This situation is depicted in Figure 4.8.

Finding the best user association for sum rate maximization in a NxN-IC turns easily into a highly complex problem. However, similar to the simultaneous SIC technique in section 4.2.6, changing the user association is useful in reducing the effect of corner degradation. The main principle states that a non-external corner may be less degraded under a non-conventional user

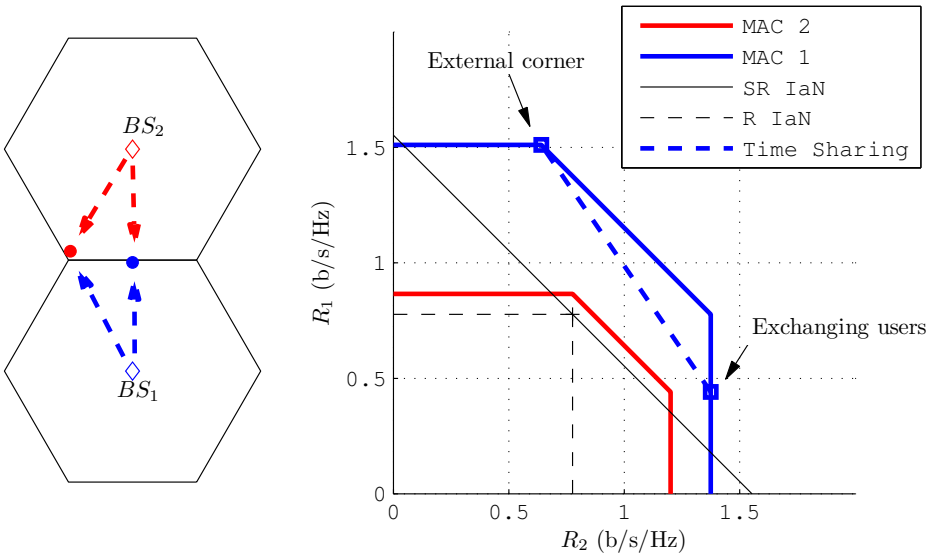

Figure 4.8: Flexible user association delivers larger sum rates by means of SIC even in a cellular context.

association henceforth, yielding a new operating point where SIC provides a larger sum rate. In this regard, a general rule to find a better user association is described as follows. Consider the following non-external corner at the $N-$dimensional capacity region of user i ($i \neq 1$) with decoding order $[1, 2 \dots N]$

$$\text{Corner}_i^{[12\dots N]} = \left[C\left(P_1\right), \dots C\left(\frac{P_{ni}}{1+\sum_{j=1}^{n-1} P_{ji}}\right), \dots C\left(\frac{P_{Ni}}{1+\sum_{j=1}^{N-1} P_{ji}}\right)\right]. \quad (4.42)$$

In a conventional user association the $N-1$ rates different from R_i should be degraded according to

$$R_{n\neq i} = \min\left\{ C\left(\frac{P_{ni}}{1+\sum_{j=1}^{n-1} P_{ji}}\right), \text{SINR}_n \right\}, \text{where } \text{SINR}_n = \frac{P_n}{1+\sum_{j\neq n}^{N} P_{jn}}. \quad (4.43)$$

We denote a given non-conventional user association, pairing the decoding order (i.e. the Tx's order) to a given Rx's order as $[1, 2 \dots N] \rightarrow [N, N-1, \dots 1]$, where Tx_1 serves Rx_N and so on. Consequently, the new degradation implies

$$R_{n\neq i} = \min\left\{ C\left(\frac{P_{ni}}{1+\sum_{j=1}^{n-1} P_{ji}}\right), \text{SINR}_{nl} \right\}, \text{where } \text{SINR}_{nl} = \frac{P_{nl}}{1+\sum_{j\neq n}^{N} P_{jl}}. \quad (4.44)$$

where n is the index of the Tx's order and l is the corresponding index for the Rx's order. Therefore, the sum rate for the conventional association is

$$\begin{aligned} \mathrm{SR}_{\mathrm{SIC^i}}^{[12\ldots\mathrm{N}]} &= \min\left\{C(P_{1i}), C(\mathrm{SINR}_1)\right\} + \min\left\{C\left(\frac{P_{2i}}{1+P_{1i}}\right), C\left(\mathrm{SINR}_2\right)\right\}, \ldots \\ &+ \min\left\{C\left(\frac{P_{Ni}}{1+\sum_{j=1}^{N-1} P_{ji}}\right), C\left(\mathrm{SINR}_N\right)\right\}, \end{aligned} \tag{4.45}$$

and the sum rate for the non-conventional association is

$$\begin{aligned} \mathrm{SR}_{\mathrm{SIC^i[N,N-1\ldots1]}}^{[12\ldots\mathrm{N}]} &= \min\left\{C(P_{1i}), C(\mathrm{SINR}_{1N})\right\} + \min\left\{C\left(\frac{P_{2i}}{1+P_{1i}}\right), C\left(\mathrm{SINR}_{2,N-1}\right)\right\}, \ldots \\ &+ \min\left\{C\left(\frac{P_{Ni}}{1+\sum_{j=1}^{N-1} P_{ji}}\right), C\left(\mathrm{SINR}_{N1}\right)\right\}. \end{aligned} \tag{4.46}$$

Finally, the system should operate in the non-external corner with the non-conventional association, if a centralized scheduling entity verifies that

$$\mathrm{SR}_{\mathrm{SIC^i[N,N-1\ldots1]}}^{[12\ldots\mathrm{N}]} > \mathrm{SR}_{\mathrm{SIC^i}}^{[12\ldots\mathrm{N}]}. \tag{4.47}$$

Using flexible user associations does not avoid corner degradation. Instead, it seeks at finding a Tx-Rx pairing to lessen the degradation sum rate loss. Since the number of sum rates that should be considered grows with $N!$ as well as the number of user associations, efficient algorithms to find the best operating point are needed. Ideally, the solution should combine user association and simultaneous SIC to find non-external feasible corners where the system can operate at larger sum rates providing much greater fairness compared to external corner points.

4.3.3 Bounds on SIC Gain for 2-cells

To illustrate the potential use of SIC in ad hoc scenarios a simplified network is used. Consider two transmitters whose coverage ranges are the semi circles shown in Figure 4.9. A minimum distance is reserved to avoid very high (non realistic) rate allocations due to the use of ideal Shannon codes (where $R = \log_2(1+\mathrm{SINR})$). Since the cellular case was already evaluated (see results in Figure 4.4), both users will be placed inside the red cell (cell 2). In a classical approach the network is designed to serve both users with Tx_2 in different time-frequency resources.

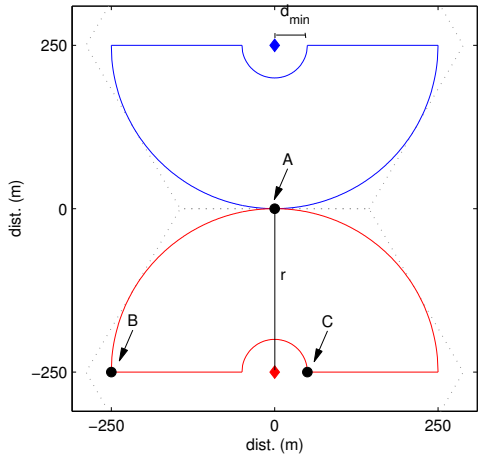

Figure 4.9: Simplified network for SIC gain bounds. Both users will be placed in the lower cell. Positions [A, B] and [C, A], represent the worst case and the best case for SIC gain respectively.

To increase the sum rate, the network could serve each user with a different transmitter. In such a case, the generated interference could be reduced applying the cooperative SIC method proposed in (4.9). As will be shown in this section, it is possible to find bounds for the SIC gain in such scenarios.

To take an example, the SIC gain condition at Rx_2, $\mathrm{SIC}^2 : P_{12} > \frac{P_1}{1+P_{21}}$ is evaluated. The worst case for SIC^2 is presented when P_{12} and P_{21} are at their minimum values and P_1 at its maximum. To achieve this, Rx_1 should be placed at point A and Rx_2 at point B as indicated in Figure 4.9. Let $p = Pr^{-\alpha}$ and $p_x = Pd_{min}^{-\alpha}$ be the minimum and maximum SNR received from Tx_2 respectively. On the other hand, $\hat{p}$ and $\hat{p}_x$ are the minimum and maximum SNR received from Tx_1. Having both users inside cell 2 implies that the variables in the SIC^2 condition are confined in the following ranges

$$p \geq P_{12} \geq \hat{p}, \;\; p_x \geq P_{21} \geq p, \;\; p \geq P_1 \geq \hat{p}. \tag{4.48}$$

Additionally, the net gain (in b/s/Hz) for the use of SIC at Rx_2 is defined as $\mathrm{G}_{\mathrm{net}} := \mathrm{SR}_{\mathrm{SIC}^2} - \mathrm{SR}_{\mathrm{IaN}}$. Based on these conditions, bounds on the SIC gain can be derived as stated in the

following lemma.

Lemma 2. *Assuming the network model described in section 4.3.3, the SIC gain can be bounded as*

$$\log_2\left(\frac{(1+p)(1+\hat{p})}{1+2p}\right) < \mathrm{G_{net}} < \log_2\left(\frac{(1+p)(1+p_x)}{1+\hat{p}+p_x}\right) \tag{4.49}$$

where $p = Pr^{-\alpha}$*,* $\hat{p} = (5)^{-\alpha/2}p$ *and* $p_x = Pd_{min}^{-\alpha}$ *is the maximum received* SNR*.*

Proof. Since Rx_1 and Rx_2 are placed at points A and B respectively (see Figure 4.9), the rate for Rx_1 is

$$\min\left\{C\left(\frac{P_1}{1+P_{21}}\right), C\left(\frac{P_{12}}{1+P_2}\right)\right\} = C\left(\frac{P_{12}}{1+P_2}\right). \tag{4.50}$$

Replacing $\mathrm{G_{net}} = \log 2(1+\mathrm{G}) = \mathrm{C(G)}$ (4.50) can be written as

$$\begin{aligned} C(\mathrm{G}) + C\left(\frac{P_1}{1+P_{21}}\right) + C\left(\frac{P_2}{1+P_{12}}\right) &= C(P_2) + C\left(\frac{P_{12}}{1+P_2}\right) \\ (1+\mathrm{G})\left(1+\frac{P_1}{1+P_{21}}\right) &= 1+P_{12} \\ 1+\mathrm{G} &= \frac{(1+P_{12})(1+P_{21})}{1+P_{21}+P_1} \\ \mathrm{G_{net}} &= \log_2\left(\frac{(1+P_{12})(1+P_{21})}{1+P_{21}+P_1}\right). \end{aligned} \tag{4.51}$$

The minimum value for the gain is found where the inequality for SIC^2 gain condition is as tight as possible. That is, if $P_1/(1+P_{21})$ is as big as possible and P_{12} is as small as possible. In our case this is equivalent to having users at points A and B, where $P_{12} = \hat{p}$, $P_{21} = p$ and $P_1 = p$. That is,

$$\mathrm{G_{net}} = \log_2\left(\frac{(1+p)(1+\hat{p})}{1+p+p}\right). \tag{4.52}$$

Similarly, the best case for the inequality in (4.50) requires that Rx_1 and Rx_2 are located at points C and A respectively, which corresponds to $P_{12} = p$, $P_1 = \hat{p}_x$ and $P_{21} = p_x$. Replacing these values in (4.51) the upper bound is obtained. □

Following the same derivations, it is also possible to find bounds for the SIC gain in presence of OCI. Setting the SNR received from other cells as $P_{Oi} = \kappa\hat{p}$ (with $\kappa > 1$) the result is expressed in the following corollary.

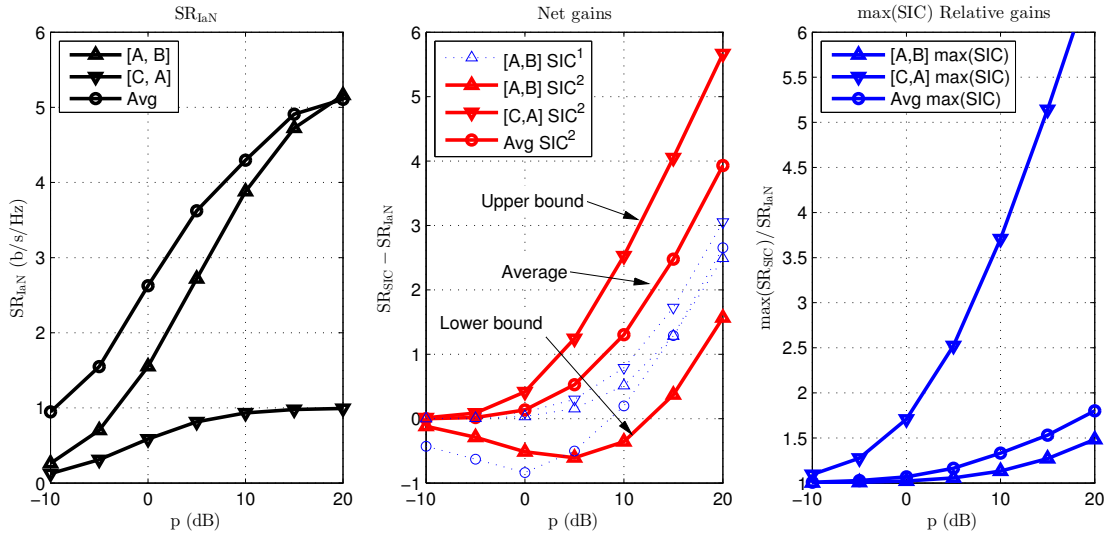

Figure 4.10: Relative and net SIC gains, for two users inside a semi-circular cell.

Corollary 6. *According to the scenario described in lemma 2, the inclusion of an average value of OCI equal for both receivers $P_{O1} = P_{O2} = \kappa\hat{p}$, the lower bounds for SIC gain are modified as*

$$\log_2\left(\frac{(1+p+\kappa\hat{p})\,(1+(\kappa+1)\hat{p})}{(1+\kappa\hat{p})\,(1+2p+\kappa\hat{p})}\right) < \mathrm{G_{net}} < \log_2\left(\frac{(1+p+\kappa\hat{p})\,(1+\kappa\hat{p}+p_x)}{(1+\kappa\hat{p})\,(1+\hat{p}+p_x+\kappa\hat{p})}\right) \quad (4.53)$$

Additionally, having found bounds for the SIC gain when two users are placed in the same cell, its average value can also be calculated, evaluating the gain expression in (4.51) over all possible positions inside cell 2, $[\omega_1, \omega_2] \in \Omega$ as

$$\overline{\mathrm{G_{net}}} = \iint_{\Omega} C\left(\frac{(1+Pd_{12}(\omega_2)^{-\alpha})\,(1+Pd_{21}(\omega_1)^{-\alpha})}{1+Pd_{21}(\omega_1)^{-\alpha}+Pd_1(\omega_1)^{-\alpha}}\right)\mathrm{d}\omega_1\,\mathrm{d}\omega_2, \quad (4.54)$$

where d_i and d_{ji} are functions of ω_i such that every pair $[d_1, d_{21}] = f(\omega_1)$ and $[d_2, d_{12}] = f(\omega_2)$ is a valid set of distances having both users inside cell 2.

Figure 4.10 validates the bounds found in (4.49). Three situations are depicted: Rx_1 and Rx_2 placed at points $[A, B]$ for the worst case of SIC^2, then placed at $[C, A]$ for the best case and finally, the values averaged over all possible positions where both users lay inside cell 2. It can be seen how the largest values of gains correspond to the smallest values of $\mathrm{SR_{IaN}}$. The

net gains may be negative in the worst case for values of $p < 12$ dB. However in the same layout $[A, B]$, the blue dashed line shows that $\mathrm{SR}_{\mathrm{SIC}^1}$ is always positive; establishing that even if one user is in the worst case for SIC gains, the other user can use SIC to improve the sum rate. Highlighting this result, the right hand side axes presents the maximum value of SIC gains divided by $\mathrm{SR}_{\mathrm{IaN}}$. Remarkably, the average value is always positive, concluding that in average SIC could increase the sum rate from 20% in the low-SNR to 80% in the high-SNR regime. Additionally, in some extreme cases with low $\mathrm{SR}_{\mathrm{IaN}}$, SIC can provide a staggering five-fold increase at $p = 15$ dB.

4.3.4 The limits of the SIC Gain condition

In a purely theoretical perspective, a user could perform an infinite number of SIC loops to decode and suppress interference signals received below a given outage threshold. But in wireless networks, those signals are spread around a given area and therefore may arrive with largely different powers at the SIC receiver, failing to reach the decodability edge. Hence, it is valid to ask if there is a network layout such that SIC gains are maximized. Moreover, in such a layout is there a limit for the number of signals that SIC can treat?

In section 4.2.2, it was shown where should users be placed to maximize SIC gains in the case of 2 hexagonal cells. A similar answer is needed for the case of N Tx-Rx pairs, and can be found with a rather simple argument. Given a network where $N = 3$, the most natural layout to increase the coverage is to place the transmitters in the corners of an equilateral triangle, whose side is given by a compromise between the minimum achievable rate and the coverage area. The best configuration for SIC gains, i.e. where the inequality (4.13a) $1 + \sum_{j\neq u}^{N} P_{ju} > \prod_{i\neq u}^{N} (1 + \mathrm{SINR}_i)$ gives the largest margin, is found when each P_{ju} is maximized and each SINR_i is minimized. There is indeed one point where these conditions hold simultaneously: the only common vertex of the three hexagonal cells centered on the transmitters, as seen in Figure 4.11. If any transmitter is moved from its position or any receiver is not placed in the vertex, SIC gains will be reduced. It is then straightforward to see that the same argument is valid for N transmitters and N receivers in a circular layout as explained in the following

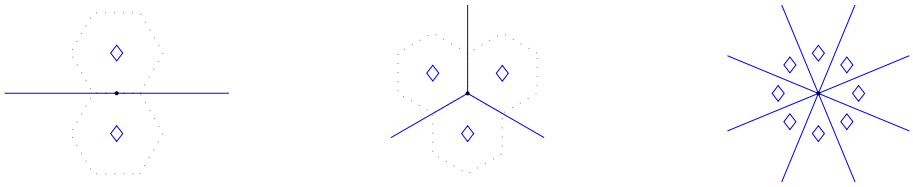

Figure 4.11: The best position for enabling cooperative SIC for $2, 3$ or 8 Tx-Rx pairs.

proposition.

Proposition 12. *If N transmitters are placed in a circumference of radius r (with equal angular separation), the best user location to increase SIC gain is having all users at the center of the circumference.*

In the case described in proposition 12, called the *ring network* in the sequel, and shown in Figure 4.12, the SIC gain condition can be evaluated as N grows indefinitely, where the following result is derived.

Theorem 7. *For any configuration of a ring network with N Tx-Rx pairs, there is always a region of non zero area where the SIC gain condition holds true at any transmitted* SNR.

Proof. The SIC gain condition in (4.13a) is written for the case of a ring network as

$$\begin{aligned} 1+\sum_{j\neq u}^{N} P_{ju} &> \prod_{i\neq u}^{N}(1+\mathrm{SINR}_i) \\ 1+\sum_{j\neq u}^{N} p &> \prod_{i\neq u}^{N}\left(1+\frac{p}{1+\sum_{j\neq i}^{N} p}\right). \end{aligned} \tag{4.55}$$

Then, the above inequality can be reduced to

$$\begin{aligned} 1+(N-1)p &> \left(\frac{p}{1+(N-1)p}\right)^{N-1} \\ (1+(N-1)p)^{N} &> p^{N-1} \\ \frac{(1+(N-1)p)^{N}}{p^{N-1}} &> 1. \end{aligned} \tag{4.56}$$

Finally, it is easily verified that the inequality (4.56) is always true for any value p and any number of Tx-Rx pairs. For the smallest possible value $N = 2$, the inequality holds true

$$(1+p)^2 > p, \tag{4.57}$$

or for asymptotically large value of N

$$\lim_{N\to\infty} \frac{(1+(N-1)p)^N}{p^{N-1}} = \infty > 1, \tag{4.58}$$

which proves that a non-empty region exists where SIC gain holds true in a ring network at any transmitted SNR and any number of Tx-Rx pairs. □

Another important feature of a ring network is that if all users are placed in the middle, then any user could perform SIC and all corners are achievable without degradation. This implies that the SIC sum rate is

$$\mathrm{SR}_{\mathrm{SIC}} = \sum_{i=1}^{N} C\left(\frac{p}{1+(i-1)p}\right). \tag{4.59}$$

In order to quantify the advantage of a ring network configuration, we denote the relative SIC gain as

$$\mathrm{G}_{\mathrm{rel}} = \frac{\mathrm{SR}_{\mathrm{SIC}}}{\mathrm{SR}_{\mathrm{IaN}}}. \tag{4.60}$$

To have a simpler expression, the relative gain is tightly bounded as follows.

Lemma 3. *The SIC gain obtained from a ring network of N Tx-Rx pairs can be upper-bounded as*

$$\mathrm{G}_{\mathrm{rel}} \leq 1 + \frac{\log_2\left(\left[\prod_{i=2}^{N-1} \frac{Ni-i}{Ni-N}\right]\left[1+\frac{2(N-1)p}{N}\right]\right)}{N\log_2\left(\frac{1+Np}{1+(N-1)p}\right)}. \tag{4.61}$$

Proof. See Appendix C.0.4. □

In Figure 4.12 the gains due to the use of SIC show the immense potential of ring network configurations. For large number of Tx-Rx pairs the network capacity can achieve a 2, 5, or up to 10-fold increase in the high-SNR regime. Ring networks remain an interest benchmark for hot spots and scenarios where users concentrate on reduced areas.

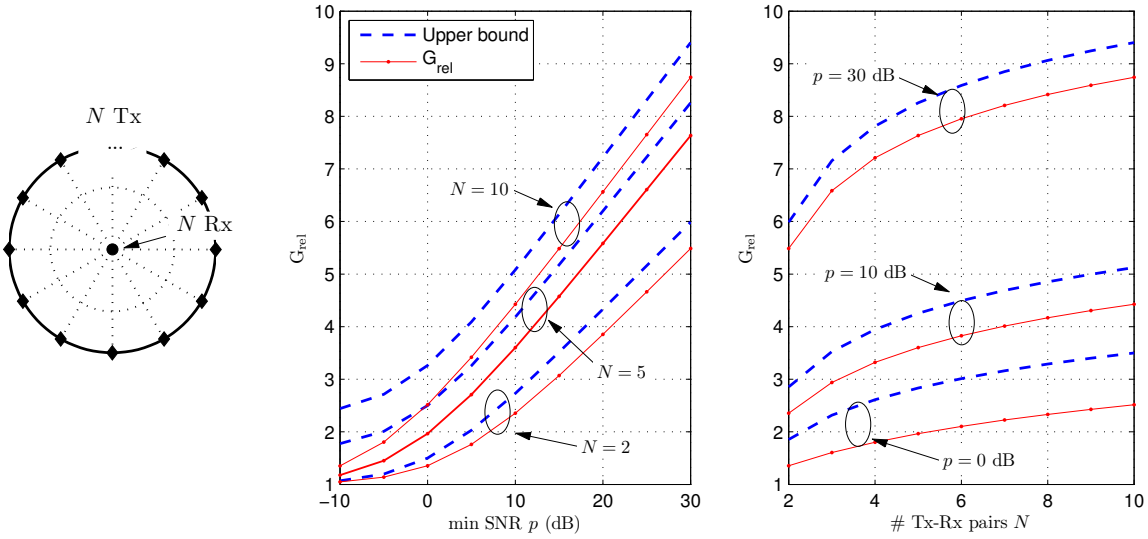

Figure 4.12: Ring network: N transmitters in a circle and N receivers in its center. Gains and upper bounds.

4.4 Effect of small-scale fading

Since all the analysis has been applied on received SNR values, the SIC gain conditions and their derived results may also apply for fading channels if the coherence time completely spans the coding block duration and the link adaptation loop latency provides the necessary conditions to guarantee the scheduling of cooperative SIC. As the study of the effects of fading and multi-antenna systems requires a thorough and extensive analysis, this section seeks to point out preliminary results on the impact of small-scale fading and the use of SIC on multi-antenna channels.

4.4.1 Fading on SIC gain condition

On the 2x2-IC we consider initially the SISO case to evaluate the ergodic sum rates obtained with SIC and IaN receivers. Let $P_{ji} = Pd_{ji}^{-\alpha}|h_{ji}|^2$, where h_{ji} accounts for the effective channel

gain from small-scale fading.

$$\begin{aligned} \mathrm{SR}_{\mathrm{SIC}^1} &= \mathbb{E}_H \left[C(P_1) + \min \left\{ C\left(\frac{P_{21}}{1+P_1}\right), C\left(\frac{P_2}{1+P_{12}}\right) \right\} \right] \\ \mathrm{SR}_{\mathrm{IaN}} &= \mathbb{E}_H \left[C\left(\frac{P_1}{1+P_{21}}\right), C\left(\frac{P_2}{1+P_{12}}\right) \right]. \end{aligned} \tag{4.62}$$

For notation simplicity $\mathbb{E}_H$ denotes the expectation over all fading variations. Additionally $P_{ji} = \gamma_{ji}|h_{ji}|^2$ is a short-hand notation used to state the SIC gain condition under small-scale fading in the following theorem.

Theorem 8. *The SIC gain condition for Rx$_1$ in the 2x2-IC under a small-scale fading is expressed in terms of the ergodic achievable rates as*

$$e^{1/\gamma_{21}} E_1\left(\frac{1}{\gamma_{21}}\right) > \frac{\gamma_2}{\gamma_{12}-\gamma_2} e^{-1/\gamma_{12}} E_1\left(\frac{-1}{\gamma_{12}}\right) + \frac{\gamma_2}{\gamma_2-\gamma_{12}} e^{1/\gamma_2} E_1\left(\frac{1}{\gamma_2}\right) \tag{4.63}$$

where $E_1(x)$ is the exponential-integral function of the first order.

Proof. See Appendix C.0.5. □

Equation (4.63) shows the inequality of the SIC gain condition in terms of the expected values of the Shannon capacity as expressed in equation (4.64), stating that in average, the sum rate using SIC at Rx$_1$ will be greater than using IaN receivers. But it is difficult to understand what the effect of small-scale fading is from (4.63). A graphical comparison is useful for understanding. The initial (non-fading) SIC gain condition in (4.3a) is equivalent to $C(P_{21}) > C(\mathrm{SINR}_2)$ which can be directly compared to the condition derived in Theorem 8 in order to evaluate the effect of small-scale fading. Figure 4.13 depicts the relative SIC gains as defined in (4.60) $\mathrm{G}_{\mathrm{rel}} = \mathrm{SR}_{\mathrm{SIC}}/\mathrm{SR}_{\mathrm{IaN}}$, with and without small-scale fading. In the presence of small-scale fading, although the sum rate is reduced with respect to a non-fading channel, the relative gain is increased. The reason is that the $\mathrm{SR}_{\mathrm{IaN}}$ is more affected than $\mathrm{SR}_{\mathrm{SIC}}$.

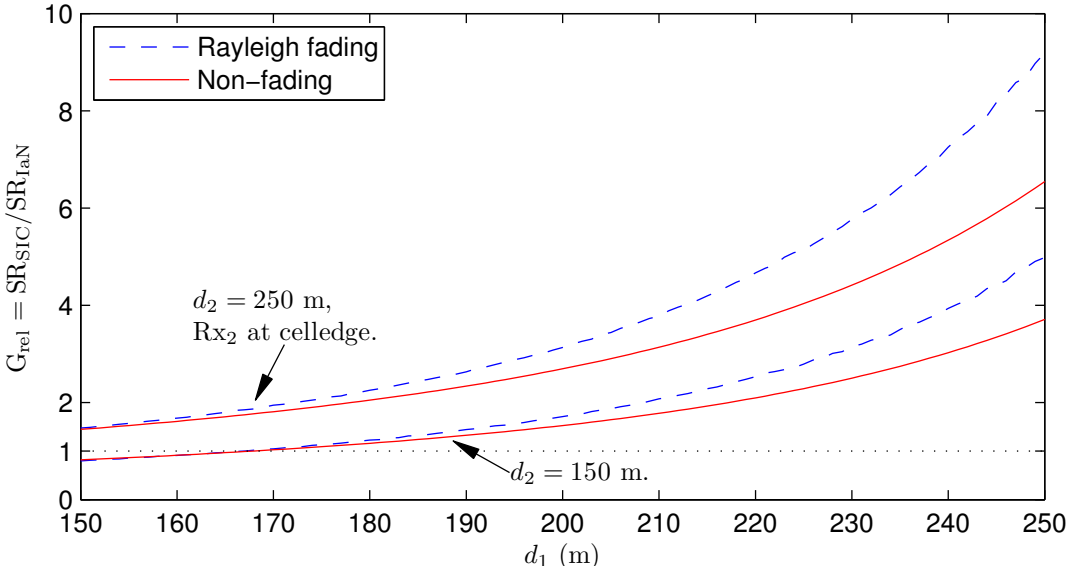

Figure 4.13: Relative SIC gains for Rayleigh fading and non-fading channels.

4.4.2 Multi-antenna systems on the SIC gain condition

The SIC gain condition in terms of the ergodic capacity

$$\begin{aligned} \mathrm{SR}_{\mathrm{SIC}^1} &> \mathrm{SR}_{\mathrm{IaN}} \\ \mathbb{E}_H\left[C(P_{21})\right] &> \mathbb{E}_H\left[C\left(\frac{P_2}{1+P_{12}}\right)\right] \end{aligned} \tag{4.64}$$

may be further analyzed in MISO and SIMO systems.

- *Multiple antennas at the transmitter:* The use of multiple antennas at the transmitter will require an additional feedback mechanism to provide the spatial CSI. If the multiple antennas are used to provide transmission diversity, the desired SNR values (P_i) will enjoy a power gain (in the order of the number of transmit antennas) while the interference SNR values (P_{ij}) will remain similar in average as the signal precoding is independent of the interference channels. This fact goes in contradiction with the SIC gain condition as stated in (4.64), note that P_{21} and P_{12} will in average remain equal, while P_2 should increase. Thus, reducing SIC gains. In contrast, if the multiple antennas are used for spatial multiplexing, additional interference signals will arrive from the same distance. These

additional signals may be treated as OCI (impacting SIC gains) or may be considered in a for SIC by increasing the MAC level as described in section 4.2.5. Since the distance is the same of the multiple interference signals, the situation becomes similar to the ring network described in section 4.3.4, which is clearly favorable for the use of cooperative SIC.

- *Multiple antennas at the receiver:* Multiple antennas at the receiver can also be used either for multiplexing or diversity. In the case of diversity, the received power is boosted proportionally to the number of non correlated copies of the signal that can be effectively combined determined by the number of properly separated antennas. Both the IaN and SIC receivers will obtain an increased SINR however, the SIC receiver benefits twice of this effect in a 2-MAC case (or N times in a N-MAC) whereas the IaN receiver only once. The difference lies in the number of times a SIC receiver has to decode a signal; $N-1$ interference signals and 1 desired signal; taking advantage several times of the diversity gain. When the multiple antennas at the receiver are used for spatial multiplexing, a thorough analysis is needed to determine whether SIMO or SIC is better to deal with interference and ultimately increase the system capacity. This analysis is outside the scope of this thesis.

4.4.3 Success probability analysis

The event of successfully decoding the desired signal at Rx_i is composed by the success in decoding the interference signal and the success of decoding the desired signal once the interference has been suppressed [75]. Consider that the link ji takes place over a MISO channel with η_{ji} antennas. The received SNR, P_{ji} follows a gamma distribution $Gamma(\eta_{ji}, \gamma_{ji})$ where $\gamma_{ji} = d_{ji}^{-\alpha}$ is the scale parameter and η_{ji} is the shape parameter.

Theorem 9. *If a system operates in the (feasible) external corner of a $2x2$ IC, the success probability for Rx_i is*

$$\mathbb{P}_{succ}^{\mathrm{SIC^i}} = e^{-\beta/\gamma_{ji}} \sum_{k=0}^{\eta_{ji}-1} \sum_{l=0}^{k} \binom{k}{l} \frac{(\beta/\gamma_{ji})^k}{k!} \frac{\partial^l \mathcal{L}_{P_i}(\beta/\gamma_{ji})}{\partial (\beta/\gamma_{ji})^l} e^{-\beta/\gamma_i} \sum_{k=0}^{\eta_i-1} \frac{(\beta/\gamma_i)^k}{k!}. \tag{4.65}$$

where $\mathcal{L}$ denotes the Laplace transform and β is the outage threshold. Additionally, if the system operates in the corresponding degraded corner point, the success probability for Rx_i is

$$\mathbb{P}_{succ}^{*\mathrm{SIC^i}} = e^{-\beta/\gamma_j} \sum_{k=0}^{\eta_j-1} \sum_{l=0}^{k} \binom{k}{l} \frac{(\beta/\gamma_j)^k}{k!} \frac{\partial^l \mathcal{L}_{P_{ij}}(\beta/\gamma_j)}{\partial (\beta/\gamma_j)^l} e^{-\beta/\gamma_i} \sum_{k=0}^{\eta_i-1} \frac{(\beta/\gamma_i)^k}{k!}. \tag{4.66}$$

Proof. See Appendix C.0.6. □

In the SISO case, the χ^2 distributions of the fading random variables lose their degrees of freedom (scale parameter in the gamma distribution) that appear in MISO case. Hence, following the derivations in Appendix C.0.6, the expressions (4.65) and (4.66) are reduced to

$$\begin{aligned} \mathbb{P}_{succ}^{\mathrm{SIC^i}} &= e^{-\beta\left(\frac{1}{\gamma_{ji}}+\frac{1}{\gamma_i}\right)} \frac{\beta^2}{\gamma_i(\gamma_{ji}+\gamma_i\beta)} \\ \mathbb{P}_{succ}^{*\mathrm{SIC^i}} &= e^{-\beta\left(\frac{1}{\gamma_j}+\frac{1}{\gamma_i}\right)} \frac{\beta^2}{\gamma_i(\gamma_j+\gamma_{ij}\beta)} \end{aligned} \tag{4.67}$$

4.5 Centralized Cell Scheduling under Cooperative SIC

Applying the cooperative SIC scheme in a cellular network with many cells may be challenging as the number of combinations of cells for which the SIC gain conditions need to be checked can be prohibitively high. Moreover, a central processor has to know all the received power values to compute the SIC gain conditions and decide which pairs of BSs and users should perform SIC. In a network formed by transmitters arranged in a hexagonal grid, a Tx can be paired with any of its six neighbors if the corresponding SIC gain conditions are verified. Furthermore, a receiver can be selected by multiple transmitters as the one whose signal should be suppressed. In this section, we present an algorithm for centralized cell scheduling so as to maximize the system sum rate. We assume that all the values P_i and P_{ij} are available at the central processor unit and that the cooperative SIC strategy is only used for at most two cells (i.e. 2-level MACs). For ease of exposition, the following definitions are used:

Master cell (M): a Tx-Rx pair that imposes a rate to another cell in order to perform SIC and decode the interfering signals. *Slave cell (S)*: a Tx-Rx pair whose rate is imposed by a master

cell. For instance, in a two-cell network operating at an external corner point such that Rx_1 performs SIC to decode and suppress the signal from Tx_2, the Tx_1-Rx_1 pair forms the master cell while the Tx_2-Rx_2 link is in a slave cell. Consequently, a scheduler that maximizes the sum rate should be designed under the following premises:

- A master cell cannot be a slave cell simultaneously.
- A master cell has only one slave (only 2-level MACs considered).
- A slave cell may have several masters if the sum rate is increased (cf. equation (4.35)).

Algorithm 1 is used in a network where each cell has already selected one user. This implies that if there are multiple users on each cell another algorithm should determine which user should be served.

Once all SIC gain conditions are checked, the scheduler verifies that each slave is linked to the best master(s) set. Note that if several masters impose a rate constraint on the same slave, the slave should take the minimum of all rates, which may reduce the SIC gains. Having a list of slaves paired to the best master(s) $\mathrm{S}^*_{\mathrm{list}}$, where the best master(s) are those producing the largest sum rate, all conflicts should be identified. For each pair $(\mathrm{S}, \mathrm{M}) \in \mathrm{S}^*_{\mathrm{list}}$ a conflict is formed by all pairs where the slave S is also a master or the master M is also a slave. Finally, an exhaustive search over all valid combinations of Master/Slave allocations is done to find the largest sum rate. Although fairness is not analyzed, it can be pointed out that the SIC gain conditions activate mainly for celledge users.

4.6 Numerical Results

4.6.1 Two-cell network

The cooperative SIC is tested initially in a two-cell network. The purpose is to understand how often is the SIC gain condition activated and what is the average value of the SIC gain. To consider OCI, is important to note that if a user is very close to a celledge, the network will

Algorithm 1 Sum rate maximization using SIC in multicell networks

$N \Leftarrow$ number of cells.

$U \Leftarrow$ number of users per cell.

1. Check SIC gain conditions for all cells, users and neighbors.

for all $n = 1$ to N, $i = 1$ to U, $j = 1$ to 6 **do**

if: $P_{ji}/(1 + P_{Oi}) > P_j/(1 + P_{ij} + P_{Oj})$, then $[i, j] \rightarrow \mathrm{SIC}_{\mathrm{list}}$

end for

return $\mathrm{SIC}_{\mathrm{list}}$, where $L = |\mathrm{SIC}_{\mathrm{list}}|$.

return $\mathcal{M} \Leftarrow$ set of all Masters (M).

return $\mathcal{S} \Leftarrow$ set of all Slaves (S).

2. Find the best Master(s) for each slave.

for $i = 1$ to L **do**

find all possible M for S_i.

find the subset of M with $\max$ Sum Rate.

end for

return $\mathrm{S}^*_{\mathrm{list}}$ where $S = |\mathrm{S}^*_{\mathrm{list}}|$.

3. Find the best M-S allocation without conflicts

for $i = 1$ to S **do**

Find all M-S conflicts for (S_i, M_i) where:

$conflict := \{(S_i, M_i)|S_i \in \mathcal{M} \cup M_i \in (\mathcal{S} \cup \mathcal{M} \backslash M_i)\}$

end for

return $\mathrm{Conflicts}_{\mathrm{list}}$ where $C = |\mathrm{Conflicts}_{\mathrm{list}}|$

return $V = \prod_j^C |conflict_j|$ where V is the number of valid M-S combinations.

if $V = 0$, then S^*_{list} is the M-S allocation $\mathbb{A}$.

for $i = 1$ to V **do**

Calculate the system Sum Rate for each feasible allocation

end for

return $\mathbb{A}$, where $\mathbb{A} \in \mathbb{N}^{2\times n}$ is the best M-S allocation and n is the number of M-S pairs.

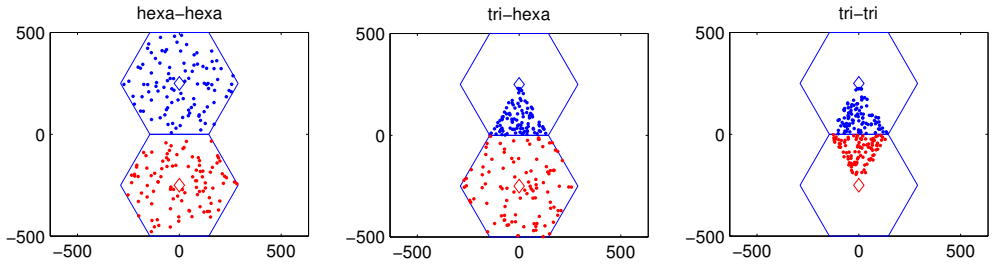

Figure 4.14: User distributions in a 2-cell network.

probably decide to apply cooperative SIC between those two cells. Hence, OCI will probably not include the strongest interferer for a given receiver, but since not all the six cells can be included on the cooperative scheme, some OCI will be present in a real network. To consider different levels of OCI, there are three different scenarios where the users will be randomly placed as shown in Figure 4.14

The SIC success rate is defined as the rate of activation of the SIC gain condition. Figures 4.15, 4.16 and 4.17, show that cooperative SIC gives large gains in the absence of OCI, but when OCI is included, the SIC success rate and the SIC gain are strongly reduced. The only gain that preserves a considerable value is seen in the 5% rate, where in the *tri-tri* case reaches a 25% increase.

Finally, considering only the case where users are randomly placed in both triangles (see Figure 4.14), the variation of the gains with respect to the minimum SNR received in the corner hexagon is shown in Figure 4.18. The encouraging result is that for reasonable values of received SNR, celledge users (5%-rate) see their average rate increase between 20% and 25%. This gain is only obtained having cancelled the strongest interferer and includes all other OCI sources around, showing the great potential of cooperative SIC for $N > 2$.

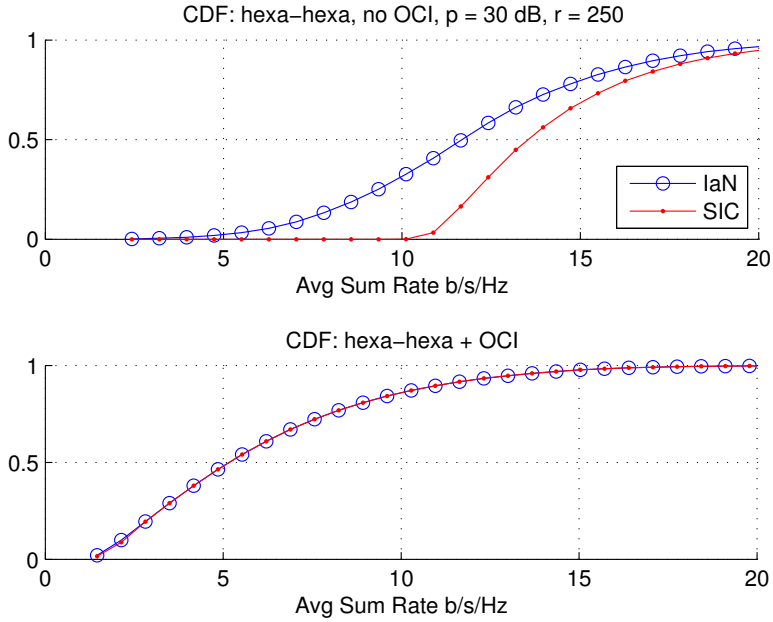

SIC succ rate = 82%

Sum rate gain = 18%

5% rate gain = 75%

SIC succ rate = 3.4%

Sum rate gain = 0.2%

5% rate gain = 4.2%

Figure 4.15: Sum rate CDF for random users in both hexagons.

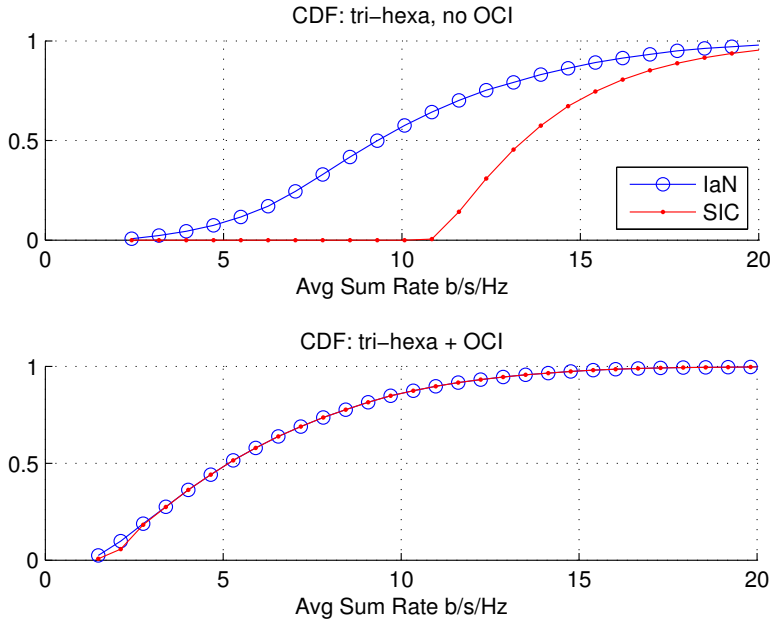

SIC succ rate = 96%

Sum rate gain = 40%

5% rate gain = 159%

SIC succ rate = 12%

Sum rate gain = 0.6%

5% rate gain = 16%

Figure 4.16: Sum rate CDF for random users in one hexagon and one triangle.

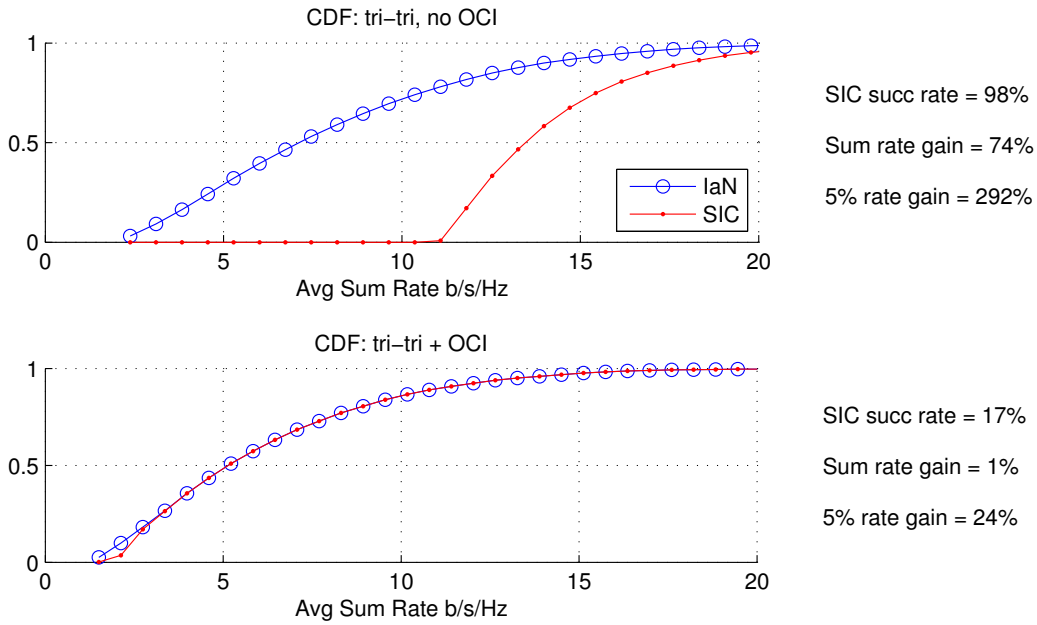

Figure 4.17: Sum rate CDF for random users in both triangles.

4.6.2 21-Cell Network

A network of 7 tri-sector BSs forms a 21-cell hexagonal grid as shown in Figure 4.19. Observe that OCI is present at each cell differently; the outer cells have 2 or 3 neighbors while the inner cells have 6.

The system parameters are based on LTE simulation scenario known as "3GPP case 1" described in [81]. Its main values are summarized in table 4.1. CAP is the cell antenna pattern and the link budget adjustment of -7 dB includes minor factors explained in the cited reference.

In this case, the SIC success rate indicates the average number of cells involved in the cooperative SIC scheme (either as master or slave) at any given realization. In Figure 4.19, $1/3$ of the cells have receivers performing SIC. The system gain is the gain in terms of sum rate when cooperative SIC is performed as compared to IaN considering all cells, even those not using SIC. The SIC gain is the gain in sum rate with respect to IaN considering only those cells

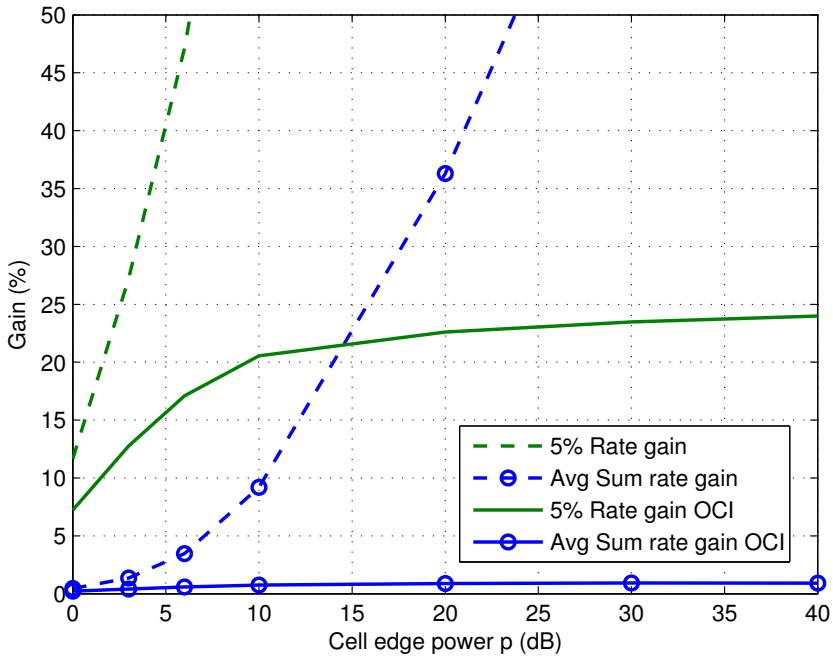

Figure 4.18: Sum rate and 5%-rate gains for radom users in both triangles.

involved in the cooperative SIC.

In Figure 4.20, the effect of increasing the transmit power and the number of users is studied. The left subfigure shows how the SIC success rate increases with the system SNR. This is explained by the fact that higher transmit power enlarges the SIC gain region. On the right subfigure the SIC gain averaged over different user locations is compared to the average system sum rate. Clearly, when the number of users/cell is increased, the probability of finding the best pair for SIC gains is increased, yielding in significant system performance gain. However, the proposed centralized algorithm may become computationally complex and efficient decentralized scheduling algorithms are required to determine the best user sets to select.

Table 4.1: Simulation parameters and values.

Parameter	**Value**
Inter-BS distance (km)	0.5
Min BS-UE distance (km)	0.02
Pathloss (d in km)	$148.1 + 37.6 \log_{10}(d)$ dB
Horizontal CAP, θ in (°)	$-\min(12(\theta/70)^2, 20)$ dB
Noise power + Noise figure	-174dBm + 9dB
Link budget adj.	-7dB.

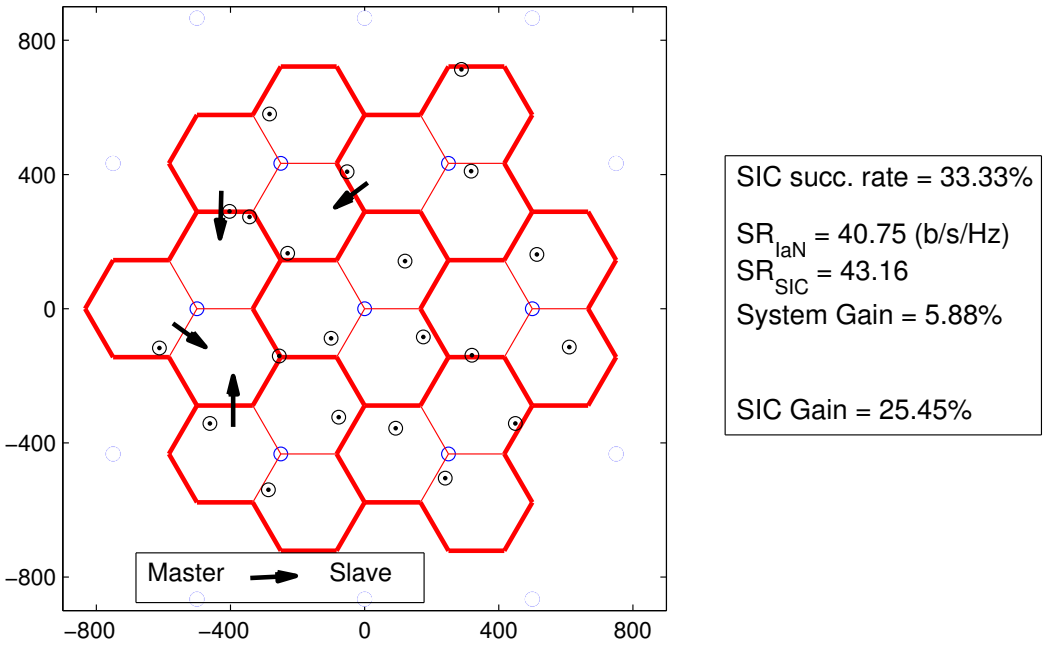

Figure 4.19: 21-cell network layout. Users are placed randomly, arrows indicate Master-Slave relations. The values on the right-hand side are calculated for this particular realization.

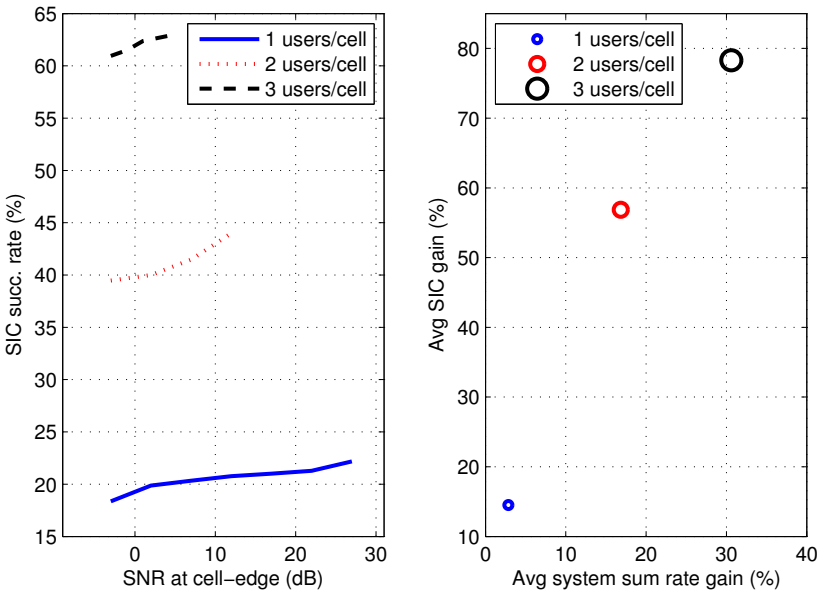

Figure 4.20: System performance with respect to the number of users per cell.

Appendices

Appendix C

Appendix C

C.0.3 Proof of proposition 8

Take any internal corner of a polyhedron where SIC gain condition is attained. Without lose of generality, we use the polyhedron of the capacity region of the MAC at Rx_u where $1 + \sum_{j\neq u}^{N} P_{ju} > \prod_{i\neq u}^{N} (1 + \mathrm{SINR}_i)$. The internal corner is

$$[R_{1u}, R_{2u}, \ldots R_u] = \left[C\left(P_{1u}\right), C\left(\frac{P_{2u}}{1+P_{1u}}\right), \ldots C\left(\frac{P_u}{1+\sum_{j\neq u}^{N} P_{ju}}\right)\right]$$

If the corner is feasible, then

$$R_{ju} < C\left(\mathrm{SINR}_j\right),\ \forall j,$$

and the sum rate in the corner would be

$$\begin{aligned} \mathrm{SR}_{\mathrm{SIC^u}} &< \sum_{j=1}^{N} C\left(\mathrm{SINR}_j\right) \\ &< \mathrm{SR}_{\mathrm{IaN}}, \end{aligned}$$

which implies that the interior corner feasibility and the SIC gain condition $\mathrm{SR}_{\mathrm{SIC^u}} < \mathrm{SR}_{\mathrm{IaN}}$ are in contradiction. Then, if the corner is degraded to obtain its feasibility

$$R_{ju} = C\left(\mathrm{SINR}_j\right), \forall j$$

and therefore, comparing the sum rates

$$\mathrm{SR}_{\mathrm{SIC^u}} = \sum_{j=1}^{N} C\left(\mathrm{SINR}_j\right) = \mathrm{SR}_{\mathrm{IaN}},$$

which proves that there is no SIC gain.

C.0.4 Proof of Lemma 3

The relative gain for the ring network can be expressed as

$$\begin{aligned} \mathrm{G}_{\mathrm{rel}} = \frac{\mathrm{SR}_{\mathrm{SIC}}}{\mathrm{SR}_{\mathrm{IaN}}} &= \frac{\sum_{i=1}^{N} C\left(\frac{p}{1+(i-1)p}\right)}{NC\left(\frac{p}{1+(N-1)p}\right)} \\ &= \frac{\log_2\left(\prod_{i=1}^{N}\frac{1+ip}{1+(i-1)p}\right)}{\log_2\left(\frac{1+Np}{1+(N-1)p}\right)}. \end{aligned} \tag{C.1}$$

The argument of the logarithm can be simplified as follows

$$\begin{aligned} \frac{\frac{1+ip}{1+(i-1)p}}{\frac{1+Np}{1+(N-1)p}} &= \frac{1+(N+i-1)p+(Ni-i)p^2}{1+(N+i-1)p+(Ni-N)p^2} \\ &= \frac{1+(N+i-1)p+(Ni-N)p^2-(i-N)p^2}{1+(N+i-1)p+(Ni-N)p^2}. \end{aligned}$$

In the case where $i = 1$

$$\begin{aligned} \frac{1+p}{\frac{1+Np}{1+(N-1)p}} &= \frac{1+Np+(N-1)p^2}{1+Np} \\ &\leq 1+\lim_{p\to\infty}\frac{(N-1)p^2}{1+Np} \\ &\leq 1+2\frac{(N-1)}{N}p. \end{aligned} \tag{C.2}$$

And in the case where $i > 1$

$$\begin{aligned} \frac{1+p}{\frac{1+Np}{1+(N-1)p}} &= 1+\frac{(N-i)p^2}{1+(N+i-1)p+(Ni-N)p^2} \\ \lim_{p\to\infty}\frac{(N-i)p^2}{1+(N+i-1)p+(Ni-N)p^2} &= \frac{N-i}{Ni-N}. \end{aligned} \tag{C.3}$$

After replacing (C.2) and (C.3) and some algebraic manipulation we get

$$\begin{aligned}\frac{\log_2\left(\prod_{i=1}^{N}\frac{1+ip}{1+(i-1)p}\right)}{N\log_2\left(\frac{1+Np}{1+(N-1)p}\right)} &\leq \frac{\log_2\left(\left[\frac{1+Np}{1+(N-1)p}\right]^N\left[\prod_{i=2}^{N}1+\frac{N-i}{Ni-N}\right]\left[1+2\frac{N-1}{N}p\right]\right)}{N\log_2\left(\frac{1+Np}{1+(N-1)p}\right)}\\ &= 1+\frac{\log_2\left(\left[\prod_{i=2}^{N}1+\frac{N-i}{Ni-N}\right]\left[1+2\frac{N-1}{N}p\right]\right)}{N\log_2\left(\frac{1+Np}{1+(N-1)p}\right)}\\ &= 1+\frac{\log_2\left(\left[\prod_{i=2}^{N-1}\frac{Ni-i}{Ni-N}\right]\left[1+2\frac{N-1}{N}p\right]\right)}{N\log_2\left(\frac{1+Np}{1+(N-1)p}\right)}.\end{aligned}$$

C.0.5 Proof of Theorem 8

First, the case where $C(P_{21}/(1+P_1)) > C(P_2/(1+P_{12}))$ can be discarded since in average the inequality always holds true. Then $C(P_{21}/(1+P_1)) < C(P_2/(1+P_{12}))$ is considered. Using the linearity of the expectation operator, the inequality in (4.3b) yields

$$\begin{aligned}\mathrm{SR}_{\mathrm{SIC}^1} &> \mathrm{SR}_{\mathrm{IaN}}\\ \mathbb{E}_H\left[C(P_{21})\right] &> \mathbb{E}_H\left[C\left(\frac{P_2}{1+P_{12}}\right)\right].\end{aligned} \tag{C.4}$$

Considering Rayleigh fading and SISO channels, any received SNR e.g. $P_i = \gamma_i|h_i|^2$ follows an exponential distribution with cdf

$$F_{P_i}(x) = 1 - e^{x/\gamma_i}. \tag{C.5}$$

Using the law of total probability

$$\begin{aligned}F_{\mathrm{SINR}_2}(x) &= \mathbb{P}\left(\mathrm{SINR}_2 < x\right)\\ &= \mathbb{P}\left(h_2 < x(1+h_{12})\right)\\ &= 1-\left[\frac{\gamma_2}{x\gamma_{12}+\gamma_2}\right]e^{-x/\gamma_2}.\end{aligned}$$

Then substituting the ergodic rates with Lemma A.0.1 both expected values are reduced to

$$\begin{aligned}\mathbb{E}_H\left[C(P_{21})\right] &= \int_0^\infty \frac{e^{-x/\gamma_{21}}}{1+x}\,\mathrm{d}x\\ \mathbb{E}_H\left[C\left(\frac{P_2}{1+P_{12}}\right)\right] &= \int_0^\infty \frac{\gamma_2 e^{-1/\gamma_2}}{(1+x)(\gamma_2+\gamma_{12}x)}\,\mathrm{d}x.\end{aligned}$$

Finally, using the exponential integral definition and a useful integral from [82] as

$$\begin{aligned}\int_x^\infty \frac{e^{-x}}{x}\mathrm{d}x &= E_1(x),\\ \int_0^\infty \frac{e^{-ax}}{(x+b)(x+1)}\mathrm{d}x &= (1-b)^{-1}e^{ab}E_1(ab)+(b-1)^{-1}e^{a}E_1(a),\end{aligned}$$

the proof is completed.

C.0.6 Proof of Theorem 9

$$\begin{aligned}\mathbb{P}_{succ}^{\mathrm{SIC^i}} &= \mathbb{P}_{succ}^{Int}\times\mathbb{P}_{succ}^{Sig}\\ &= \mathbb{P}\left(\frac{P_{ji}}{1+P_i}>\beta\right)\times\mathbb{P}\left(P_i>\beta\right)\end{aligned} \tag{C.6}$$

Following the same derivations as in Appendix A.0.8, we prove first the success probability for the interferer term

$$\mathbb{P}_{succ}^{Int} = e^{-\beta/\gamma_{ji}}\sum_{k=0}^{DoF_{ji}-1}\sum_{l=0}^{k}\binom{k}{l}\frac{\left(\beta/\gamma_{ji}\right)^k}{k!}\frac{\partial^l\mathcal{L}_{P_i}\left(\beta/\gamma_{ji}\right)}{\partial\left(\beta/\gamma_{ji}\right)^l},$$

then the success probability for the signal term

$$\mathbb{P}_{succ}^{Sig} = e^{-\beta/\gamma_i}\sum_{k=0}^{DoF_i-1}\frac{\left(\beta/\gamma_i\right)^k}{k!}. \tag{C.7}$$

For the degraded case, the only variation is to replace the interferer term as

$$\mathbb{P}_{succ}^{Int} = \mathbb{P}\left(\frac{P_j}{1+P_{ij}}>\beta\right). \tag{C.8}$$

Part IV

Conclusions and Perspectives

Conclusions

Recently, cellular networks have become denser, and need to provide a diversified palette of communication services, which resulted in both traffic volume and data rate increase. As a result, increasing the capacity of cellular networks is crucial, and interference mitigation has been identified as one of the key issues and has attracted significant attention from both industry and academia. This dissertation provided performance analysis and evaluation of interference mitigation techniques for the downlink of future cellular networks, and in particular techniques such as CoMP at the transmitter side and SIC at the receiver side. Although in theory network cooperation has shown promising results, in practice the gains do not seem to materialize and better cooperation techniques need to be evaluated in realistic scenarios suitable for implementation.

Coordinated Multi-Point Transmission

First cooperative techniques at the transmitter side, also known as CoMP, were investigated in two of the most commonly used transmission modes: CBF and JT. A theoretical framework was derived (see section 2.2) to precisely measure the impact of different impairments that are often discarded in previous work in the literature. The quantization error is considered by extending RVQ analysis. The different delays incurred in the feedback process are included using a Gauss-Markov process, while unequal path-loss and OCI are accounted by means of moment matching approximations of gamma distributions. The validity of the derived closed form expressions for both achievable sum rate and success probability was extensively verified by simulations and comparisons with LTE parameters. CoMP was proved to be highly sensitive to quantization and delay errors requiring more advanced feedback techniques for an efficient implementation.

To maximize the sum rate of different types of CoMP transmissions, a multi-mode transmission scheme was proposed (section 2.4) based exclusively on known system parameters. MU-JT achieves the best ergodic capacity in the high-SNR and high feedback resolution regimes. However, the rates are only slightly larger than those obtained with CBF without the need for data sharing and strict synchronization requirements as in JT. Finally, CoMP was also compared with a non-CoMP transmission (MRT) in section 2.6, to identify the cell regions where CoMP yields capacity gains. The result shows that CoMP is only beneficial when the users are very close to the cell-edge and the region can be extended towards the center of the cell by increasing the feedback resolution. Additionally, the need for more efficient feedback mechanisms was investigated in chapter 3, proposing adaptive feedback allocation techniques for SU-JT and CBF. Both allocation solutions are based on tight approximations of the ergodic capacity and the quantization error. However, different from previous solutions on this subject, the optimization problem was jointly solved without separating the solution into one for the desired signal and another for the interference terms, avoiding thus suboptimal results. The proposed schemes not only perform significantly better than the known ones, but may also increase the network capacity up to 50% with respect to equal bit allocation at the expense of some extra feedback bits required to inform the users each time the vector allocation is changed.

Cooperative Successive Interference Cancellation

Opposite from CoMP techniques, SIC takes place at the receiver side. SIC is generally related to the uplink as is known for many years to be a capacity achieving technique for the MAC, i.e. multiple sources transmit to the same destination. Similarly, many mobiles may transmit to the same base station in the same time-frequency resource on a given cell. However, chapter 4 proves that SIC can be very useful in the downlink of wireless networks by means of network cooperation. A basic two cell network is an instance of an IC and can be decomposed in two related MACs. Under this perspective, it was shown that there is a condition and a transmission strategy guaranteeing that the use of a SIC receiver brings gains with respect to IaN receivers (see section 4.2.1). This condition allows to identify the cell regions where SIC is useful as well

as it allows to quantify the gain provided. This new transmission strategy is named cooperative SIC and is extended for the case of N transmitter and receiver pairs where only one of the receivers uses its SIC capability to decode and suppress all the $N-1$ interference signals. Additionally, it was shown that in the case of N cells, there are $\sum_i^N \binom{N}{i}$ possible SIC gains conditions in which the cooperative SIC strategy could be applied. The conditions under which several users can activate the SIC receiver simultaneously are also explored in section 4.2.6. Bounds for the SIC gains were found for the cellular case, where each user is placed in a different cell obtaining around 150% in the high-SNR regime. Similar bounds were derived in the case where both users are placed in the same cell. In that scenario, assuming no OCI, the sum rate can be smaller but the relative gain of SIC with respect to IaN can achieve a six-fold increase in the high-SNR regime. Furthermore, a different network layout where all transmitters are placed in a circle and serve an equal number of receivers located in the center of the circle is identified as the best possible configuration to increase the SIC gain. For this layout called ring network, it was shown that there is always a region where the SIC gain condition holds true for any number of transmitter-receiver pairs (see section 4.3.4). The SIC gain condition was also evaluated under small-scale fading yielding an increase of the relative gain (SIC vs IaN, see section 4.4.1). In a more practical perspective, the implementation of the cooperative SIC strategy in a large network was evaluated in section 4.5. An algorithm was proposed to find the cooperative SIC clusters that maximize the network sum rate for each network realization, in order to take the largest possible benefit from the SIC usage. Important gains are observed specially for cell-edge users. Having only one user per cell, the probability of employing cooperative SIC is low, and the system gains remain lower than 5%. However, with only 3 users per cell, the SIC gain condition is easily activated and the system capacity can be increased up to a 60%. Additional numerical results confirm considerable gains both on the cell-edge and at the system level.

Future work

The theoretic framework derived for CoMP can be readily extended for different subjects that need to be assessed before the technology is suitable for implementation. For instance, the Gauss-Markov model can be used to differentiate the different delays that feedback suffers: in the air interface, in the backhaul and the processing time. In this regard, some transmission modes will be more likely used for cooperation between the different sectors of the same BS (known as intra-BS CoMP) or for cooperation between sectors of different BS (inter-BS CoMP). The adaptive feedback allocation technique proposed for SU-JT cannot be easily extended for MU-JT. The main difficulty lies in the fact that for the multi-user case, it is not easy to find an approximation of the SINR such that the optimization problem becomes convex. Therefore, extending our results to the MU-JT case requires a different approach. Integrating the adaptive feedback allocation techniques with the analytical expressions obtained for CoMP throughput can be very useful evaluating how more efficient feedback mechanisms enlarge the regions where CoMP performs better than non-CoMP transmissions, in particular for technologies such as Distributed Antenna Systems.

Cooperative SIC is a new strategy for interference mitigation and should be analyzed in multiple practical settings in wireless networks. The role of power control has to be investigated, while flexible power allocation to the different transmitters may generate the necessary conditions for cooperative SIC in situations where equal power allocation cannot. Additionally, a meticulous analysis of the performance of SIC for MIMO links is needed. It is crucial to determine what kind of interference should be counter by means of multiple antennas or by means of SIC. The impact of imperfect feedback and delay in the cooperation process or scheduling stages can also reduce the SIC performance. In an information theory perspective, the cooperative SIC strategy can be compared with different transmission schemes used for the different regimes of the IC. Finally, the problem of flexible user association combined with simultaneous cooperative SIC and scheduling appears to be a highly complex and non convex optimization problem. Efficient solutions are needed to avoid exhaustive search, allowing for an easier implementation of a centralized scheduler that takes into account all these variables.

Part V

Bibliography

Bibliography

[1] ICT facts and figures 2013. International Telecommunications Union, 2013.

[2] D. Tse and P. Viswanath. *Fundamentals of wireless communication*. Cambridge University Press, 2005.

[3] T. S. Rappaport. *Wireless communications, principles and practice*. Prentice Hall, 2002.

[4] A. Goldsmith. *Wireless communications*. Cambridge University Press, 2005.

[5] Y. Bouguen, E. Hardouin, A. Maloberti, and F.X. Wolff. *LTE et les réseaux 4G*. EYROLLES, 2012.

[6] A. Lozano and N. Jindal. Transmit diversity vs. spatial multiplexing in modern mimo systems. *IEEE Trans. on Wireless Commun.*, 9(1):186–197, 2010.

[7] L. R. Kahn. Ratio squarer. *Proc. IRE*, 42:1704, Nov 1954.

[8] S. M. Alamouti. A simple transmit diversity technique for wireless communications. *IEEE Journal on Sel. Areas in Commun.*, 16(8):1451 – 1458, October 1998.

[9] E. Telatar. Capacity of multi-antenna Gaussian channels. *European Trans. Telecommun.*, 6:585–595, 1999.

[10] G.J Foschini and M.J. Gans. On limits of wireless communications in a fading environment when using multiple antennas. *Wireless Pers Commun*, 6:311–335, March 1998.

[11] V. Tarokh, N. Seshadri, and A. R. Calderbank. Space-time codes for high data rate wireless communication: Performance criterion and code construction. *IEEE Trans. on Inform. Theory*, 44(2):744–765, March 1998.

[12] L. Zheng and D. Tse. Diversity and multiplexing: A fundamental tradeoff in multiple antenna channels. *IEEE Trans. on Inform. Theory*, 49(5), May 2003.

[13] J. Zhang, R.W. Heath, M. Kountouris, and J. G. Andrews. Mode switching for the multi-antenna broadcast channel based on delay and channel quantization. *EURASIP Journal on Adv. Sig. Proc., Sp. Issue on Multiuser Limited Feedback*, 2009.

[14] D. Gesbert, S. Hanly, H. Huang, S. Shamai, O. Simeone, and Wei Yu. Multi-cell mimo cooperative networks: A new look at interference. *IEEE Journal on Sel. Areas in Commun.*, 28(9):1380–1408, 2010.

[15] J. Jose, A. Ashikhmin, T.L. Marzetta, and S. Vishwanath. Pilot contamination and precoding in multi-cell TDD systems. *IEEE Trans. on Wireless Commun.*, 10(8):2640–2651, 2011.

[16] F. Rusek, D. Persson, B.K. Lau, E.G. Larsson, T.L. Marzetta, O. Edfors, and F. Tufvesson. Scaling up MIMO: Opportunities and challenges with very large arrays. 30(1):40–60, 2013.

[17] D. López-Pérez, I. Guvenc, G. De la Roche, M. Kountouris, T.Q.S. Quek, and J. Zhang. Enhanced intercell interference coordination challenges in heterogeneous networks. *IEEE Wireless Communications Magazine*, 18(3):22–30, 2011.

[18] J.G. Andrews, H. Claussen, M. Dohler, S. Rangan, and M.C. Reed. Femtocells: Past, present, and future. *IEEE Journal on Sel. Areas in Commun.*, 30(3):497–508, 2012.

[19] A. Lozano, Andrews J.G., and Heath R.W. On the limitations of cooperation in wireless networks. *Proc., Information Theory and its Applications (ITA)*, pages 123–130, 2012.

[20] V.R. Cadambe and S.A. Jafar. Interference alignment and degrees of freedom of the k -user interference channel. *IEEE Trans. on Inform. Theory*, 54(8):3425–3441, 2008.

[21] B. Clerckx, H. Lee, Y.-J. Hong, G. Kim,. Rank recommendation-based coordinated scheduling for interference mitigation in cellular networks. In *Global Telecommunications Conference (GLOBECOM 2011), 2011 IEEE*, pages 1–6, Dec 2011.

[22] H. Dahrouj and Wei Yu. Coordinated beamforming for the multicell multi-antenna wireless system. *IEEE Trans. on Wireless Commun.*, 9(5):1748–1759, 2010.

[23] G. J. Foschini and K. Karakayali and R. A. Valenzuela. Coordinating multiple antenna cellular networks to achieve enormous spectral efficiency. 153(4):548–55, August 2006.

[24] D. Lee, H. Seo, B. Clerckx, E. Hardouin, D. Mazzarese, S. Nagata, and K. Sayana. Coordinated multipoint transmission and reception in lte-advanced: deployment scenarios and operational challenges. *IEEE Commun. Mag.*, 50(2):148–155, 2012.

[25] B. Clerckx, Y. Kim, H. Lee, J. Cho and J. Lee. Coordinated multi-point transmission in heterogeneous networks: A distributed antenna system approach. In *Circuits and Systems (MWSCAS), 2011 IEEE 54th International Midwest Symposium on*, pages 1–4, Aug 2011.

[26] F. Rashid-Farrokhi, K.J.R. Liu, and L. Tassiulas. Transmit beamforming and power control for cellular wireless systems. *IEEE Journal on Sel. Areas in Commun.*, 16(8):1437–1450, 1998.

[27] M. Schubert and H. Boche. Solution of the multiuser downlink beamforming problem with individual SINR constraints. *IEEE Trans. on Veh. Technology*, 53(1):18–28, 2004.

[28] H. Dahrouj and Wei Yu. Coordinated beamforming for the multi-cell multi-antenna wireless system. In *Information Sciences and Systems, 2008. CISS 2008. 42nd Annual Conference on*, pages 429–434, 2008.

[29] N. Jindal. High SNR analysis of MIMO broadcast channels. In *Proc., IEEE Intl. Symp. on Inform. Theory (ISIT)*, pages 2310–2314, 2005.

[30] O. Somekh, O. Simeone, Y. Bar-Ness, and A.M. Haimovich. CTH11-2: Distributed multi-cell zero-forcing beamforming in cellular downlink channels. In *Proc., IEEE Globecom*, pages 1–6, 2006.

[31] P. Marsch and G. Fettweis. On base station cooperation schemes for downlink network mimo under a constrained backhaul. In *Proc., IEEE Globecom*, November 2008.

[32] D.J. Love, V.K.N. Lau, D. Gesbert, B.D. Rao and M. Andrews. An overview of limited feedback in wireless communication systems. *IEEE Journal on Sel. Areas in Commun.*, 26(8):1341–1365, October 2008.

[33] N. Jindal. MIMO broadcast channels with finite-rate feedback. *IEEE Trans. on Inform. Theory*, 52(11):5045–5060, November 2006.

[34] J. Zhang, M. Kountouris, J.G. Andrews, and R.W. Heath. Multi-mode transmission for the MIMO broadcast channel with imperfect channel state information. *IEEE Trans. on Commun.*, 59(3):803–814, March 2011.

[35] M. Kobayashi, N. Jindal and G. Caire. Training and feedback optimization for multiuser MIMO downlink. *IEEE Trans. on Commun.*, 59(8):800–811, August 2011.

[36] N. Lee, W. Shin, Y.-J. Hong and B. Clerckx,. Two-cell MISO interfering broadcast channel with limited feedback: Adaptive feedback strategy and multiplexing gains. In *Communications (ICC), 2011 IEEE International Conference on*, pages 1–5, June 2011.

[37] F. Boccardi, H. Huang, and A. Alexiou. Network MIMO with reduced backhaul requirements by MAC coordination. In *42nd Asilomar Conference on Signals, Systems and Computers*, pages 1125–1129, 2008.

[38] P. Marsch and G. Fettweis. Uplink CoMP under a constrained backhaul and imperfect channel knowledge. *IEEE Trans. on Wireless Commun.*, 10(6):803–814, June 2011.

[39] J. Hoydis, M. Kobayashi and M. Debbah. On optimal channel training for uplink network MIMO systems. In *Proc., IEEE Intl. Conf. on Acoustics, Speech, and Sig. Proc. (ICASSP)*, pages 3056 – 3059, 2011.

[40] Y. Rui, M. Li, P. Cheng, L. Yinhui, A. Guo. Achievable rates of coordinated multi-point transmission schemes under imperfect CSI. In *Proc., IEEE Intl. Conf. on Communications*, 2011.

[41] B. Makki, Jingya Li, T. Eriksson, and T. Svensson. Throughput analysis for multi-point joint transmission with quantized CSI feedback. In *Proc., IEEE Veh. Technology Conf.*, pages 1–5, 2012.

[42] R. Bhagavatula and R. W. Heath Jr. Adaptive limited feedback for sum-rate maximizing beamforming in cooperative multicell systems. *IEEE Trans. on Sig. Process.*, 59(2):800–811, February 2011.

[43] J. Zhang and J.G. Andrews. Adaptive spatial intercell interference cancellation in multicell wireless networks. *IEEE Journal on Sel. Areas in Commun.*, 28(9):1455–1467, December 2010.

[44] N. Seifi, M. Viberg, R.W. Heath, J. Zhang, and M. Coldrey. Multimode transmission in network MIMO downlink with incomplete CSI. *EURASIP Journal on Advances in Signal Processing*, page 4, 2011.

[45] R. Ahlswede. Multi-way communication channels. In *IEEE International Symposium on Information Theory (ISIT)*, pages 103 – 135, 1971.

[46] H. Liao. A coding theorem for multiple access communications. In *IEEE International Symposium on Information Theory (ISIT)*, 1972.

[47] S. Verdu. *Multiuser Detection*. Cambridge University Press, 2008.

[48] A. Carleial. A case where interference does not reduce capacity (corresp.). *IEEE Trans. on Inform. Theory*, 21(5):569–570, 1975.

[49] T. Han and K. Kobayashi. A new achievable rate region for the interference channel. *IEEE Trans. on Inform. Theory*, 27(1):49–60, January 1981.

[50] H. Sato. The capacity of the gaussian channel under strong interference. *IEEE Trans. on Inform. Theory*, 27(6):786–788, November 1981.

[51] S. Shamai and B. Zaidel. Enhancing the cellular downlink capacity via co-processing at the transmitting end. In *Proc., IEEE Veh. Technology Conf.*, pages 1745–1749, May 2001.

[52] H. Weingarten, Y. Steinberg, and S. Shamai (Shitz). The capacity region of the Gaussian multiple-input multiple-output broadcast channel. *IEEE Trans. on Inform. Theory*, 52(9):3936–3964, September 2006.

[53] P. Marsch and G. Fettweis. A framework for optimizing the uplink performance of distributed antenna systems under a constrained backhaul. In *Proc., IEEE Intl. Conf. on Communications*, pages 975–979, 2007.

[54] P. Marsch and G. Fettweis. *Coordinated Multi-Point in Mobile Communications*. Cambridge University Press, 2011.

[55] V. Jungnickel, L. Thiele, T. Wirth, T. Haustein, S. Schiffermuller, A. Forck, S. Wahls, S. Jaeckel, S. Schubert, H. Gabler, C. Juchems, F. Luhn, R. Zavrtak, H. Droste, G. Kadel, W. Kreher, J. Mueller, W. Stoermer, and G. Wannemacher. Coordinated multipoint trials in the downlink. In *GLOBECOM Workshops (GC Wkshps), 2009 IEEE*, pages 1–7, 2009.

[56] Irmer, R. and Droste, H. and Marsch, P. and Grieger, M. and Fettweis, G. and Brueck, S. and Mayer, H.P. and Thiele, L. and Jungnickel, V. Coordinated multipoint: Concepts performance and field trial results. *IEEE Commun. Mag.*, 49(2):102–111, February 2011.

[57] E. Biglieri, J. Proakis, and S. Shamai (Shitz). Fading channels: Information-theoretic and communications aspects. *IEEE Trans. on Inform. Theory*, 44(6):2619–2692, October 1998.

[58] K.K. Mukkavilli, A. Sabharwal, E. Erkip, and B. Aaf. On beamforming with finite rate feedback in multiple-antenna systems. *IEEE Trans. on Inform. Theory*, 49(10):2563–79, October 2003.

[59] C. Au-Yeung and D.J. Love. On the performance of random vector quantization limited feedback beamforming in a MISO system. *IEEE Trans. on Wireless Commun.*, 6(2):458–462, February 2007.

[60] P. G. Moschopoulos. The distribution of the sum of independent gamma random variables. *Ann. Inst. Statist. Math. (Part A)*, 37:541–544, 1985.

[61] S. B. Provost. On sums of independent gamma random variables. *Statistics*, (20):583–591, 1989.

[62] C. A. Coelho and J. T. Mexia. On the distribution of the product and ratio of independent generalized gamma-ratio random variables. *The Indian Journal of Statistics*, 69:221–255, 2007.

[63] D. Jaramillo-Ramírez, M. Kountouris, and E. Hardouin. Coordinated multi-point transmission with quantized and delayed feedback. In *Proc., IEEE Globecom*, December 2012.

[64] A.M. Hunter, J.G. Andrews, and S. Weber. Transmission capacity of ad hoc networks with spatial diversity. *IEEE Trans. on Wireless Commun.*, 7(12):5058–5071, 2008.

[65] 3gpp ts 36.211 v10.4.0 (2011-12), physical channels and modulation. http://www.3gpp.org, December 2011. [Accessed: Jan, 2012].

[66] D. Jaramillo-Ramírez, M. Kountouris, and E. Hardouin. Coordinated multi-point transmission with imperfect channel knowledge and other-cell interference. In *Proc., IEEE PIMRC*, September 2012.

[67] H.L Maattanen and K. Schober and O. Tirkkonen and R. Wichman. Precoder partitioning in closed-loop MIMO systems. *IEEE Trans. on Wireless Commun.*, August 2009.

[68] N. Lee and W. Shin. Adaptive feedback scheme on K-cell MISO interfering broadcast channel with limited feedback. *IEEE Trans. on Wireless Commun.*, 10(2):401–406, February 2011.

[69] R. Bhagavatula and R. W. Heath Jr. Adaptive bit partitioning for multicell intercell interference nulling with delayed limited feedback. *IEEE Trans. on Commun.*, 59(8):3824–3836, August 2011.

[70] S. Yu and H.-B. Kong and Y.-T. Kim and S.-H. Park and I. Lee. Novel feedback bit allocation methods for multi-cell joint processing systems. *IEEE Trans. on Wireless Commun.*, 11(9):3030–3036, September 2012.

[71] A. El Gamal and Y.-H. Kim. *Network Information Theory*. Cambridge University Press, 2012.

[72] F. Baccelli, A. El Gamal and D. Tse. Interference networks with point-to-point codes. *IEEE Trans. on Inform. Theory*, 57(5):2582–2596, May 2011.

[73] J. Axnas, Y.-P. Eric Wang, M. Kamuf and N. Andgart. Successive interference cancellation techniques for LTE downlink. In *Proc., IEEE PIMRC*, 2011.

[74] Miridakis, N.I. and Vergados D.D. A survey on the successive interference cancellation performance for single-antenna and multiple-antenna OFDM systems. *IEEE Communications Surveys and Tutorials*, 15(1):312–335, 2013.

[75] J. Blomer and N. Jindal. Transmission capacity of wireless ad hoc networks: Successive interference cancellation vs. joint detection. In *Proc. IEEE Int. Conf. on Commun.*, 2009.

[76] S. Sen and N. Santhapuri and R.R. Choudhury and S. Nelakuditi. Successive interference cancellation: a back-of-the-envelope perspective. In *Proc. ACM SIGCOMM Workshop on Hot Topics in Networks*, 2010.

[77] X. Zhang and M. Haenggi,. The performance of successive interference cancellation in random wireless networks. In *Proc., IEEE Globecom*, December 2012.

[78] M. Wildemeersch, T.Q.S. Quek, M. Kountouris, A. Rabbachin and C.H. Slump. Successive interference cancellation in heterogeneous cellular networks. In *http://arxiv.org/abs/1309.6788*, Sep 2013.

[79] C. Avin, A. Cohen, Y. Haddad, E. Kantor, Z. Lotker, M. Parter and D. Peleg. SINR diagrams with interference cancellation. In *Proc. 23rd Annual ACM-SIAM Symposium on Discrete Algorithms*, January 2012.

[80] E. Hardouin, M. S. Hassan and A. Saadani. Downlink interference cancellation in LTE: Potential and challenges. In *Proc., IEEE Wireless Networking and Comm. Conf.*, April 2013.

[81] Further advancements for e-utra physical layer aspects (release 9). 3GPP TS 36.814, March 2010.

[82] I. S. Gradshteyn and I. M. Ryzhik. *Table of Integrals, Series, and Products*. Academic, San Diego, CA, 5 edition,, 1994.